Transcytosis of Interleukin (IL-)11 and apical redirection of gp130 is mediated by IL-11 α-receptor

and

Identification of MAD2B as a novel regulatory protein of IL-6 classic signaling

Dissertation

This dissertation is submitted

for the degree of the Doctor of Philosophy

to the faculty of Mathematics and Natural Sciences

at the Heinrich-Heine-University Düsseldorf

presented by

Niloufar Monhasery

from Tehran, Iran

Düsseldorf, February 2016

Der IL-11 α-Rezeptor vermittelt die Transzytose vom Interleukin (IL-)11 und den apikalen Transport von gp130

und

Identifikation von MAD2B als regulatorisches Protein des klassischen IL-6 Signalwegs

Dissertation

zur Erlangung des Doktorgrades

der Mathematisch-Naturwissenschaftlichen Fakultät

der Heinrich-Heine-Universität Düsseldorf

vorgelegt von

Niloufar Monhasery

aus Tehran-Iran

Düsseldorf, Februar 2016

aus dem Institut für **Biochemie und Molekularbiologie II,**

Medizinische Fakultät, Heinrich Hein Universität Düsseldorf

Gedruckt mit der Genehmigung der

Mathematisch-Naturwissenschaftlichen Fakultät der

Heinrich-Heine-Universität Düsseldorf

Referent: Prof. Dr. rer. nat. Jürgen Scheller

Korreferent: Prof. Dr. rer. nat. William F. Martin

Tag der mündlichen Prüfung: 14.04.2016

Eidesstattliche Erklärung zur Dissertation

Hiermit versichere ich, dass die vorliegende Dissertation von mir selbständig und ohne unzulässige fremde Hilfe unter Beachtung der Grundsätze zur Sicherung guter wissenschaftlicher Praxis an der Heinrich-Heine-Universität Düsseldorf verfasst worden ist. Die Dissertation wurde in der vorgelegten oder in ähnlicher Form noch bei keiner anderen Institution eingereicht. Ich habe bisher keine erfolglosen Promotionsversuche unternommen.

Düsseldorf, den

Niloufar Monhasery

Table of Content

1. Introduction 1

1.2 The Interleukin (IL)-6 family 1

1.3 The cytokine Interleukin-6 3

1.3.1 IL-6 Signaling 5

1.3.2 The IL-6 receptor 6

1.3.4 IL-6 Roles in Vivo 8

1.4 The cytokine Interleukin-11 10

1.4.1 The IL-11 receptor 11

1.4.2 IL-11 roles in vivo 12

1.5 IL-6 and IL-11 signaling pathways 14

1.6 Cell Polarity 16

1.6.1 Trafficking routs in epithelial cells 17

1.6.2 Apical sorting mechanisms 18

1.6.3 Basolateral sorting signals 19

1.6.4 IL-6R, IL-11R, and gp130 sorting in polarized cells 19

1.7 The mitotic arrest deficiency 2 (MAD2) protein 20

1.7.1 The mitotic spindle assembly checkpoint protein MAD2B 21

1.8 Aim of the studies 22

2 Material and Methods 24

2.1 Material 24

2.1.1 Antibiotics 24

2.1.2 Primary Antibodies 24

2.1.3 Secondary Antibodies 25

2.1.4 Chemicals 26

2.1.5 Enzymes 27

Table of Content

2.1.6 Devices 27
2.1.7 Kits 28
2.1.8 Oligonucleotides 28
2.1.9 Buffers and Solutions 28
2.1.10 Recombinant Cytokines and Inhibitors 30
2.1.11 Common dishes and material 31
2.1.12 Cell culture media and reagents 31
2.1.13 Cells 32
2.2 Methods 32
2.2.1 Molecular Methods 32
2.2.1.1 Plasmid-DNA extraction via Mini-prep 32
2.2.1.2 Plasmid–DNA extraction via Midi-prep 33
2.2.1.3 RNA extraction 33
2.2.1.4 Measurement of RNA and DNA concentration 33
2.2.1.5 cDNA synthesis 34
2.2.1.6 Polymerase chain reaction (PCR) 34
2.2.1.7 Quantitative real time-PCR (qPCR) 36
2.2.1.8 DNA digestion 37
2.2.1.9 Agarose gel electrophoresis 37
2.2.1.10 DNA-fragment extraction from agarose gel 37
2.2.1.11 DNA Ligation 38
2.2.1.12 Transformation of DNA into E.coli 38
2.2.1.13 DNA sequencing 38
2.2.1.14 Flow cytometry analysis 38
2.2.1.15 Immunofluorescence staining and confocal microscopy 39
2.2.2 Protein Methods 40
2.2.2.1 Cell lysis 40
2.2.2.2 Protein concentration measurement with BCA assay 40

Table of Content

2.2.2.3 Immunoprecipitation (IP) 41

2.2.2.4 Nano-trap 41

2.2.2.5 SDS-PAGE and Western blotting 42

2.2.2.6 ELISA 43

2.2.3 Cultivation and Manipulation of mammalian cells 43

2.2.3.1 Cell culture 43

2.2.3.2 Polarization of cells 44

2.2.3.3 Preparing Cryotube for cell freezing 44

2.2.3.4 Transient transfection 45

2.2.3.5 Retroviral transduction fo Ba/f3 cells 45

2.2.3.6 Stable transfection of MDCK cells 46

2.2.3.7 Cytokine stimulation 46

2.2.3.8 Cell synchronization (Double Thymidine Block) of HEK-293 cells 46

2.2.3.9 Transcytosis assay 47

3 Results 48

3.1 Transcytosis of Interleukin (IL-)11 and apical redirection of gp130 is mediated by IL-11 α-receptor 48

3.1.1 IL-11R1 is sorted to apical and basolateral membranes of polarized MDCK cells 48

3.1.2 IL-6 and IL-11 stimulation do not change the sorting pattern of IL-6R and IL-11R1 in polarized MDCK cells 51

3.1.3 Apical and basolateral stimulation of polarized MDCK-IL-11R1 with recombinant IL-11 induced phosphorylation of STAT3 52

3.1.4 The cell surface half-life of IL-6R and IL-11R is comparable 54

3.1.5 Internalization of IL-6R and IL-11R1 is clathrin-dependent 55

3.1.6 Generation of IL-6R/IL-11R1 chimeras to determine the apical sorting motif within the IL-11R1 60

3.1.7 Apical sorting signal is located in the intracellular domain of IL-11R1 62

3.1.8 Apical sorting of IL-11R1 forced the typically basolateral-restricted gp130 to the apical membrane and enabled IL-11 classic signaling and IL-6 trans-signaling 65

3.1.9 Detection of gp130 via confocal microscopy on the apical surface of MDCK-gp130-IL-11R1 cells 68

Table of Content

3.1.10 IL-11R1 is a cytokine transcytosis receptor 70

3.1.11 Transcytosed IL-6 and IL-11 were biologically active 72

3.1.12 No transcytosis of IL-11R1 from the apical to basolateral side of polarized MDCK cells 74

3.1.13 gp130 is transcytosed by IL-11R1 75

3.2 Identification of MAD2B as a novel regulatory protein of IL-6 classic signaling 77

3.2.1 OOxPxxxpP is the binding motif of MAD2B in the IL-6R intracellular domain .. 77

3.2.2 MAD2B and IL-6R interaction has no influence on the cell cycle progression 84

3.2.3 Interaction of MAD2B and IL-6R led to an increased number of IL-6R and gp130 molecules on the surface of HepG2 cells 87

3.2.4 Interaction of MAD2B and IL-6R led to an increased number of IL-6R and gp130 on the surface of Ba/F3-gp130-IL-6R cells 91

3.2.5 Expression of MAD2B resulted in the stronger phosphorylation of STAT3 through classic IL-6 signaling 93

3.2.6 Co-expression of MAD2B and IL-6R has no effect on IL-6 trans-signaling 96

4 Discussion 98

4.1 Transcytosis of Interleukin (IL-)11 and apical redirection of gp130 is mediated by IL-11 α-receptor 98

4.1.1 IL-11R1 is sorted to apical and basolateral membranes of polarized MDCK cells 98

4.1.2 The apical sorting signal of IL-11R1 is located on the intracellular domain 100

4.1.3 IL-11R1 is a cytokine transcytosis receptor 101

4.1.4 gp130 is transcytosed by IL-11R1 102

4.2 Identification of MAD2B as a novel regulatory protein of IL-6 classic signaling 105

4.2.1 “OOxPxxxpP” is the binding motif of MAD2B in the IL-6R intracellular domain 105

4.2.2 Co-expression of MAD2B and IL-6R has no influence on the cell cycle progression 106

4.2.3 Interaction of MAD2B and IL-6R resulted in an increased number of IL-6R and gp130 molecules on the surface of HepG2 cells and stronger STAT3 phosphorylation via classic signaling 107

Summary 109

Zusammenfassung 110

Table of Content

Literature 112

Appendix 129

Abbreviations 131

Acknowledgments 134

1. Introduction

1.2 The Interleukin (IL)-6 family

The IL-6 family of cytokines has numerous physiological functions and is tightly involved in health and disease. Moreover, they prompt the transcription of genes which are engaged in survival, differentiation, apoptosis, and proliferation; remarkably, they are involved in immune responses and haematopoiesis. The name "IL-6" for this family of cytokines is due to IL-6, one of the members of the family, which is prominently engaged in pro- and anti-inflammatory processes. The IL-6 family consists of IL-6, IL-11, IL-27, IL-30, IL-31, LIF (Leukaemia inhibitory factor), OSM (oncostatin M), CNTF (ciliary neurotropic factor), CT-1 (cardiotrophin-1) and CLC (cardiotrophin-like cytokine). They belong to the four-helical bundle cytokine family. The bundle folding in up-up-down-down topology has been recognized in several mediator proteins such as interleukins, cytokines and growth factors (Bazan, 1990). Generally, these proteins share little sequence homology and were grouped in one family by bundle folding formation (Bazan, 1989) (Fig 1.2).

IL-6-type cytokines bind to a complex of trans-membrane receptors which belong to the immunoglobulin superfamily (Bazan, 1989; Bazan, 1990). The complex contains two types of receptors, the non-signaling α-receptors IL-6R, IL-11R, EBI/3 and CNTFRα and the transducing β-receptors gp130, leukaemia inhibitory factor receptors (LIFR), oncostatin M receptors (OSMR), and WSX-1 (IL-27R). α-receptors are specific for each cytokine and their expressions are limited to some types of cells. This leads to enhanced specificity of target cells. β-receptors are signal transducing receptors which form homo- or hetero-dimers (Taga and Kishimoto, 1997). Glycoprotein 130 (gp130) is the common β-receptors in all receptor complexes of cytokine family.

IL-6 and IL-11 are the only members of the IL-6 family which signal via homo-dimerization of gp130 whereas the other members use hetero-dimerization of gp130 and one type of the other β-receptors. There is an exception in the case of cytokine IL-31 which binds to a heterodimer of OSMR and the IL-31 receptor A (Cornelissen *et al.*, 2012)(Fig.1).

α-receptors can be present either in the transmembrane form like IL-6R, IL-11R, CNTFR or in soluble form such as Epstein-Barr virus induced gene 3 (EBI3) for IL-30 to form the composite cytokine IL-27 (Pflanz *et al.*, 2002; Heinrich *et al.*, 1998; Senaldi *et al.*, 1999). Moreover, the cytokine OSM, LIF and IL-31 signaling proceed without the need of an α-receptor (Robledo *et al.*, 1997) (Fig 1.2).

Binding of IL-6 type cytokines to their receptors is generally based on ionic and hydrophobic interactions (Grötzinger *et al.*, 1997). All IL-6 type cytokines, except IL-31, bind to the β-receptor gp130 with a high degree of plasticity within gp130 and the binding site of the respective cytokines (Boulanger *et al.*, 2003; Grötzinger *et al.*, 1997). Binding sites of IL-6 type cytokine are known as site I, II and III. Site II and III within the cytokines mediate the interaction with the β-receptors, site I is the specific binding site for α-receptors. Interestingly, the electrostatic potential of site II in IL-6, CNTF, LIF and OSM and gp130 cytokine binding module (CBM) indicates nearly no similarity. Therefore, chemical plasticity of the interaction of IL-6 type cytokines from site II and CBM of gp130 leads to kind of various orientations of cytokines and the CBM of gp130 (Boulanger and Garcia, 2004).

Binding of IL-6 type cytokines to β-receptors triggers several signaling pathways. These signaling cascades comprise signal transducer and activators of transcription (STAT) transcription factor, mitogen-activated protein kinases (MAPK), extracellular regulated kinases (ERK 1/2) and phosphoinositide 3-kinase (PI3K). Moreover, there are negative regulators in different steps of the signaling pathways. Intracellularly suppressor of cytokine signaling 3 (SOCS3), protein inhibitor of activated STATs (PIAS) and protein tyrosine phosphatases (PTP) are main negative feedbacks mediators. In addition, receptor internalization and soluble forms of β-receptors act antagonistically on cytokine signaling (Heinrich *et al.*, 1998; Rabe *et al.*, 2008).

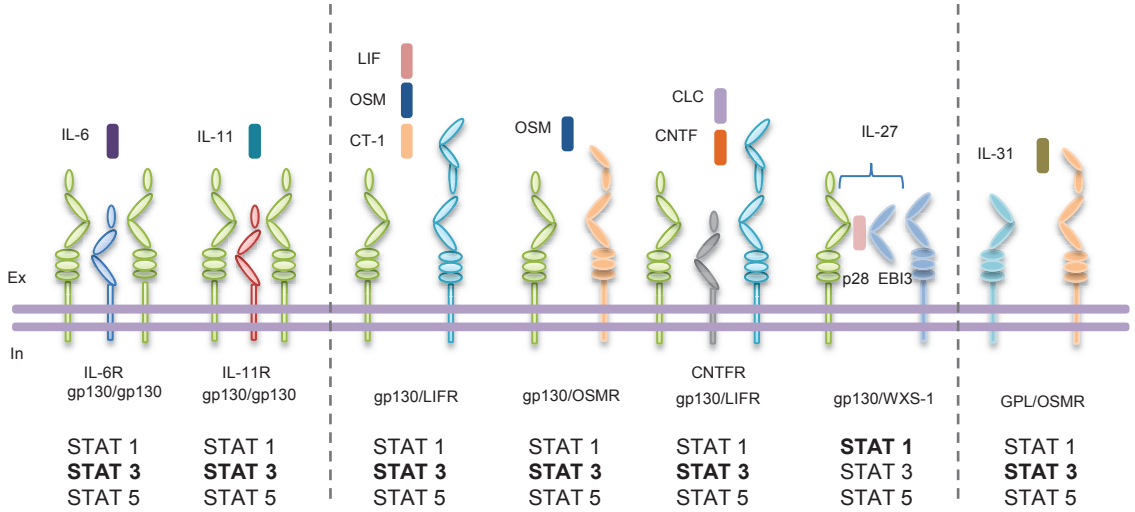

Figure 1.2: schematic illustrations of IL-6 type cytokine receptor complexes. IL-6, IL-11, CLC, and CNTF have specific transmembrane α-receptors whereas LIF, OSM, CT-1, and IL-31 have no α-receptors. Moreover, IL-27 consists of the α-receptor EBI-3and the cytokine IL-30. gp130 is one of the β-receptors which is present in all of the receptor complexes except IL-31. IL-6 family members can activate different STAT molecules, but the most prominent one in each case is marked in bold. Ex: Exracellular; In: Intracellular.

1.3 The cytokine Interleukin-6

Interleukin 6 (IL-6) is a multifunctional small secreted glycoprotein which is outstanding for its pro- and anti-inflammatory properties (Scheller *et al.*, 2011). IL-6 is involved in a wide range of physiological processes. Notably, it plays a promoting role in haematopoiesis and regeneration, and on the other hand acts as a cancer promoting factor (Chang *et al.*, 2014). IL-6 levels in the plasma serum of healthy individuals is low, about 1 pg/ml (Rose-John, 2012), but during inflammation, the level of IL-6 can be dramatically increased. For example in patients with rheumatoid arthritis IL-6 levels raise up to 150 pg/ml (Nowell *et al.*, 2003). IL-6 was described in 1980 and named interferon β2, as it was a novel mRNA which was detected in fibroblasts under the stimulation of interferon β (Weissenbach *et al.*, 1980; Sehgal and Sagar, 1980). IL-6 mRNA encodes a protein with 212 amino acids length which consists of a 29 amino acids as signal peptide and 183 amino acids of the mature protein. According to the

N-linked glycosylation, secreted IL-6 is found in different isoforms of 21-28 kDa (Schiel *et al.*, 1990). Interestingly, IL-6 glycosylation does not have any effect on the function of IL-6, but might affect the half-life or the stability of the protein (Parekh *et al.*, 1992; Simpson *et al.*, 1997). The expression of IL-6 mRNA and its destination are under the control of several factors either on the transcriptional or post-transcriptional levels. On the transcriptional level, the production of IL-6 mRNA is governed by the TATA box sequence motifs in the promoter region. TATA box motif is the binding site of NF-κB (Shimizu *et al.*, 1990; Libermann and Baltimore, 1990; Ray *et al.*, 1988), AP-1 (Lee *et al.*, 1987b; Angel *et al.*, 1987), a cyclic AMP (cAMP)-responsive element (Lee *et al.*, 1987a), and CCAAT enhancer binding protein β (C/EBPβ) (Matsusaka *et al.*, 1993). As shown in figure 3.1 NF-κB has a prominent role in the regulation of IL-6 mRNA expression. There are some factors which induce the expression of IL-6 via activation of NF-κB such as lipopolysaccharide (LPS) (Fong *et al.*, 1989), the pro-inflammatory cytokines TNFα and IL-1α (Kohase *et al.*, 1986; Kohase *et al.*, 1987), and viral infections (Sehgal *et al.*, 1988). On the post-transcriptional level, RNase 1 (regnase-1, encoded by the Zc3h12a gene) has been shown to have a negative impact on IL-6 mRNA (Iwasaki *et al.*, 2011), whereas bromodomain-containing protein 4 (BRD4) has been proved to affect IL-6 production in a positive way (Barrett *et al.*, 2014). Recently, a novel regulatory protein Arid5a (RNA-binding protein AT-rich interactive domain protein 5A) was identified. Arid5a binds to 3´UTR of IL-6 mRNA which results in the stabilization of mRNA through the inhibition of regnase-1 action (Masuda *et al.*, 2013).

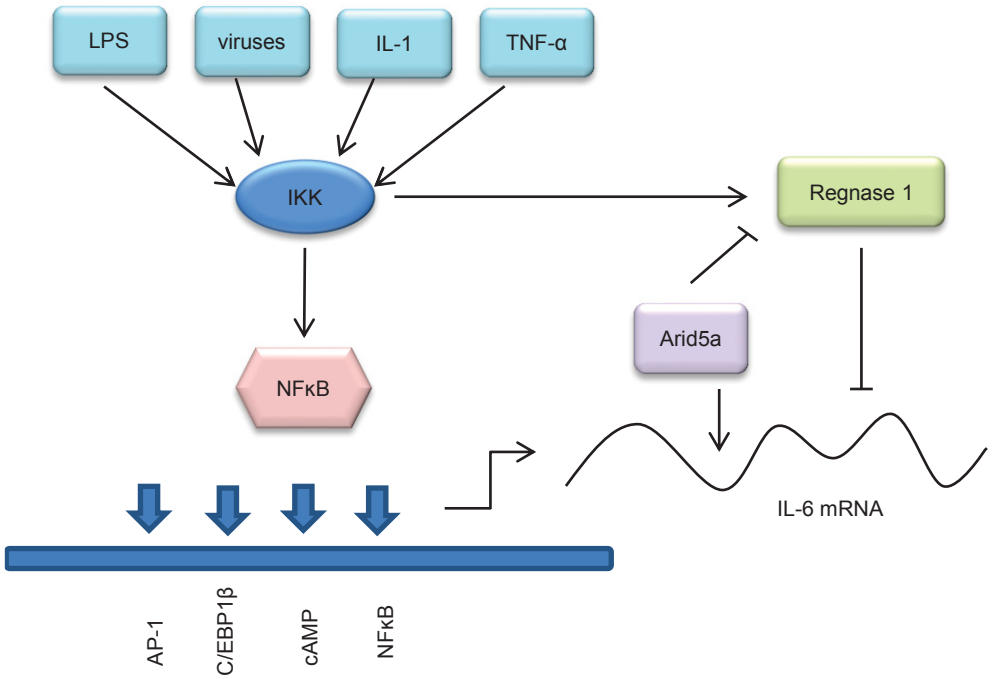

Fig 1.3: regulation of IL-6 mRNA generation. IL-6 mRNA generation is mainly under the control of NF-κB which regulation is under the influence of IKK. However, Regnase and Arid5a have negative and positive regulatory effects on mRNA level of IL-6, respectively.

1.3.1 IL-6 Signaling

IL-6 activates cells via two mechanisms: 1. Classical signaling and 2. Trans-signaling. In classic signaling, IL-6 binds to the non-signaling transmembrane α-receptor (IL-6R) whereas in trans-signaling, IL-6R is found in a soluble form. However, in both signaling pathways, the complex of IL-6 and IL-6R leads to the homo-dimerization and activation of the signal transducing β-receptor (gp130) with high affinity (Garbers *et al.*, 2012). Signal transduction leads to the activation of Janus-kinase/Signal transducer and activator of transcription (Jak/STAT), mitogen activated protein kinase (MAPK) and phosphatidyl-inositol-3-kinase (PI3K) pathways (Heinrich *et al.*, 2003). Several studies have shown that regenerative and

anti-inflammatory activities of IL-6 are mediated by classical signaling, while trans-signaling has been counted for the pro-inflammatory properties of IL-6 (Rose-John, 2012).

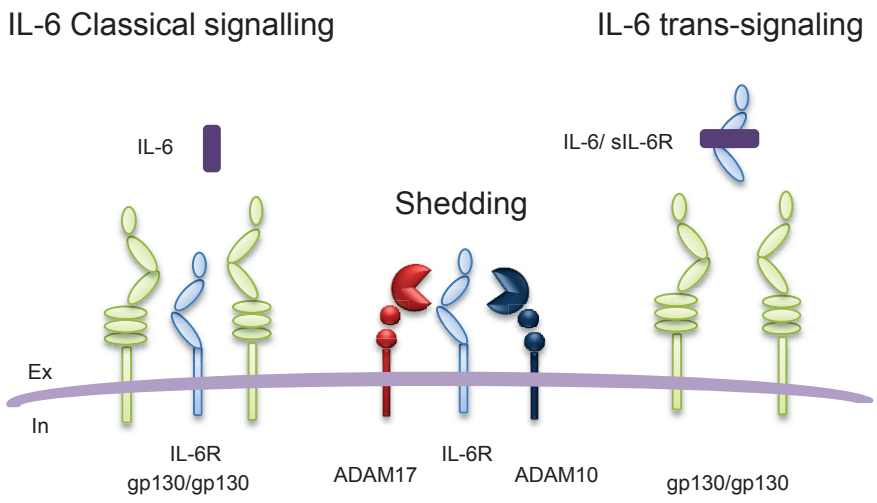

Figure 1.3.1: IL-6 signaling pathways. IL-6 can affect cells via two signaling pathways. Classic signaling that can be triggered by binding of IL-6 to transmembane α-receptors and trans-signaling can be activated via binding of IL-6 to its soluble IL-6R. ADAM17 is a metalloproteases which mediates the cleavage of the IL-6R and releases the soluble form of this α-receptor into the extracellular space (sIL-6R).

1.3.2 The IL-6 receptor

The IL-6R is a type I transmembrane glycoprotein which is also known as CD126 or gp80 with a molecular weight of 80 kDa. The ectodomain of IL-6R consists of an Ig like domain (D1), the cytokine binding module (CBM comprises D2 and D3) and a stalk region with 52 amino acid residues (Sprecher *et al.*, 1998). It is follow by a transmembrane domain and intracellular domain with 83 amino acid residues. IL-6R expression is limited to a small number of cell types such as hepatocytes, megakaryocytes, and some leukocytes including monocytes, macrophages, B cells and various subtypes of T cells (Scheller and Rose-John,

2006; Rose-John *et al.*, 2006) and leads to the selective activation of definite target cells via classical signaling.

Moreover, the soluble form of IL-6R (sIL-6R) is found in human plasma (around 50 ng/ml). In contrast to classical signaling which needs the transmembrane IL-6R, IL-6/sIL-6R can mediate IL-6 trans-signaling pathway in all cell types (signal transducer receptor gp130 is ubiquitously expressed). sIL-6R lacks the transmembrane and intracellular domain and is generated *via* two different mechanisms. The first and most prominent one is the result of proteolytic cleavage of the transmembrane IL-6R by the activity of metalloproteases (90%) (Mullberg *et al.*, 1993). The second mechanism is the alternative splicing of IL-6R mRNA which leads to the production of the IL-6R without transmembrane and cytosolic domain (10%) (Lust *et al.*, 1992).

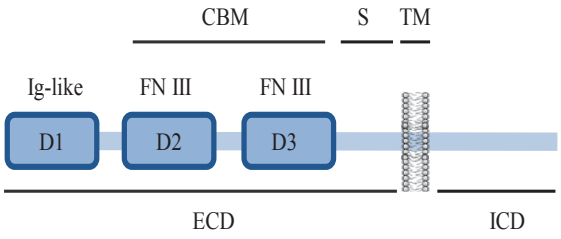

Fig 1.3.1: IL-6R structure. IL-6R consists of 3 regions. 1. Extracellular region which comprise of Ig-like (D1) domain, cytokine binding module (CBM; D1+D2), and the stalk region (S) 2. Transmembrane domain (TM) 3. Intracellular domain (ICD).

ADAM (A Disintegrin And Metalloprotease) proteases are type I transmembrane proteins which are responsible for the proteolysis (shedding) of many cytokine receptors such as IL-6R, TNFR, and IL-1R (Edwards *et al.*, 2008). ADAM10 and ADAM17 are members of the ADAM family which are involved in the shedding of IL-6R but it has been shown that ADAM17 causes inducible fast shedding whereas ADAM10 activity results in slow constitutive IL-6R proteolysis (Baran *et al.*, 2013). The stalk region adjacent to the transmembrane domain between Gln357 and Asp358 of IL-6R is the cleavage site for ADAM17 (Mullberg *et al.*, 1994). Recently it has been shown that conserved ADAM17 Dynamic Interaction Sequence (CANDIS) of ADAM17 is involved in IL-6R recognition (Düsterhöft *et al.*, 2014).

The single nucleotide polymorphism (SNP) rss2228145 results in about 2 fold increase in the level of sIL-6R in the serum (Rafiq *et al.*, 2007; Galicia *et al.*, 2004). The rss2228145 SNP is an adenine (Asp358) to cysteine (Ala358) mutation which is located in the exon 9 of the IL-6R (Galicia *et al.*, 2004). The mutation site is exactly located at the cleavage site of ADAM17 which results in an increase of ectodomain shedding of IL-6R (Garbers *et al.*, 2014). Moreover, humans homozygous for the rss2228145 SNP show a high level of the differentially spliced sIL-6R (dsIL-6R) on the mRNA level (Stephens *et al.*, 2012; Lamas *et al.*, 2013).

1.3.4 IL-6 Roles *in vivo*

IL-6 is a multifunctional cytokine which is not only involved in inflammation and infection but has critical roles in metabolic regulation, control of bone metabolism, pain, regenerative and neural processes. Interestingly, the numerous activities of IL-6 are dependent on the activation of different extracellular signaling pathways. Studies suggest that IL-6 trans-signaling is responsible for the pro-inflammatory roles of IL-6, whereas classical signaling of IL-6 accounts more for the anti-inflammatory and homeostatic effects of IL-6 (Wolf *et al.*, 2014). In the following paragraphs, there are some examples of IL-6 roles on the physiology of the body.

1.3.4.1 IL-6 and the immune system

IL-6 plays critical roles in regulation of the immune system especially in acute and chronic phases of inflammation. After the initiation of inflammation, release of IL-6 from damaged epithelial and endothelial cells as well as tissue resident macrophages leads to the attraction of neutrophils. Infiltration of neutrophils results in secretion of high amount of proteases and reactivation of oxygen species at the inflammatory site and results in tissue damage. However, infiltration of monocytes and T-cells reduce the destructive effect of neutrophilic activities. Activity of proteases at inflammatory sites leads to shedding of IL-6R from the neutrophils

and enhancement of trans-signaling in resident tissues and release of monocytes-attracting chemokine such as CCL2/MCP-1, CCL8/MCP-2, andCXCL5/ENA-78 and attraction of monocytes. (Jones, 2005). Interestingly, IL-6 signaling improves differentiation of monocytes to macrophages by increasing the expression of M-CSF receptors (Chomarat *et al.*, 2000). IL-6 is a necessary cytokine for T-cell differentiation, recruitment and apoptosis. IL-6 progresses the differentiation of T cells towards helper T-cells (T_H); T_H2 and T_H17 cells. The differentiation of T_H2 cells is regulated by induction IL-4 expression and suppression of IFNγ signaling via SOCS3 (Diehl and Rincon, 2002; Sofi *et al.*, 2009). Intriguingly, IL-6 can inhibit the differentiation of naïve $CD4^+$ T-cells into the regulatory T-cells (T_{reg}) by suppression of TGFβ which normally prevent autoimmunity and protect against tissue injury (Bettelli *et al.*, 2006). Moreover, it was shown that IL-6 trans-signaling is critically needed for the efficient induction of T_H17 cells (Dominitzki *et al.*, 2007).

1.3.4.2 IL-6 and bone metabolism

IL-6 trans-signaling plays a prominent role in the regulation of bone homeostasis. It was proven that osteoclast formation was stimulated by IL-6 and sIL-6R. Activation of JAK/STAT signaling pathway via IL-6 trans-signaling induces the expression of RANKL which is an important factor for osteoclastogenesis (Hashizume *et al.*, 2008). Interestingly, after ovariectomy in IL-6 knockout mice, bone loss in female after menopause was inhibited (Poli *et al.*, 1994).

1.3.4.3 IL-6 and metabolism

IL-6 emerged as one of the regulatory factors of metabolism. Most results were obtained from IL-6 knockout mice. A comparison between wild type mice and $IL\text{-}6^{-/-}$mice illustrated that glucose tolerance and insulin resistance was developing in the absence of IL-6. In addition, $IL\text{-}6^{-/-}$ mice demonstrated symptoms of liver inflammation (Matthews *et al.*, 2010). Interestingly, it was demonstrated that adipocyte of obese individuals secrete IL-6, an activity which correlated with the adipocytes volume (Skurk *et al.*, 2007). Therefore, obesity was regarded as a state of chronic, low-grade inflammation (Hotamisligil, 2006). Strikingly, $IL\text{-}6^{-/-}$

mice were found to develop late onset of besity (Wallenius *et al.*, 2002). On the other hand, inhibition of IL-6 signaling by applying neutralizing monoclonal antibodies (tocilizumab) in patients with Reumatoid Arthritis (RA) resulted in an increase in body weight and hypertriglyceridemia and hypercholsterinemia (Nishimoto *et al.*, 2005). However, transgenic mice which were over-expressing IL-6 and sIL-6R, were drastically smaller in size and have less visible fat pad volume in comparison to wild type mice (Peters *et al.*, 2001).

1.3.4.4 IL-6 and heart diseases

It is suggested that IL-6 and particularly IL-6 trans-signaling are pathophysiological responses which contributes to hypertrophy and progression of heart failure. Therefore, inhibition of IL-6 trans-signaling can be a potential therapy (Coles *et al.*, 2007). In rats, IL-6 trans-signaling results in myocardial fibrosis, hypertension, and diastolic dysfunction (Melendez *et al.*, 2010). Furthermore, neutralizing of IL-6 signaling in the heart of rats leads to the partially reduction of cardiac hypertrophy and collagen synthesis (Mir *et al.*, 2012). Intriguingly, it was shown that IL-6 and sIL-6R expression was up-regulated in an autoimmune myocarditis model, whereas inhibition of IL-6 signaling blocks the progression of the disease (Camporeale *et al.*, 2013).

Interestingly, patients who were carrying the IL-6R rs2228145 SNP demonstrated a reduced risk of coronary heart disease and reduced production of acute-phase proteins, due to the lower level of transmembrane IL-6R (Sarwar *et al.*, 2012).

1.4 The cytokine Interleukin-11

Like IL-6, IL-11 signals through a homodimer of the ubiquitously expressed β-receptor glycoprotein 130 (gp130) and the specificity is gained through the individual IL-11 α-receptor (IL-11R), which is involved in the initial binding of the cytokine and receptor complex formation. The pathways which can be activated by IL-11 are similar to the pathways which activated by IL-6. The mitogen-activated protein kinase (MAPK)-cascade and the Janus kinase/signal transducer and activator of transcription (Jak/STAT) pathways are the most

prominent ones. IL-11 was found as a soluble factor in the supernatant of the primate bone marrow derived cell lines (transformed PU-34 stromal cells). The mature form of IL-11 is 178 amino acid residues long with a molecular mass of approximately 19 kDa (Paul *et al.*, 1990). The genomic sequence is about 7 kb and contains 5 coding exons which are located on chromosome 19 (Yin *et al.*, 1994). IL-11 mRNA was detected in low levels in the murine thymus, spleen, bone, heart, lung, kidney, brain, spinal cord, testis, uterus and ovaries (Davidson *et al.*, 1997; Du *et al.*, 1996). IL-11 can be produced by wide variety of cell types in response to different stimuli; for instance sub-epithelial myofibroblasts (which is believed to be the highest source of IL-11) yield high amount of IL-11 in response to stimulation with TGF-β, IL-1β or IL-22 (Bamba *et al.*, 2003; Andoh *et al.*, 2005).

Although IL-6 and IL-11 reveal the same topology and transcribed with canonical signal peptides and signal via homo-dimerization of two gp130, they share little sequence homology (about 22%) (Garbers and Scheller, 2013). There is an overlapping between the tissues that respond to both IL-11 and IL-6, whereas, they harbour their own specific functions. For example, in heart, IL-6 activation leads to hypertrophy and fibrosis, however IL-11 has role in the regeneration of the heart (Aitsebaomo *et al.*, 2011; Dawn *et al.*, 2004). In table 2, tissues and organs which response to IL-11 are named.

1.4.1 The IL-11 receptor

IL-11R is a unique α-receptor for IL-11 which gives the specificity to IL-11 signaling pathway. The 10 kb long human IL-11Rα gene consists of 13 exons and is located on chromosome 9(p13) (Van Leuven *et al.*, 1996). Human IL-11R, as a result of differentially splicing has two isoforms (IL-11R1 and IL-11R2) which are different in the structure of their cytoplasmic domain. IL-11R2 lacks the 32 amino acid residues of c-terminus and the intracellular domain consists of only four alternative amino acid residues. Murine IL-11R1 consists of 14 exons and shares 99% exon coding sequence similarity with IL-11R2 murine (Cherel *et al.*, 1995). Human and murine IL-11R1 has 84% amino acid homology. The regulation of IL-11R is not clear but it has been shown that it comprise putative p53 and AP-1

binding motifs (Putoczki and Ernst, 2015). In mice expression of IL-11R1 was reported for a wide range of organs and cells such as brain, bone, bladder, heart, lung, kidney, macrophages, T-cells, and osteoblasts, whereas expression of IL-11R2 is limited to the testis, lymph nodes, and thymus (Romas *et al.*, 1996; Trepicchio *et al.*, 1997; Robb *et al.*, 1997).

Cells that do not express IL-11 α-receptors can be sensitive to the complex of cytokine/soluble cytokine α-receptor and the fact fits to the responsive of non-expressed IL-11R cells to IL-11. IL-11 can bind to the recombinant soluble IL-11R (sIL-11R) and the complex can stimulate gp130 which leads to the signal transduction. The recombinant sIL-11R act in vitro agonistically and antagonistically.(Curtis *et al.*, 1997; Baumann *et al.*, 1996; Karow *et al.*, 1996). Recently, a report was published regarding to the presence and activity of endogenous sIL-11R *in vivo* (Lokau et al., 2016).

1.4.2 IL-11 roles *in vivo*

The physiological roles of IL-11 were characterized via generation of the IL-11R1 deficient mice. It has been shown that under standard condition these mice appeared normal but females have a defective decidua formation which abrogated embryonic development (Robb *et al.*, 1998). The result of the investigation suggests that the other engaged cytokines are able to maintain the haemostasis of tissues in the absence of IL-11 signaling. Nevertheless, IL-11 signaling has key role in immune activities, mucosal and cell injury, onset and progression of cancers.

1.4.2.1 IL-11 in hematopoietic and immune activities

IL-11 has a prominent role in proliferation of megakaryocytes in the bone marrow. Megakaryocytes but not platelets express IL-11R1. When recombinant IL-11 was applied in mice, an increase of 30-50% in the number of platelets was detected. It shows that IL-11 can cause the increase in the number of platelets by stimulating the mature megakaryocytes

(Weich *et al.*, 1997; Gordon, 1996). Bone metabolism is regulated by the balanced activities of osteoblasts and osteoclasts. A transgenic mouse which has high expression of IL-11 undergoes increased osteoblastogenesis which results in high bone mass accumulation during aging (Takeuchi *et al.*, 2002). Interestingly, treatment of breast cancer patients before chemotherapy with recombinant IL-11 reduced the bone marrow transplants after chemotherapy (Gordon *et al.*, 1996). IL-11 has role in the stimulation of erythropoiesis and regulation of macrophages proliferation and differentiation (de Haan *et al.*, 1995). Stimulation of macrophages with IL-11 leads to the increase of IκB which results in the inhibition of NFκB nuclear translocation and reduction of the pro-inflammatory cytokine production such as TNF-α, IL-6, IL-1β (Trepicchio *et al.*, 1997; de Haan *et al.*, 1995). IL-11 plays an important role in differentiation of T-helper cells which is associated with a reduction of inflammatory tissue damage. IL-11 restricts the differentiation of T-helper cells by regulation of cytokine production from activated $CD4^+$ T-cells which results in production of IL-4 and IL-19 and inhibition of IL-12 and IFN-γ (Hill *et al.*, 1998).

1.4.2.2 IL-11 in mucosal regulation and cell injury

IL-11 is a critical factor for treatment of mucosal damage and cell injury. It was suggested that IL-11 has evolved to execute efficient wound-healing responses. Expression of IL-11 via different types of mesenchymal cells such as fibroblasts, chondrocytes, and placental stromal cells might be due to its effective role in response to mucosal damage (Maier *et al.*, 1993). IL-11 is applied as a clinical treatment for patients with mucositis and Crohn's disease. In ulcerative colitis and Crohn's disease mouse models, application of recombinant IL-11 relieves features of inflammation and intestinal damage (Neddermann *et al.*, 1996; Keith *et al.*, 1994). In another study, it was demonstrated that treatment of mice with recombinant IL-11 played a protective role in the small intestine from bowel injury associated with graft-versus-host disease, lethal gamma and neutron body irradiation, chemotherapy damage and ischemia (Keith *et al.*, 1994; Burnett *et al.*, 2013; Yang *et al.*, 2014). Application of recombinant IL-11 in all of the modes illustrated a protecting role which reduced mucosal damage, elevated the wound-healing response and increased the overall survival. Furthermore, IL-11 has a critical role in hepatocyte damage. IL-11 induces the production of

acute-phase response proteins in hepatocytes and decreases the rate of hepatocyte necrosis and apoptosis (Nishina *et al.*, 2012b; Maeshima *et al.*, 2004). Intriguingly, IL-11 is a potential factor in regulation of lung morphology and can induce the remodelling of airways and sub-epithelial fibrosis (Zheng *et al.*, 2001). In a lung injury mouse model, treatment of mice with recombinant IL-11 led to the reduction of hyperoxic lung injury and improvement of survival after thoracic radiation (Redlich *et al.*, 1996).

1.4.2.3 IL-11 in cancer onset and progression

High expression of IL-11 was reported in different types of human cancers with the origin of either hematopoietic or epithelial cells. Wide varieties of cancer cells were expressing IL-11 such as melanoma, breast, colon, and non-small-cell lung (Morinaga *et al.*, 1998; Furugaki *et al.*, 2011; Luis-Ravelo *et al.*, 2014). Interestingly, not only cancer cells, but also tumour infiltrating macrophages and T-lymphocytes were expressing IL-11 at high levels (Torroella-Kouri *et al.*, 2003). Expression of IL-11 in various types of cancer can be interpreted differently. For example, in breast cancer the level of IL-11 might be a proper tool for prediction of metastasis development (Sotiriou *et al.*, 2001; Ren *et al.*, 2013), whereas in adenocarcinoma IL-11 expression is associated with the grade of tumour (Maeshima *et al.*, 2004; Necula *et al.*, 2012). In order to investigate the role of IL-11 signaling for tumour progression, IL-11 deficient mice were tested. The result of experiments revealed that IL-11 signaling was essential for onset and progression of tumours in colitis-associated cancer and sporadic colon cancer models (Putoczki *et al.*, 2013). Intriguingly, in a gastric cancer mouse model that is dependent on STAT3 activation for tumor progression, even partial inhibition of IL-11 signaling resulted in a significant decrease in tumor burden (Putoczki *et al.*, 2013)

1.5 IL-6 and IL-11 signaling pathways

IL-6 and IL-11 can activate the JAK-STAT pathways, MAPK cascades and PI3K-Akt signaling. Binding of IL-11 and IL-6 to their specific α-receptors leads to homo-dimerization

of gp130 (Matadeen *et al.*, 2007). The formation of this complex results in the activation of Jak molecules, which causes the phosphorylation of five tyrosine (Y) residues in the cytoplasmic region of gp130. The four membrane distal pYs are required for binding and subsequent phosphorylation of the latent transcriptional factors STAT and STAT3 (Heinrich *et al.*, 2003). This phosphorylation enables the phosphorylation of a conserved Y residue in the carboxyl-terminal part of STAT molecules which results in the dimerization and translocation of homo- or heterodimers of STAT proteins into the nucleus. STAT proteins bind to sequence-specific sites of DNA and leads to the transcriptional regulation of target genes (Zhong *et al.*, 1994). However, the membrane-proximal tyrosine (Y_{759}) provides a binding site SHP2 (SH2 containing phosphatase), which mediates the activation of the mitogen activated kinase (MAPK)-cascade, the phosphatidyl-inositol-3-kinase (PI3K)-cascade (Schmitz *et al.*, 2000; Tebbutt *et al.*, 2002). SOCS3 is an important negative regulator of IL-6 signaling that limits the duration of signaling in response to cytokines using gp130 as a part of receptor complex. In order to inhibit the signaling, SOCS3 binds to Y_{759} on gp130 and JAK molecules simultaneously. SOCS3 binds *via* its SH2 domain to a membrane-proximal motif of gp130 and *via* its N-terminal KIR (kinase inhibitory region) domain to the JAK molecule and inhibits the kinase function of JAKs (Kershaw *et al.*, 2013).

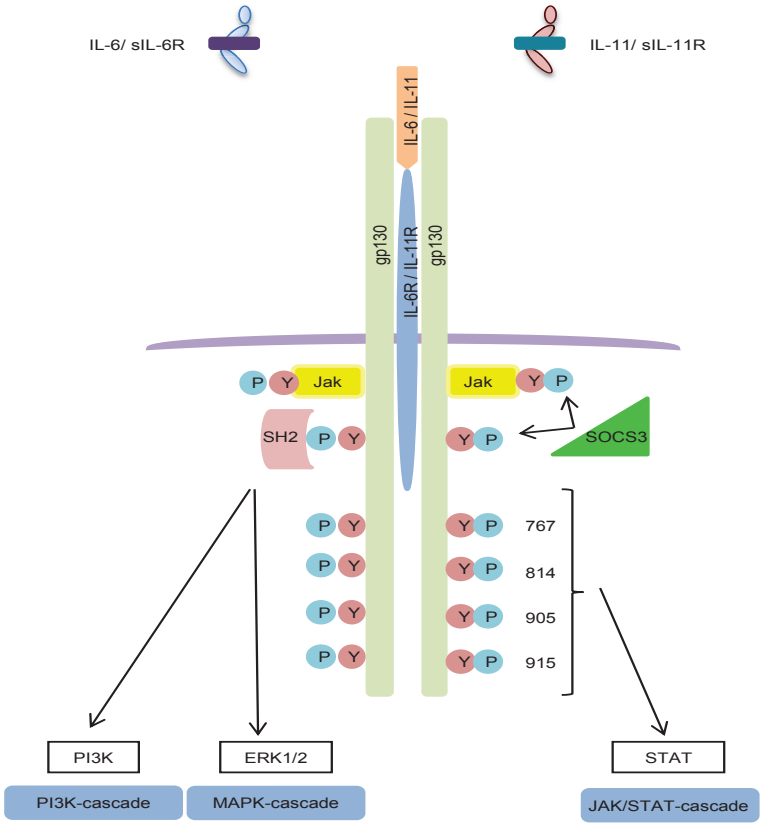

Figure 1.5: IL-6 and IL-11 can trigger several signaling pathways. Complex formation of IL-6/IL-6R or IL-11/sIL-11R results in homo-dimerization of gp130 and phosphorylation of tyrosine residues in the c-terminus and activation of JAK/STAT, PI3K or MAPK cascades.

1.6 Cell Polarity

Cell polarity refers to spatial differences in the shape, structure, and function of the cell surfaces and leads to the commitment of a cell to a special function. The well-known examples of polarized cells are epithelial cells with apical-basal polarity and neurons in which signals are conducted in one direction from dendrites to axons. This arises from the polarized localization of proteins in specific areas of the membrane. This fact requires the polarized vesicle transport *via* cytoskeletal filaments to deliver the trans-membrane proteins from Golgi apparatus to the membrane and involves regulatory molecules. In a sheet of epithelial cells, cells adhere to one another through adherent junctions, tight junctions, and desmosomes. These cellular junctions discriminates the apical and basolateral membrane with distinct protein and lipid composition (Orlando and Guo, 2009). Sheets of polarized epithelial cells form a physical barrier between external or luminal environments and the internal milieu by

covering all body cavities. Formation and preservation of this barriers demands biochemically and functionally divers membrane surface establishment which is due to the different lipid and protein arrangements (Martin-Belmonte and Mostov, 2008). The apical membrane exposes to external and luminal environments which performs the role of protective barriers, and control the uptake of nutrients and ions. The lateral membrane is in contact with neighbour cells and is involved in cell-cell communication, whereas the basal membrane exposes to the extracellular matrix. Basal and lateral surface were called as basolateral part of the cells which has critical roles in regulation of ion gradients, signal transduction and cell adhesion (Rodriguez-Boulan and Nelson, 1989). Deregulation of the cell polarity leads to a wide variety of diseases (Stein *et al.*, 2002). For instance, defects in N- and O-linked glycosylation as apical sorting signals results in congenital sucrase-isomaltase deficiency (CSID) which is an autosomal recessive intestinal disorder (Alfalah *et al.*, 2002; Jacob *et al.*, 2000). Moreover, mutation on the tyrosine-based basolateral sorting motif of low-density lipoprotein receptor leads to familial hypercholesterolemia (FH) which is as an autosomal dominant disorder resulting from the inability of patients to remove low-density lipoprotein from their plasma (Koivisto *et al.*, 2001; Matter *et al.*, 1992).

1.6.1 Trafficking routs in epithelial cells

To generate the asymmetric and polarized epithelial cells, the apical and basolateral compartments should be translocated to their final destination. To establish and maintain this asymmetry, newly made plasma membrane proteins are sorted in the trans-Golgi network (TNG) and directing to apical or basolateral surfaces (Griffiths and Simons, 1986). Generally, signals for basolateral sorting of proteins are located in the cytoplasmic domain, whereas signals for apical sorting can be located in any part of the protein and also O- and/or N-linked glycosylation can act as apical delivery signal. In addition to TNG-sorting system, there are two distinct classes of early endosomes which are apical early endosomes and basolateral early endosomes which play significant roles in this system (Sheff *et al.*, 2002).

1.6.2 Apical sorting mechanisms

Apical sorting signals are needed to guide the transportation of the newly synthesised proteins to the apical surface of the cell. Interestingly, the apical sorting signal could be localized in different parts of the apically sorted proteins such as extracellular, trans-membrane, and cytoplasmic domains (Weisz and Rodriguez-Boulan, 2009)

1. N- and O-linked protein glycosylation is one of the apical sorting signals (Yeaman *et al.*, 1997; Fiedler and Simons, 1995). Glycan structures are diverse and general molecular mechanisms which regulate the apical sorting of glycosylated proteins have not exactly been determined but there are some specific reports. For example, the sequential addition of one to five N-glycans to the basolaterally located Na^+-K^+-ATPase β1-subunit led to the translocation of the subunit to the apical domain in HGT-1 cells (Vagin *et al.*, 2005)

2. A well known apical sorting signal is the glycosylphosphatidylinositol (GPI) anchor, GPI-anchored proteins are predominantly localized to the apical membrane of epithelial cells (Mayor and Riezman, 2004).

3. Lipid rafts are another key regulator of apical sorting proteins (Simons and van Meer, 1988). Lipid rafts are defined as dynamic, nanometer-sized, sterol-sphingolipid-enriched, and tightly packed lipid-protein assemblies that fluctuate on a sub-second time scale (Lingwood and Simons, 2010). The influenza virus HA localization in apical part is the best example of apical sorting *via* the attachment to lipid rafts (Skibbens *et al.*, 1989).

4. The transcytotic pathway is another regulator of apical sorting of receptors. In principle transcytosis is a process which is important to transfer macro-molecules to the opposite cell surface of polarized cells. However, these mechanisms are responsible for sorting of receptors which were localized first on the basolateral membrane and then according to the endocytosis process be directed to the apical surface (Orzech *et al.*, 2000). The best example of transcytosis is related to the

polymeric immunoglobulin receptors (pIgR) (Mostov, 1994). In the case of pIgR, the basolateral and apical sorting motifs are located in the cytoplasmic domain of the receptors. According to the basolateral sorting signal, the receptor is transferred to the basolateral surface. Then, either with or without stimulation of the ligand the receptor is internalized via clathrin-mediated endocytosis. Afterwards, the endosomal vesicles are translocated to the apical membrane according to the apical signal of receptors (Mostov, 1994; Luton *et al.*, 2009).

1.6.3 Basolateral sorting signals

In comparison to the apical sorting signals, basolateral sorting signals are very well defined. For the first time in 1992 Mellman's group reported the existence of basolateral sorting motifs within the cytoplasmic domain of LDL-receptors (Matter *et al.*, 1992). Basolateral delivery is generally dependent on signals which are located in the cytoplasmic domain of the protein. The most common basolateral sorting signals are: 1. Tyrosine based motifs YXXO or NPXY (X can be any amino acid and O is a bulky hydrophobic residue); 2. Di-leucine motifs (Mellman and Nelson, 2008). However, there is a wide variety of basolateral sorting signals in the case of different proteins, for example the total number of charged residues was found to be crucial for basolateral sorting of P2Y receptors (Wolff *et al.*, 2010).

1.6.4 IL-6R, IL-11R, and gp130 sorting in polarized cells

IL-6 receptors are expressed by polarized cells such as hepatocytes and intestinal epithelial cells. In intestinal epithelial cells, endogenous IL-6R expression was found on the basolateral surface of T84 cells (human colonic adenocarcinoma), while it was sorted in apical and basolateral membrane of Caco-2 cells (intestinal epithelial cells) (Molmenti *et al.*, 1993). In

2000, it was revealed that the basolateral sorting signal of IL-6R is related to two discontinues motifs in its cytoplasmic domain and any mutation or deletion in these motifs led to the apical delivery of IL-6R. The membrane-proximal tyrosine-based motif (YSLG) and a more membrane-distal dileucine-type motif (LI) are the basolateral signals for IL-6R sorting. It was shown that stimulation of polarized MDCK cells which were stably transfected with IL-6R from basolateral side led to the activation of STAT3, whereas there was no activation of STAT3 as a result of the stimulation of cells from apical side (Martens *et al.*, 2000). gp130 is ubiquitously expressed in all cell types of cells. It was shown that the di-leucine motif (L^{786} L^{787}) in the cytoplasmic domain of gp130 was responsible for the internalization of the receptor (Dittrich *et al.*, 1996). In 2005, it was revealed that the same motif is responsible for sorting of gp130 in polarized MDCK cells (Doumanov *et al.*, 2006). IL-11R is expressed on polarized cells such as hepatocytes and intestinal epithelial cells. However, there is no report regarding to the sorting of IL-11R in polarized cells.

1.7 The mitotic arrest deficiency 2 (MAD2) protein

In order to investigate the binding proteins of IL-6R intracellular domain, yeast-two-hybrid assay was done in our group. MAD2B was identified as one of the binding proteins of IL-6R.

The mitotic arrest deficiency 2 (MAD2) protein is one of the members of the MAD family which is a critical molecular component of the spindle checkpoint. Genomic DNA duplicated during the cell cycle and the duplicated sister genomes are physically tethered through the process of sister-chromatid cohesion (Nasmyth, 2002; Onn *et al.*, 2008). At the metaphase to anaphase transition, a ubiquitin ligase complex forms which called the anaphase-promoting complex or cyclosome (APC/C) ubiquitinates securin and cyclin B (Yu, 2007; Peters, 2006). Degradation of securin and cyclin B activates separase, which cleaves the cohesion complex that maintains sister-chromatid cohesion (Nasmyth, 2002; Onn *et al.*, 2008). A cell-cycle surveillance system called the spindle checkpoint monitors the proper attachment of microtubules to kinetochores (Bharadwaj and Yu, 2004; Musacchio and Salmon, 2007). Unattached kinetochores activate this checkpoint, which inhibits APC/C and stabilizes

securing and cyclin B, thereby delaying separase activation and the onset of anaphase. Throughout the cell cycle, MAD2 forms a constitutive core complex with MAD1 which is the upstream regulator of MAD2. During mitosis, MAD2 is recruited to unattached kinetochores in a MAD1-dependent manner. MAD2 inhibites the ability of Ddc20 to activate APC/C (Yu, 2007), however the mechanism is not solved.

1.7.1 The mitotic spindle assembly checkpoint protein MAD2B

The mitotic arrest deficient 2-like protein (named MAD2B, MAD2L2) is one of the members of MAD family and acquired its name regarding to 54% amino acid similarity to mitotic arrest-deficient 2 (MAD2) (Cahill *et al.*, 1999; van den Hurk *et al.*, 2004). MAD2B contains a conserved HORMA domain which is engaged in protein-protein interaction, protein oligomerization, and chromatin state recognition (Cahill *et al.*, 1999) MAD2B can bind to CDH1 and CDC20 which are known as the activators of anaphase promoting complex/cyclosome (APC/C). Therefore, MAD2B can affect the cell cycle progression by inhibiting the activity of APC/C *via* the inhibition of ubiquitin ligase CDH1-APC and CDC20-APC (Chen and Fang, 2001; Pfleger *et al.*, 2001; Sudakin *et al.*, 2001). In addition, it was found that during mitosis clathrin is localized to kinetochore fibres of the spindle and clathrin light chain interacts with MAD2B (Medendorp *et al.*, 2010).

1.8 Aim of the studies

IL-11 is one of the members of IL-6 family with the highest homology to IL-6. IL-11 signaling is important in intestinal epithelial cell homeostasis and mucosal protection, thrombopoiesis, embryogenesis, (gastric) tumor development, immunomodulation, haematopoiesis, macrophage and osteoclast differentiation and promotion of stem cell development (Putoczki and Ernst, 2010). Intestinal wound-healing critically depends on polarized intestinal epithelial cells and hematopoietic cell-derived IL-11 and both processes are severely impaired in IL-11R1 deficient mice. Administration of IL-11 is protective in several disease states, among them colitis, renal ischemia and reperfusion injury, experimental autoimmune encephalomyelitis, acute liver injury and cardiac fibrosis after myocardial infarction (Gurfein *et al.*, 2009; Lee *et al.*, 2012; Nishina *et al.*, 2012a; Obana M *et al.*, 2010; Qiu *et al.*, 1996). In gastric tumors, IL-11R1 deficient mice displayed a delayed onset and reduced overall tumor formation (Putoczki *et al.*, 2014). According to the high expression of IL-11R in polarized cells, in this study, we are going to examine the localization of IL-11R is polarized cells and investigate the controlling mechanisms of IL-11R sorting.

IL-6 is known as an anti- and pro-inflammatory cytokine and is one of the key molecules in regulation of immune system. IL-6 can affect cells by binding to its specific α-receptor (IL-6R) and homo-dimerization of β-receptors (gp130). IL-6R is a transmembrane receptor which can be present as a soluble form due to the activity of metalloproteases or alternative splicing of mRNA. Intracellular domain of IL-6R has a 83 amino acids long (ICD) and no specific roles have been identified for this domain so far. To have a deeper insight for transportation, localization, internalization, and degradation of IL-6R, we need to examine the role of IL-6R intracellular domain. In our group, MAD2B has been discovered as a novel IL-6R binding protein according to the result of yeast-two-hybrid assay. MAD2B has been known as the inhibitor of ubiquitin ligases CDH1-APC and CDC20-APC and also has a critical role in regulation of cell cycle. gp130 is the IL-6 signal transducing receptor which degradation depend on the ubiquitin pathway. c-CbI is responsible for gp130 ubiquitination, internalization, degradation and signal termination. Consequently, MAD2B can be assumed as an inhibitor of gp130 ubiquitination *via* interacting with IL-6R intracellular domain. Consequently, we will examine the interaction and binding sites of IL-6R and MAD2B. The

effect of their interaction, on one hand on the cell cycle, and on the other hand, on STAT3 signaling pathway will be investigated.

2 Material and Methods

2.1 Material

2.1.1 Antibiotics

Ampicillin	Carl Roth, Karlsruhe	100 ng/ml
Hygromycin	Carl Roth, Karlsruhe	1 mg/ml
Kanamycin	Carl Roth, Karlsruhe	50 µg/ml
Geneticin (G418)	(G418) Genomycin, Genaxxon, Ulm	1.6 mg/ml
Puromycin	PAA Laboratories GmbH, Cölbe	1.5 µg/ml

2.1.2 Primary Antibodies

Anti-hIL-6R (4-11)	1 mg/ml, 1:1000 Western blot & ELISA, 1:100 FACS; Production described in Chlaris et al., 2007
Anti-hIL-11R (4D12)	2 mg/ml, 1:100 Immunocytochemistry; Santa Cruz Biotechnology, Heidelberg
Anti-hIL-11R (AF490)	100 µg/ml, 1:100 FACS & ELISA; R&D, Minneapolis, USA
Anti-c-myc (71D10)	100 µg/ml, 1:1000 Western blotting, 1:500 Immunocytochemistry; Cell Signaling Biotechnology, Frankfurt
Anti-pSTAT1 (Y^{701}) (58D6)	200 µg/ml, 1:1000 Western blotting; Cell Signaling Biotechnology, Frankfurt
Anti-STAT1 (42H3)	100 µg/ml, 1:1000 Western blotting; Cell Signaling Biotechnology, Frankfurt
Anti-pSTAT3 (Y^{705}) (D3A7)	100 µg/ml, 1:1000 Western Blotting; Cell Signaling Biotechnology, Frankfurt

Anti-STAT3 (124H6)	100 µg/ml, 1:1000 Western Blotting; Cell Signaling Biotechnology, Frankfurt
Anti-pERK1/2 (T^{207}/Y^{204})	100 µg/ml, 1:1000 Western Blotting; Cell Signaling Biotechnology, Frankfurt
Anti-ERK	100 µg/ml, 1:1000 Western Blotting; Cell Signaling Biotechnology, Frankfurt
Anti-pAkt (S473) (D9E)	100 µg/ml, 1:1000 Western Blotting; Cell Signaling Biotechnology, Frankfurt
Anti-Akt	100 µg/ml, 1:1000 Western blot; Cell Signaling Biotechnology, Frankfurt
Anti-β-actin (C4)	200 µg/ml, 1:1000 Western blot; Santa Cruz Biotechnology, Heidelberg
Anti-CD130 (gp130) [B-S12]	100 µg/ml, 1:100 FACS; Abcam, Cambridge, England
Anti-CD130 (gp130) [B-T2]	100 µg/ml, 1:200 Immunocytochemistry; Thermo, Waltham, USA
Anti-GFP	100 µg/ml, 1:1000 Western Blotting; Roche, Mannheim, Germany
Anti-Na^+-K^+ ATPase (H-300)	20 µg/ml, 1:200 Immunocytochemistry; Santa Cruz Biotechnology, Heidelberg
Anti-Ezrin	100 µg/ml, 1:500 Immunocytochemistry; Sigma-Aldrich, Steinheim
Anti-Clathrin heavy chain(D3C6)	100 µg/ml, 1:200 Immunocytochemistry; Cell Signaling Biotechnology, Frankfurt

2.1.3 Secondary Antibodies

Anti-Mouse IgG-POD	1 mg/ml, 1:5000 Western Blotting; Thermo scientific, Waltham, USA
Anti-Rabbit IgG-POD	1 mg/ml, 1:5000 Western Blotting; Thermo scientific, Waltham, USA
Rabbit anti-Human IgG-POD	1 mg/ml, 1:5000 Western Blotting; Thermo scientific, Waltham, USA
Alex Flour®546 goat anti-mouse IgG	1 mg/ml, 1:200 Immunocytochemistry; Life Technology, Eugene, OR, USA
Alex Flour®488 goat anti-rabbit IgG	1 mg/ml, 1:200 Immunocytochemistry; Life Technology, Eugene, OR ,USA
Fluorescein(FITC)-conjugated Affinity Purified, Anti-mouse IgG	1 mg/ml, 1:100 FACS; Life Technology, Eugene, OR, USA
Allophycocyanin (APC)-conjugated Affinity Purified , Anti-rabbit	1 mg/ml, 1:100 FACS; Jackson ImmunoResearch

2.1.4 Chemicals

Chemicals which are not in the list were purchased from Carl Roth GmbH, Karlsruhe.

6x orange DNA loading dye	Thermo Scientific, Waltham, USA
Acrylamide, 30% solution	Sigma-Aldrich, Steinheim
Agarose	Biozym Scientific, Hessisch Oldendorf
Bovines Serum Albumin (BSA)	Biomol, Hamburg
Bromphenol blue	Sigma-Aldrich, Steinheim
Cell Titer-Blue	Promega, Mannheim
DMSO	Sigma-Aldrich, Steinheim
Double Tymidine	Sigma-Aldrich, Steinheim
Dynasore	Abcam, Cambridge, England
Ethanol	Merck, Darmstadt
Ethylene glycol tetraacetic acid (EGTA)	Sigma-Aldrich, Steinheim
Ethylenediaminetetraacetate (EDTA)	Sigma-Aldrich, Steinheim
Gene Ruler 1kb DNA ladder	Thermo Scientific, Waltham, USA
LB-agar-powder	Applichem, Darmstadt
Methanol	Merck, Darmstadt
Sodium chloride	Applichem, Darmstadt
Sodium fluoride	Sigma-Aldrich, Steinheim
Sodium orthovanadate	Sigma-Aldrich, Steinheim
Sodium hygro genoho phosphate	Merck, Darmstadt
Sodium pyrophosphate	Sigma-Aldrich, Steinheim
Negative Pitstop 2	Abcam, Cambridge, England
Nonidet P-40	Sigma-Aldrich, Steinheim
Page Ruler Prestained (Protein marker)	Thermo Scientific, Waltham, USA
Pitstop 2	Abcam, Cambridge, England
Potassium acetate	Merck, Darmstadt
Potassium chloride	Applichem, Darmstadt
TEMED	Sigma-Aldrich, Steinheim
Triton x-100	VWR, Radnor, USA
Trypan blue	Bio-Rad, München
Tween 20	Sigma-Aldrich, Steinheim

β-Glycerophosphate	Sigma-Aldrich, Steinheim
Mercaptoethanol	Sigma-Aldrich, Steinheim

2.1.5 Enzymes

All enzymes including restriction enzymes and polymerases were purchased from Thermo Scientific, Waltham, USA. RNase was purchased from Qiagen, Hilden.

2.1.6 Devices

7500 Real-Time-PCR System	Applied Biosystems, Warrington, UK
Analytical Balance	Kern, Balingen-Frommern
ChemoCam Imager	Intas, Göttingen
CO_2-Incubator	Binder, Tuttlingen
Confocal Microscope LSM-510	Zeiss, Jena
Freezer container Mr.Frosty	Thermo Scientific, Waltham, USA
Gel iX Imager	Intas, Göttingen
Horizontal Electrophoresis System	Bio-Rad, München
Inverse Microscope Axiovert 25	Zeiss, Jena
Mastercycler	Eppendorf, Hamburg
Multichannel Pipette	Eppendorf, Hamburg
Multipipette	Eppendorf, Hamburg
Nano drop ND-2000	Peq-Lab, Erlangen
Neubauer cell counter	Brand, Werthein
One channel Pipette	Eppendorf, Hamburg
pH-Meter	Sartorious, Göttingen
Plate Centrifuge	Eppendorf, Hamburg
Precision Balance	Kern, Balingen-Frommern
Roll mixer	Neolab, Heidelberg
Tecan infinite M200 PRO reader	Tecan, Crailsheim
Thermo block	Eppendorf, Hamburg
Trans-Blot Turbo^{TM} Transfer System	Bio-Rad, München
UV-table	Bio-Budget Technologies, Krefeld
Vortexer	Neolab, Heidelberg
Water bath Aqualine	Lauda, Lauda-Königshofen

2.1.7 Kits

Mini-prep, NucleoBond Xtra mini	Macherey-Nagel, Düren
Midi-prep, NucleoBond Xtra mini	Macherey-Nagel, Düren
PCR clean-up, Gel extraction	Macherey-Nagel, Düren
BCA Protein Assay	Thermo Scientific, Waltham, USA
RNA extraction	Nucleospin RNA II, Macherey-Nagel, Düren
IL-11 ELISA	R&D, Minneapolis, USA
IL-6 ELISA	Thermo Scientific, Waltham, USA

2.1.8 Oligonucleotides

All the oligonucleotides were synthesised by Eurofins Genomics Company.

Fw IL-11RΔICD	5'-GGAGACCCAAGCTGGCTAGCGTTTAAACTT-3'
Rw IL-11RΔICD	5'-TTACCAGAGCCCCAGTGCCAGGGCCC-3'
Fw gp130-puro	5'-GCCGCTAGCATGTTGACGTTGCAGACTTGG-3'
Rw gp130-puro	5'-CGCAAGCTTTTACTGAGGCATGTAGCCGCCTTGCCG-3'
Fw MAD2B-pmows	5'-GCGTTTAAACATGACCACGCTCACACGAC-3'
Rw MAD2B-pmows	5'-TTACTTGTACAGCTCGTCCATGCCGAG-3'

2.1.9 Buffers and Solutions

10x TBS	0.5 M Tris-HCl 1.5 M NaCl pH 7.5
5x Laemmli buffer	62.5 mM Tris-HCl 10% Glycerol 2% SDS 5% β-Mercaptoethanol pH 6.8 Spatula Bromophenol blue
Blocking buffer	5% Milk powder

	in TBS-T
ELISA blocking buffer	PBS 1% BSA 5% Succrose
ELISA washing buffer	PBS 0.05% Tween
IP buffer	50 mM Tris-HCl 150 mM NaCl 1 mM EDTA 1 mM EGTA 1 mM Na_3VO_4 2.5 mM Na-Pyrophosphate 1 mM β-Glycerophophate 1% Triton-X-100 complete protease inhibitor cocktail (one tablet/50 ml) pH 7.5
Lysis buffer	50 mM Tris-HCl 150 mM NaCl 1% Triton-X-100 complete protease inhibitor cocktail (one tablet/50 ml) pH 7.5
Nano-dilution buffer	20 mM Tris-HCL pH 7.5 150 mM NaCl 0.5 mM EDTA 2 mM PMSF
Nano-lysis buffer	20 mM Tris-HCL pH 7.5 150 mM NaCl 0.5 mM EDTA 2 mM PMSF 0.5 % NP40
PBS	137 mM NaCl 2.7 mM KCl 1.5 mM KH_2PO_4 8,1 mM Na_2HPO_4 pH 7.4
p-STAT3 lysis buffer	50 mM Tris-HCl 150 mM NaCl 2 mM EDTA 1 mM NaF 1 mM Na_3VO_4 1% Nonidet-P40 1% Triton-X-100 complete protease inhibitor cocktail (one tablet/50 ml) pH 7.5
S1-buffer	50 mM Tris-HCl

	10 mM EDTA 100 µg/ml RNase A pH 8.0
S2-buffer	200 mM NaOH 1% SDS
S3-buffer	2.8 mM Potassium Acetate pH 51
SDS-running buffer	25 mM Tris-HCl 192 mM Glycine 0.1% SDS pH 8.3
Separating buffer	1.5 M Tris-HCl 0.4% SDS pH 8.8
Stacking buffer	0.5 M Tris-HCl 0.4% SDS pH 6.8
Stripping buffer	62.5 mM Tris-HCl 2% SDS 0.1% β-Mercaptoethanol pH 6.8
TAE	40 mM Tris-HCl 0.1% Acetic acid 10 mM EDTA pH 8.0
TBS-T	TBS 0.05% Tween20
Transfer buffer	192 mM Glycine 25 mM Tris-HCl 20% CH_3OH, pH 8.5

2.1.10 Recombinant Cytokines and Inhibitors

Hyper-IL-6	From Prof. Dr. Rose-John Lab (Fischer et al.,1997; Schroers et al.,2005)
Interleukin-6 (IL-6)	ImmunoTools, Friesoythe
Interleukin-11 (IL-11)	ImmunoTools, Friesoythe

2.1.11 Common dishes and material

10 cm culture plate	TPP, Trasadingen, Switzerland
15 cm culture plate	TPP, Trasadingen, Switzerland
6 well plate	TPP, Trasadingen, Switzerland
12 well plate	TPP, Trasadingen, Switzerland
96 well plate	TPP, Trasadingen, Switzerland
Corning costar stripette	Sigma-Alderich, Steinheim
Syringe	B. Braun, Melsungen
Needle	B. Braun, Melsungen
Cryotube	VWR, Radnor, USA
MicroAmp, optical 96-well reaction plates	Life Technology, Darmstadt
MicroAmp, optical adhesive film	Life Technology, Darmstadt
PCR reaction tubes	Eppendorf, Hamburg
Petri dish	TPP, Trasadingen, Switzerland
PVDF-membrane	Carl Roth, Karlsruhe
1.5 ml; 2.0 ml Microtube	Eppendorf, Hamburg
15 ml; 50 ml Tube	Eppendorf, Hamburg
Transwell® cell culture insert	Corning, USA

2.1.12 Cell culture media and reagents

DMEM high Glucose (-/-)	Dulbecco's modified Eagel's Medium (DMEM), high Glucose (4.5 g/l), Life Technology, Darmstadt.
DMEM low Glucose (-/-)	Dulbecco's modified Eagel's Medium (DMEM), low Glucose (2.5 g/l), Life Technology, Darmstadt.
DMEM Low/high Glucose (+/+)	DMEM, with 10% Fetal Bovine Serum (FCS) and 1% Penicillin/Streptomycin
Fetal Calf Serum (FCS)	Life Technology, Darmstadt
Penicillin/Streptomycin	Life Technology, Darmstadt
TurboFect transfection reagent	Life Technology, Darmstadt
X-tremeGENE DNA transfection reagent	Roche, Switzerland

2.1.13 Cells

HEK293	Immortal human cell line, from embryonic kidney (ATCC-Number: CRL-1573).
HepG2	Liver epithelial cells, from Caucasian (ATCC-Number: HB-8065).
HeLa	Immortal human cell line, derived from cervical cancer (ATCC-Number: CCL-2).
COS7	Fibroblast like cell line, from kidney of monkey (ATCC-Number: CRL-1651).
MDCK	Madin-Darby Canine Kidney epithelial cells, from the kidney tissue of female cocker spaniel (ATCC-Number: CRL-2936).
Phoenix-Eco	Based on HEK293T cell line, second generation of retrovirus producer cell line, capable of producing gag-pol and envelope proteinfor ecotropic viruses (ATCC-Number: CRL-3214).
Ba/F3-gp130	Murine pro-B cells, they grow in the presence of IL-3 or HIL-6 and transduced with the cDNA of gp130 (Fischer et al., 1997).
Ba/F3-gp130-IL-6R	Ba/F3-gp130 stably transduced with IL-6R cDNA.

2.2 Methods

2.2.1 Molecular Methods

2.2.1.1 Plasmid-DNA extraction *via* Mini-prep

A plasmid extraction *via* Mini-prep is a small-scale isolation of plasmid DNA from bacteria. A single clone of bacteria was picked from a LB-agar plate and incubated in a 2 ml micro tube containing LB media in the presence of the specific antibiotic at 37°C with 1000 rpm shaking speed. After 14-16 h, the tube was centrifuged for 15 min at 18000 g and then the pelleted bacterial cells were resuspended in 100 µl S1 buffer. To lyse the cells, 200 µl of S2 buffer was added to the 2 ml microtube, inverted 5 times, and incubated for 5 min on ice. For neutralization, 150 µl S3-Neutral Buffer was added to the tube, inverted and incubated for

10 min on ice. After finishing the incubation time, the 2 ml micro tube was centrifuged for 10 min in 4°C centrifuge at 18000 g and the supernatant was transferred into a new 1.5 ml micro tube. The tube was incubated for 10 min in 96% cold ethanol and then centrifuged for 15 min in 4°C centrifuge at 18000 g. Afterwards, the supernatant was discarded and the pellet of DNA was washed with 70% ice-cold ethanol and centrifuged for 5 min at room temperature at 18000 g. In the last step, the pellet of DNA was dried at room temperature and dissolved in 30 µl dH_2O.

2.2.1.2 Plasmid–DNA extraction via Midi-prep

To extract higher amount of DNA, a single clone was picked from the LB-agar plate and incubated in 100 ml media in a 500 ml Erlenmeyer flask with the specific antibiotic at 37°C and 140 rpm. After 12-16 h, the bacteria were transferred into 50 ml falcon tubes and centrifuged for 15 min at 4°C. Afterwards plasmid DNA was prepared using the NucleoBond Xtra Midi/Maxi kits from Macherey-Nagel and according to the supplied protocol. The DNA was resuspended in 150 µl dH_2O.

2.2.1.3 RNA extraction

For the extraction of RNA at least $1x10^7$ cells were needed. Lysis of cells and RNA extraction was carried out using the Nucleospin RNAII kit from Macherey-Nagel, and all steps were performed according to the supplier's protocol. In the last step, RNA was resuspended in 30 µl RNase-free water and the concentration was assessed.

2.2.1.4 Measurement of RNA and DNA concentration

The concentration of RNA and DNA was measured by Nanodrop ND-2000. The ratio of 260 nm to 280 nm absorption showed the purity of the nucleic acid. For DNA it should be higher than 1.8 and for RNA higher than 2.0.

2.2.1.5 cDNA synthesis

For the synthesis of cDNA from extracted RNA, the following steps were done.

The RNA was incubated for 5 min at 65°C:

RNA	2 µg
Oligo-dT-primer	100 µM
ddH_2O	13 µl

After finishing the incubation time, following reagents were added to the tube:

RT Buffer (5X)	4 µl
dNTP-Mix (10 mM)	2 µl (= 1 mM)
Revert Aid Reverse Transcriptase	1 µl

and then incubated for 60 min at 42°C and for 10 min at 70°C

2.2.1.6 Polymerase chain reaction (PCR)

PCR was used to amplify the DNA. According to the size of the PCR product and types of mutations and deletions, the enzyme and the programmes were different.

Mutagenesis PCR

Reagents:

DNA	1 ng
Phusion	1 µl/2 kb
Phusion buffer 10X	5 µl
dNTP (25 mM)	0.4 µl
Forward primer (100 pmol)	0.5 µl
Reverse primer (100 pmol)	0.5 µl
DMSO	1.5 µl
H_2O	
Total volume	50 µl

PCR program:

98°C	4 min	
95°C	1 min	35 cycles
60°C	1 min	
72°C	3 min	
72°C	12 min	
4°C	10 min	

Colony PCR

Reagents:

DNA	Bacteria in 25 µl water
Master mixed was 25 µl which contained:	
Taq polymerase	0.2 µl/1 kb
Buffer 10X	5 µl
dNTP (25 mM)	0.4 µl
Forward primer (100 pmol)	0.1 µl
Reverse primer (100 pmol)	0.1 µl
H_2O	14.2 µl
Total volume	50 µl

PCR program:

99°C (for boiling of bacteria (25 µl))	10 min	
Addition of the master mix (25)		
95°C	1 min	
95°C	30 s	35 cycles
45°C	30 s	
72°C	40 s	
72°C	3 min	
4°C	10 min	

Amplifying PCR

Reagents:

DNA	50 pg-1 µg
Pfu	2 µl
Pfu buffer 10X with $MgSO_4$	5 µl
dNTP (25 mM)	0.4 µl
Forward primer (100 pmol)	0.1 µl

Reverse primer (100 pmol)	0.1 µl
H_2O	
Total volume	20 µl

Program:

95°C	3 min	
95°C	1 min	35 cycles
60°C	1 min	
72°C	3 min	
72°C	10 min	
4°C	10 min	

2.2.1.7 Quantitative real time-PCR (qPCR)

For qPCR, the Fast SYBER®Green Master Mix from Life Technology, Darmstadt was used. For each sample the mixture of the reagents was made according to the chart in below:

SYBER®Green Master Mix	12.5 µl
5'Primer (10 µM)	1 µl
3'Primer (10 µM)	1 µl
cDNA	Product of 50 ng RNA
ddH_2O	25 µl

Then the plate was placed in the qPCR machine, 7500 Real-Time-PCRSystem (Applied biosystem, Warrington, UK) and the following program was applied:

95°C	1 min	35 cycles
95°C	15 s	
60°C	1 min	

All the samples were loaded as triplicates and GAPDH was used as the internal control. The results were analysed via the comparative Ct-Method ($2^{-\Delta Ct}$).

2.2.1.8 DNA digestion

Digestion of plasmids and PCR-fragments with the help of specific restriction site via restriction enzymes was one of the key parts of all cloning procedures.

For preparing high amounts of DNA fragment for cloning, 10 µg DNA and 10 U Enzyme in a total volume of 50 µl was used. The mixture of DNA, enzyme(s), buffer, and water was incubated overnight at 37°C. Afterwards, the favourite fragment was separated by agarose gel electrophoresis and purified via gel extraction/PCR clean up kit from Macherey-Nagel, Düren with the supplied protocol of the kit.

For having the digestion as an analytic approach the lower concentration of DNA (0.5 µg) and Enzyme (1 U) in total volume of 20 µg was used.

2.2.1.9 Agarose gel electrophoresis

For separation of the favourite DNA fragment, the agarose electrophoresis (horizontal Electrophoresis System from Bio-Rad, München) was used. According to the expected DNA size, different concentrations of agarose were applied. The agarose was dissolved and boiled in TAE buffer and 0.01% ethidium bromide was added. DNA samples were mixed with 6x Orange DNA Loading Dye and loaded on the gel. In addition to the DNA samples, a suitable DNA Ladder (1 kb or 100 bp) was loaded on the gel. The gel electrophoresis was performed at 100 voltages and DNA fragments were visualized *via* the iX Imager from Intas, Göttingen.

2.2.1.10 DNA-fragment extraction from agarose gels

For extraction of the DNA fragment from an agarose gel, the gel was placed on the UV-table and the favourite fragment was cut out of the gel with a skalpell. Then the extracted DNA was purified *via* Gel extraction Kit from Macherey, Nagel, Düren. Finally the purified DNA-fragment was dissolved in 30 µl ddH_2O.

2.2.1.11 DNA Ligation

For ligation of DNA fragments into a vector, T4 DNA ligase from Thermo Scientific was used. DNA, 10x buffer, T4 and water were mixed in 20 µl total volume. In this reaction, the important point was the molar ratio of vector to insert of 5 to 1 (5:1). If the ends of the insert and vector were blunt, 2 µl of PEG 4000 was added to the reaction. In addition to the main reaction, always the empty vector was needed as a control reaction.

2.2.1.12 Transformation of DNA into *E.coli*

For transformation of DNA (plasmid or ligation product), chemical competent *Escherichia coli XL-1 blue* were used. 30 µl of the competent cells were thawn on ice for 5 min, then 100 ng DNA or the whole amount of ligation product (20 µl) was added to the test tube. A heat shock at 42°C for 45 seconds was applied for transformation of the DNA into the competent cells. Then the tube of competent cells was incubated for 5 min on ice and afterward 300 µl LB medium without any antibiotics was added to the test tube. The test tube was placed on the shaker with 100 rpm at 37°C for 1 h. For selection of clones the cells were plated on a LB agar plate containing the specific antibiotics and incubated overnight at 37°C.

2.2.1.13 DNA sequencing

DNA sequencing was performed by Seq Lab in Göttingen, Germany.

2.2.1.14 Flow cytometry analysis

For standard flow cytometry, $1x10^6$ cells were counted and washed once with PBS and 3 times at 4°C for 5 min with 500 µl FACS buffer (0.5% BSA-PBS). Next, the cells were incubated with the primary antibody for 60 min on ice. Afterwards, cells were washed 3 times with 500 µl FACS buffer and then incubated with the secondary antibody (APC-, FITC-conjugated) for 60 min on ice. In the last step, cells were washed 3 times with FACS buffer

and resuspended in 500 µl FACS buffer and cell surface expression of receptors was analyzed by BD FACSCanto^{TM} II machine.

For the receptor internalization assay, cells were pre-incubated with internalizing inhibitors such as Dynasore and Pitstop 2 for 30 min. Afterwards the cells were washed 3 times with FACS buffer and exposed to the primary antibody for 60 min on ice. Then, cells were washed 3 times with FACS buffer and incubated again for indicated time points. After finishing each incubation time, the cells were washed 3 times with FACS buffer and were exposed to secondary antibodies for 60 min on ice. The rest of the experiment was performed as described in the standard protocol.

2.2.1.15 Immunofluorescence staining and confocal microscopy

1.5x10^4 HELA cells were seeded on 15 mm cover slip in 12 well plates. Next day, cells were transiently transfected and incubated for 48 h in the incubator. After 48 h, cells were washed once with PBS and were fixed with 4% PFA for 20 min at room temperature. Afterwards, cells were permeabilized with 0.25 % Triton X-100 for 5 min. Next, cells were washed with PBS and were blocked for 1 h in PBS with 1% BSA and 0.25% Triton X-100. After washing the cells with PBS, cells were exposed overnight to the primary antibody at 4°C on the shaker. Then cells were washed 3 times with PBS and then exposed to secondary antibodies for 1 h at room temperature. In the last step, cells were washed 3 times with PBS and mounted with Prolong Gold Antifade reagent containing DAPI (Invitrogen, Karlsruhe, Germany) on the microscopy slide. Analyses were done with Leica TCS SP2/AOBS microscope equipped with a HCX PLAPO 63x immersion objective.

For internalization assays, the cells were not permeabilized. After exposing to the primary antibody, the cells were washed with PBS for 3 times and then incubated at 37°C for the indicated time points. After finishing the incubation, cells were fixed and blocked and exposed to the secondary antibody. The rest of the procedure was performed as described above.

For preparation of confocal slides for polarized cells, 8x10^3 MDCK cells were seeded on the transwell® cell culture insert (in 6 well plate) from Corning, USA. For polarization, the

cells were incubated for 5 days and subsequently stained with antibodies. The procedure of staining was exactly the same as described above. The transparent membrane was cut out from the plastic part of the culture insert and mounted with Prolong Gold Antifade reagent containing DAPI (Invitrogen, Karlsruhe, Germany) on the microscopy slide.

2.2.2 Protein Methods

2.2.2.1 Cell lysis

To lyse the cells, they were scratched from plates (6 well plates or 10 cm dishes), transferred to 1.5 ml test tubes, and centrifuged for 5 min at 4°C with 18000 rpm. Afterwards, cells were washed with 1 ml ice cold PBS and the supernatant was removed and the lysis buffer was added. For 10 cm dishes 250 µl and for 6-well plate and 6-well transwell insert 100 µl lysis buffer was used. The cells were resuspended in the lysis buffer and incubated for 1 h at 4°C on the tube roller. Afterwards, tubes were centrifuged for 20 min at 4°C and 18000 rpm. The supernatant was collected and stored at -20°C.

2.2.2.2 Protein concentration measurement with BCA assay

Protein concentration was measured by the BCA Protein Assay Kit from Thermo Fischer Scientific Company. Cellular lysate was diluted in water 1:10 and 25 µl of the diluted sample was loaded as duplicate. The A and B reagent in the kit was mixed 1:50 and 200 µl per well was applied. Then the plates were covered with the foil and incubated for 20 min at 37°C. After the incubation time, the plate was removed to the M200 PRO micro plate reader from Tecan and the absorption of samples was measured at 562 nm.

2.2.2.3 Immunoprecipitation (IP)

$1x10^7$ cells were scratched from plates and mixed with 250 µl IP lysis buffer and incubated for 1 h at 4°C on the roller. Then the test tube was centrifuged for 30 min at 13000 rpm at 4°C. Afterwards the supernatant was transferred to a new 1.5 ml test tube. 50 µl of the lysate was taken as an input control for Western blotting. Remaining lysate was divided into 2 test tubes. One was incubated overnight with primary antibody and the other without the primary antibody at 4°C on the roller. The agarose beads should be prepared for the second day; for each sample 25 µl of agarose A or G was washed 3 times with 500 µl IP washing buffer for 5 min at 800 g. The washed beads were incubated overnight in washing buffer at 4°C. On second day, beads were washed 2 times with washing buffer. For each sample the beads were resuspended in 50 µl washing buffer and were added to the tubes containing lysate with or without primary antibodies and incubated for 4 h at 4°C on the roller. After the incubation time, the tubes were centrifuged at 300 g for 5 min at 4°C. 50 µl of the supernatant was taken and stored as the non-bound fraction. The rest of the supernatant was discarded and the beads were washed for 5 times with 500 µl of washing buffer at 300 g, 4°C and for 5 min. The beads were resuspended in 50 µl Laemmli buffer. The lysate control and non-bound fraction were mixed with 15 µl of laemmli buffer, boiled and analysed by SDS-PAGE and Western blotting.

2.2.2.4 Nano-trap

$1x10^7$ cells were scratched from the plates and mixed with 200 µl Nano-trap lysis buffer to be lysed for 1 h at 4°C on the roller. Then, the test tube was centrifuged for 30 min at 20000 g and 4°C. Afterwards, the supernatant was carefully transfered to a new 1.5 ml tube. The total volume of the lysate was adjusted to 500 µl with dilution buffer. For Western blotting, 50 µl was taken and stored in -20°C.

The GFP-Nanobody protein binder coupled to NHS-Sepharose was washed 3 times with 500 µl ice cold dilution buffer at 2700 g for 2 min. The supernatant was discarded and the beads were resuspended in dilution buffer. For each sample, 15 µl of the beads were needed. Next, the lysate and beads were mixed and incubated on the roller for 2 h at room

temperature. After incubation, the tube was centrifuged for 3 min at 2700 g and 4°C. 50 µl of the supernatant was kept as non-bound fraction for Western blotting and the rest was discarded. Then, beads were washed 2 times with 500 µl dilution buffer at 4°C and 2700 g. In the last step, 15 µl of 5x Laemmli buffer was added to the lysate and supernatant and 30 µl of Laemmli buffer was added to the beads. All samples were boiled at 95°C for 10 min. The samples were analysed by SDS-PAGE and Western blotting.

2.2.2.5 SDS-PAGE and Western blotting

After calculating the concentration of the protein or preparation of the IP or Nano-trap samples, 5x Laemmli buffer was added to the 1.5 ml tubes which were containing the samples. Then, they were boiled at 95°C for 10 min and samples were analysed by horizontal polyacrylamide (SDS-Page) electrophoresis gel. In the first pocket of the SDS gel, the protein marker (PageRuler prestained protein ladder from Thermo Scientific, Waltham, USA) was loaded and then 50 µg of each sample was loaded on the gel. After loading of all samples, electrophoresis was performed at 80-100 voltage.

Next, the separated proteins were transferred from the SDS-gel on the PVDF-membrane by Western blotting. For transferring, the PVDF-membrane was activated *via* methanol for 1 min. Then, it was washed with water and finally exposed to the transfer buffer for 1 min. The filter papers were washed with transfer buffer and the gel was placed between the filter papers and exactly on the PVDF-membrane. The samples were transferred on the PVDF-membrane with 25 V, 1 Amp for 1 h. Afterwards, the membrane was incubated in 50 ml test tubes in blocking buffer (milk) for 1-3 h under constant rolling at room temperature. Then the membranes were washed with TBS-T and were exposed overnight to the primary antibody at 4°C. The day after, the primary antibody was removed and membranes were washed 5 times with TBS-T and were incubated with the secondary antibody for 1 h at room temperature. After the incubation time, the membranes were washed 5 times with TBS-T and were ready for developing. Therefore, the ECL Prime Western blotting detection reagent from GE Healthcare, München was applied and membranes were analysed with the ChemoCam imager from Intas, Göttingen.

In order to detect another protein on the same membrane, the membrane was incubated in stripping buffer for 20 min at 60°C. Finally, the membrane was washed with TBS-T and blocked with the blocking buffer (5% milk in TBS-T) for 1 h.

2.2.2.6 ELISA

R&D IL-11 ELISA kit and Novex IL-6 Elisa kit from Life technology were applied. The ELISA assays were done according to the manufactures protocol.

For quantification of human IL-6R, the ELISA plate was coated overnight with 4-11 antibody (1:1000 in PBS; 50 µl for each well). The plate was covered with aluminum foil and incubated at RT. The next day, the plate was washed 3 times with ELISA washing buffer and then coated with blocking buffer for 2 h. After 2 h, the plate was washed 3 times with washing buffer and 50 µl of the standard and samples were loaded (each sample and standards were loaded in duplicate). The plate was covered with aluminum foil and incubated for 2 h at RT. After incubation time, the plate was washed 3 times with washing buffer and then 50 µl of detection antibody (Baf227; 1:1000 PBS+1% BSA) was added to each well. The plate was incubated for 2 hours at RT. Afterwards, the plate was washed 3 times with washing buffer and then 100 µl Stretavidin-POD (1:200 PBS+1% BSA) was added to each well. The plate was incubated for 35-45 min at RT. In the last step, the plate was washed 3 times with washing buffer and the 75 µl POD-substrate was added to each well. The plate was incubated for 10-20 min at RT. Color development was stopped with 75 µl 1.8 H_2SO_4. The absorption of each sample was measured by Tecan infinite M200 PRO reader.

2.2.3 Cultivation and manipulation of mammalian cells

2.2.3.1 Cell culture

Cells were cultivated in DMEM high/ low Glucose (Life Technology, Darmstadt) with 10% Fetal Calf Serum (FCS) (Life Technology, Darmstadt) and 1% Penicillin/Streptomycin

(Life technology, Darmstadt) in 10 cm dishes. For sub-culturing of cells, in the case of non-adherent cells like Ba/F3-gp130 cells, 10 µl of the cells from a 70% confluent plate was transferred to the new plate containing media and supplementary cytokine. Regarding to sub-culturing of adherent cells, cells were washed with PBS and then each 10 cm dish of cells was incubated for 15 min with 3 ml Trypsin/EDTA (Life Technology, Darmstadt) at 37°C. Afterwards, 10 ml of DMEM high glucose (+/+) was added to the plates and then the mixture of detached cells was collected in a 15 ml tube and centrifuged for 5 min at 1200 g and room temperature. The cells were suspended in 1 ml DMEM high glucose (+/+) and sub-cultured in a new 10 cm dish containing DMEM high glucose (+/+). According to the cell type, the number of sub-cultured cells was different. For example, HEK293 cells were splitted 1:5, HepG2 1:3, Cos7 1:5, and MDCK 1:5.

2.2.3.2 Polarization of cells

To polarize MDCK cells, the transwell insert (filter) for a 6-well plate was applied. Sub-culturing of MDCK cells was exactly the same as for other detached cell lines. Polarization was completed after 4-5 days. $8x10^3$ cells were used for immunofluorescence staining and $1x10^4$ cells were used for cytokine stimulation assay. After seeding of the cells, they were incubated at 37°C for 5 days and media was changed after 3 days.

2.2.3.3 Preparing cryotube for cell freezing

For having a backup from each cell type, cells were frozen in special media at liquid nitrogen. To prepare cells for freezing, a 80% confluent 10 cm dish of attached cells was incubated with Trypsin/EDTA and cells were centrifuge at 1200 g for 5 min. The supernatant was completely removed and the cells were suspended in DMEM with 50% FCS and 10% DMSO. The cell suspension was transferred to a cryotube from VWR, Randor, USA and the cryotube was placed in the freezing container Mr.Frosty from Thermo Scientific, Waltham, USA and finally it was transferred to -80 and subsequently to liquid nitrogen.

2.2.3.4 Transient transfection

TurboFect Transfection Reagent from Thermo Scientific, Waltham, USA was applied for transient transfection. The day before transfection, cells were seeded in 10 cm dishes and the number of seeded cells was different according to the cell types, $2x10^6$ HEK293, $5x10^5$ Cos7, $6x10^5$ HepG2 and $2x10^6$ MDCK cells. On the next day, 1 ml DMEM high glucose (-/-) with 5 µg DNA and 10 µl TurboFect was mixed in 1.5 ml test tube and incubated for 15 min at room temperature. In the case of HepG2 cells, before adding the transfection mixture, the media was changed and just 4 ml media was placed in the dish but for the other types of cells this step was not needed. After the incubation time, the transfection reagent was added drop by drop to the cells. After 4-6 h at 37°C, the media of HepG2 and cos7 cells were changed. After 48 h the expression of the transferred gene was at the highest amount and the cells were ready for manipulation analysis.

2.2.3.5 Retroviral transduction for Ba/f3 cells

The retroviral transduction was used for transferring the genes to Ba/F3-gp130 cells. The plasmid was pMOWS as a retroviral vector.

The day before starting the procedure, $8x10^5$ Phoenix-eco cells were seeded in 6 well plates. The day after, Phoenix-eco cells were transfected *via* the mixture of 1 µg DNA, 2 µl TurboFect, and 200 µl DMEM (-/-). 4-6 h after transfection, the media of the Phoenix-eco cells were changed with 30% FCS DMEM containing 1% Penstrep. The next day, Ba/F3-gp130 cells were washed 2 times with PBS and $2x10^5$ cells were resuspended in 50 µl media. The cell volume was added to 200 µl of the conditional media, virus containing Phoenix-eco cells. 3 µl Polybrene was added to the mixture of the cells and viruses and then placed in the centrifuge with 1800 rpm at room temperature for 2 h. After finishing the incubation time, the supernatant was removed from the cells. The cells were transferred to the 6 well plate containing 5 ml DMEM high glucose (+/+) with cytokine. After 48 h the specific antibiotics (Puromycin or Hydromycin) were added to the media. Again after another 48 h, 500 µl of the cell suspension was transferred to a new 10 cm dish supplemented with fresh media, antibiotics, and cytokine.

2.2.3.6 Stable transfection of MDCK cells

For generation of stable MDCK cells, the cells were transfected as described in section 2.2.3.3. 48 h after transfection the cellular media was renewed and supplemented with the specific antibiotic (Puromycin or Geneticin). After 2-7 days surviving cells were grown to small colonies. The colonies were picked out and transferred to a 6-well plate. The expression of the gene of interest was examined *via* Western blotting or confocal microscopy.

2.2.3.7 Cytokine stimulation

For stimulation of HEK293 ($1x10^6$) and HepG2 ($5x10^5$) cells, the cells were grown on 6-well plates for 1 day. In the case of polarized MDCK cells, $1x10^4$ cells were grown on 6-well transwell inserts for 5 days. On the day of stimulation, cells were starved for 2 h in DMEM high glucose (-/-) and afterwards stimulated with 10 ng/ml recombinant IL-6 and 20 ng/ml recombinant IL-11 for 30 min. In the next step, cells were lysed for protein analysis.

2.2.3.8 Cell synchronization (Double Thymidine Block) of HEK-293 cells

For this assay, eight 10 cm plates containing $2x10^6$ HEK293 were needed. On the second day cells were transfected with IL-6R and MAD2B. In the morning, the media was changed and Thymidine with the concentration of 2 mM was applied. On the third day in the morning, cells were washed with PBS and fresh media was added to the plates. In the late afternoon, 2 mM Thymidin was added to the media for the second time. On the fourth day in the morning, cells were washed with PBS and fresh media was added to the cells, resulted in cell cycle release and were collected after 0, 2, 4, 6, 8, 10, and 12 h. At each time point, cells were collected and washed with PBS. The supernatant was removed and cells were suspended in 5 ml PBS. 500 µl of the suspension was taken and and transferred to a 1.5 ml tubes. Then the tube was centrifuged for 5 min with 1200 g at 4°C. In the last step, the supernatant were removed and cells were stained with 300 µl Nicoletti for 1 h on ice. Then cells were analyzed by flow cytometry.

2.2.3.9 Transcytosis assay

For polarization, $1x10^4$ MDCK cells were cultured on transwell inserts and incubated for 4 days. In the case of examination of IL-11 transcytosis, non-transfected MDCK cells as the Mock group, MDCK-IL-11R, MDCK-IL-11RΔICD and for testing the transcytosis of IL-6 non-transfected MDCK cells as Mock group, MDCK-IL-6R, MDCK-IL-6RΔICD, and MDCK-IL-$6R_{ECD}$/IL-11_{ICD} were seeded. On the fourth day, the cells were washed once with PBS and starved for 2 h at 37°C and then 50 ng/ml recombinant IL-6 or IL-11 (from ImmunoTools, Friesoythe) was added to the basolateral media. After 0, 1, and 24 h the media from basolateral and apical site was collected and cells were lysed. The concentration of IL-6 and IL-11 was quantified by ELISA.

3 Results

3.1 Transcytosis of Interleukin (IL-)11 and apical redirection of gp130 is mediated by the IL-11 α-receptor

3.1.1 IL-11R1 is sorted to apical and basolateral membranes of polarized MDCK cells

IL-6R and IL-11R1 are expressed in polarized cells such as hepatocytes and intestinal epithelial cells (Castell *et al.*, 1988; Molmenti *et al.*, 1993). It has been reported that IL-6R is sorted basolaterally in polarized MDCK cells. There are two discontinuous motifs which are responsible for the basolateral localization of IL-6R in polarized cells; the first motif is a membrane-proximal tyrosine-based motif (YSLG) and the second one is a more membrane-distal di-leucin-type motif (LI) (Martens *et al.*, 2000). To date, there is no information regarding to the sorting pattern of IL-11R1 in polarized cells, therefore we transfected MDCK cells stably with IL-6R and IL-11R1 cDNAs to compare their localization in polarized cells. MDCK cells were used as model for polarization (Balcarova-Ständer *et al.*, 1984). For examination of IL-6R and IL-11R1 sorting under polarized conditions, cells were cultured for 5 days in transwell inserts. After 5 days, they were fixed and immunofluorescence staining was performed. The nucleus of cells was stained by DAPI. DAPI (4',6-diamidino-2-phenylindole) is a fluorescent stain that binds strongly to A-T rich DNA regions. It is used extensively in fluorescence microscopy. As DAPI can pass through an intact cell membrane, it can be used to stain both live and fixed cells (Tarnowski *et al.*, 1991). Ezrin was applied as

an apical marker which is a membrane-organizing phosphoprotein that tethers actin microfilaments to cell membrane proteins and controls the localization and/or function of certain apical membrane proteins (Saotome *et al.*, 2004). Figure 3.1.1 A is a schematic illustration of polarized epithelial cells. The apical side is separated from the lateral and basal side by tight junctions, which form a strict barrier. Actin filaments and microtubules which build up the cytoskeleton of epithelial cells were shown in blue and green, respectively. Microvillis are microscopic cellular membrane protrusions that increase the surface area of cells and minimize any increase in volume. Microvillis are located in the apical surface of polarized cells and exposes to external and luminal environments which performs the role of protective barriers, and control the uptake of nutrients and ions. The xy axis shows the basolateral surface, whereas the xz axis shows the apical surface. Using confocal microscopy basolateral and apical surface can be separately visualized as shown in figure 3.1.1 B, C, D, E. The xy-axis showed the top view and did differentiate between basolateral and apical expression. By using the right layer in xz-axis, apical and basolateral surfaces were visualized (smaller pictures). Here, detected proteins on x-axis are basolaterally expressed and on the z-axis are apically expressed. In figure 3.1.1 B, IL-6R was co-stained with DAPI. IL-6R was mainly found on the x-axis, suggesting a predominantly basolateral expression and no apical expression and this was supported by the lack of co-localization of IL-6R with Ezrin in figure 3.1.1 C In figure 3.1.1 D, IL-11R1 was co-stained with DAPI and the result revealed a basolateral and apical localization. Co-localization of IL-11R1 with Ezrin in figure 3.1.1 E supported the apically expression of IL-11R1. Our data showed that IL-6R was basolateral sorted as it was reported before (Martens *et al.*, 2000), however IL-11R1 localization was not restricted to the basolateral membrane but also found on the apical side.

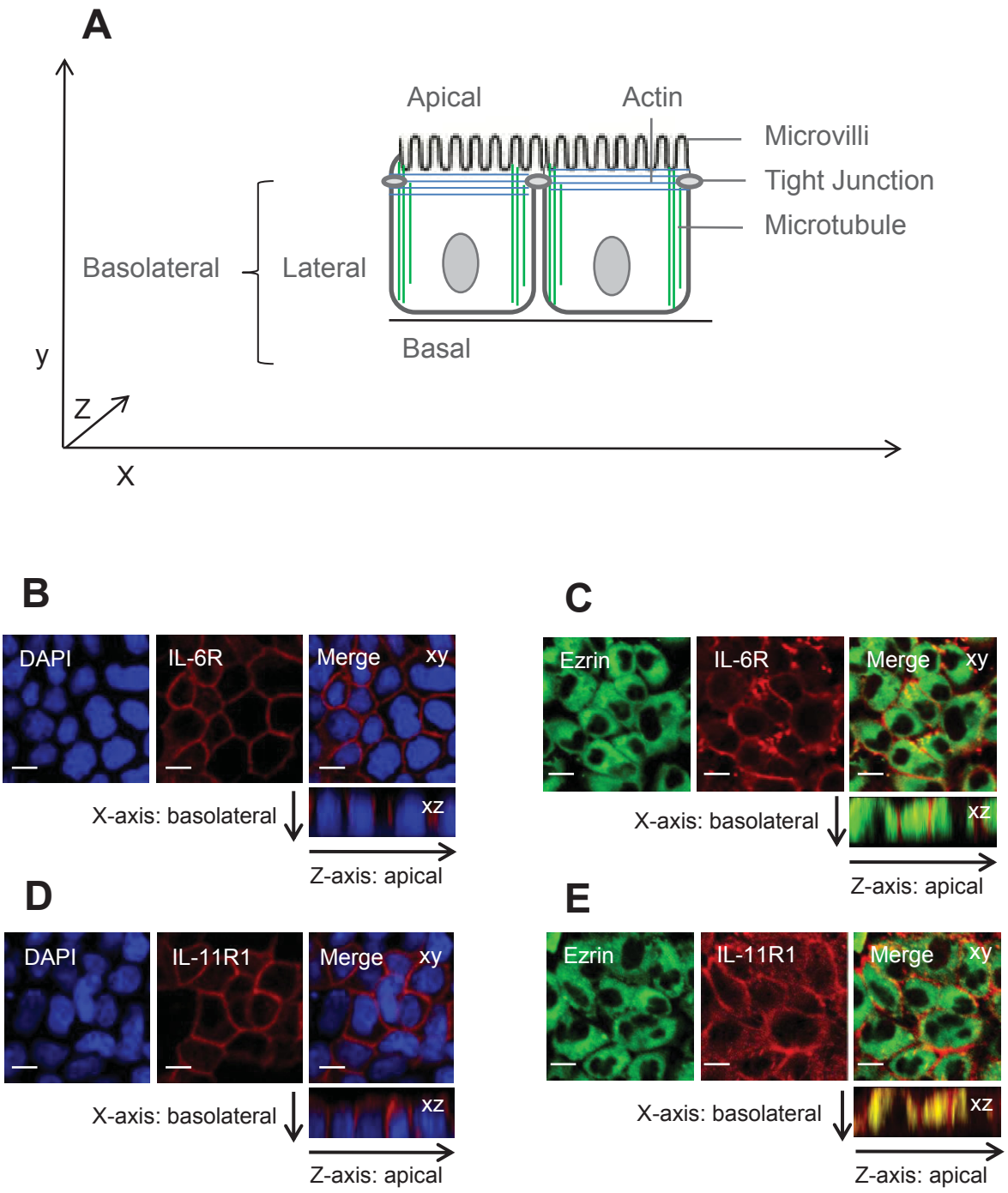

Figure 3.1.1: IL-6R is expressed on the basolateral membrane whereas IL-11R1 is sorted to the apical and basolateral membranes. A. Schematic illustration of polarized epithelial cells in which apical and basolateral surfaces are separated by tight junctions. xy-axis shows the basolateral surface and xz-axis shows the apical surface. B. and D. show the expression of IL-6R on the basolateral surface and IL-11R1 on apical and basolateral side. Blue shows DAPI staining of nucleus and red is IL-6R (4-11 mAb) and IL-11R (4D12 mAb from Santa Cruz). C. and E. show co-localization of IL-6R and IL-11R1 with Ezrin (from Sigma) as a marker of apical

membranes. IL-6R and IL-11R are shown in red and Ezrin as an apical marker is in green. Images were taken with confocal microscopy and analysed *via* LSM Image Browser. Scale bars are 10 μm. All experiments were done 3 times.

3.1.2 IL-6 and IL-11 stimulation do not change the sorting pattern of IL-6R and IL-11R1 in polarized MDCK cells

There are some reports which declare that the presence of ligand leads to the re-sorting of receptors on the apical and basolateral sides. A well-known example is the polymeric immunoglobulin receptor (pIgR). plgR biosynthetically delivers to the basolateral surface, while in the presence of pIg, pIgR are transferred to the apical surface (Luton *et al.*, 2009). In order to consider if the presence of the ligand has any effect on the localization of IL-6R and IL-11R1, polarized IL-6R- and IL-11R1-expressing MDCK cells were starved for 2 h and then stimulated for 30 min with recombinant IL-6 (10 ng/ml) and IL-11 (20 ng/ml), respectively. After 30 min, the cells were washed with PBS and fixed with 4% PFA. Receptors were stained according to the immunocytochemistry protocol and the photos were made by confocal microscopy. Staining of basolateraly sorted Na^+-K^+ ATPase was done to determine the basolateral borders (Shoshani *et al.*, 2005). It was observed that after cytokine stimulation, localization of IL-6R was still restricted to the basolateral surface of the polarized MDCK-IL-6R cells because it co-localized with Na^+-K^+ ATPase (Fig 3.1.2 A). IL-11R1 was still sorted to the apical and basolateral sides of polarized MDCK-IL-11R1 cells because some IL-11R1 did not co-localized with Na^+-K^+ ATPase (Fig 3.1.2 B). The results showed that the sorting of IL-6R and IL-11R1 is independent on the presence of cytokines (Fig 3.1.2).

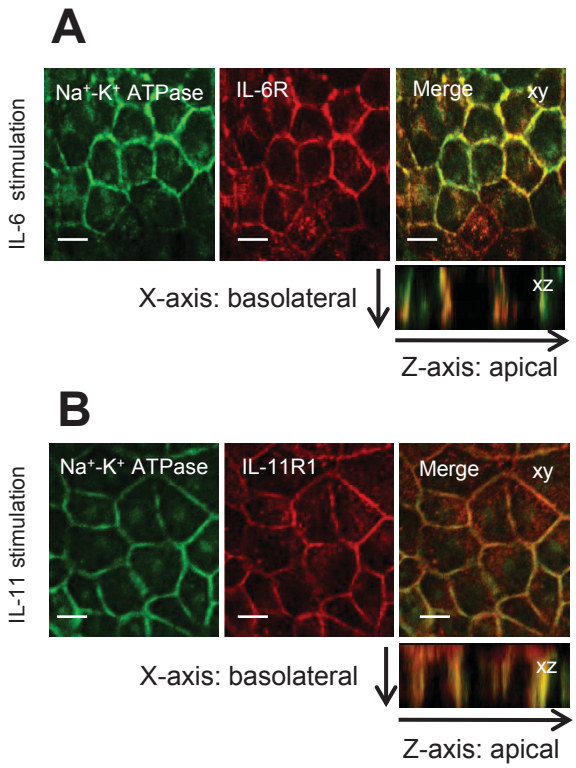

Figure 3.1.2: Sorting of IL-6R and IL-11R1 on polarized MDCK cells is independent of IL-6/IL-11 stimulation. Polarized MDCK-IL-6R and MDCK-IL-11R1 cells were starved for 2 h before stimulation and then stimulated with 10 ng/ml and 20 ng/ml recombinant IL-6 and IL-11, respectively, for 30 min. Afterwards, cells were fixed and stained. IL-6R was stained by 4-11 mAb and IL-11R1 by 4D12 mAb from Santa Cruz. Images were taken with confocal microscopy and analysed *via* LSM Image Browser. Scale bars show 10 µm. This experiment was done 3 times.

3.1.3 Apical and basolateral stimulation of polarized MDCK-IL-11R1 with recombinant IL-11 induced phosphorylation of STAT3

In order to confirm the apical and basolateral sorting of IL-11R1, $1x10^4$ MDCK-IL-6R and MDCK-IL-11R1 cells were seeded on transwell inserts in 6-well plates. After 5 days, cells were starved for 2 h and then MDCK-IL-6R and MDCK-IL-11R1 cells were stimulated with decreasing concentrations of recombinant IL-6 from 100 to 5 ng/ml and IL-11 from 100 to 8 ng/ml for 30 min from the apical and basolateral side. Afterwards, cells were lysed and

Western blotting for STAT3 and pSTAT3 was performed. Stimulation with IL-6 and IL-11 results in the activation of STAT3 which gets phosphorylated and translocated to the nucleus (Scheller and Rose-John, 2006). The results of Western blotting showed that stimulation of MDCK-IL-6R cells from the basolateral side led to the phosphorylation of STAT3 in a concentration dependent manner, while there was no STAT3 phosphorylation after apical stimulation. Non-polarized MDCK-IL-6R cells served as the stimulation control (Fig 3.1.3.A) and STAT3 served as loading control. The Western blotting result supported that IL-6R was localized on the basolateral side of polarized cells (Martens *et al.*, 2000). However, the Western blotting results of polarized MDCK-IL-11R1 cells showed the phosphorylation of STAT3 after stimulation with IL-11 from basolateral and apical side. Non-polarized MDCK-IL-11R1 cells served as stimulation control (Fig 3.1.3.B) and STAT3 served as loading control. It confirms that IL-11R1 was localized on the apical and basolateral side of polarized cells.

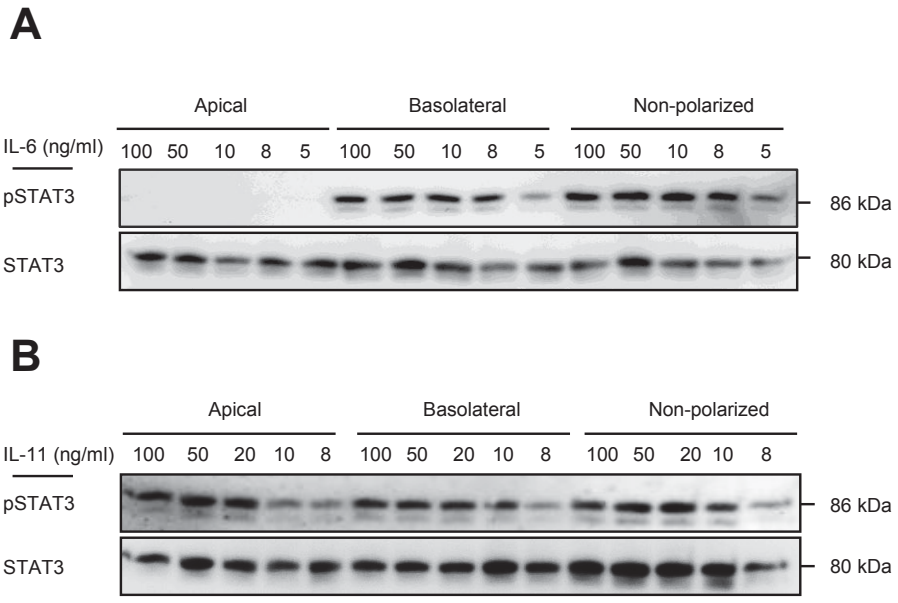

Figure 3.1.3: STAT3 phosphorylation in polarized cells. A. Polarized MDCK-IL-6R cells were stimulated with 100-5 ng/ml recombinant IL-6 from apical or basolateral side for 30 min. Non-polarized cells were stimulated as control. STAT3 served as loading control. B. Polarized MDCK-IL-11R1 cells were stimulated with 100-8 ng/ml recombinant IL-11 from apical or basolateral side for 30 min. STAT3 phosphorylation was detected after the stimulation from both sides. STAT3 served as loading control. 124H6 and D3A7 antibodies from Cell Signaling Biotechnology were used for pSTAT3 and STAT3, respectively. This experiment was done 3 times.

3.1.4 The cell surface half-life of IL-6R and IL-11R is comparable

The half-life of IL-6R was determined to be about 2.5 h in stably transfected MDCK cells and was independent on the presence of IL-6 (Gerhartz *et al.*, 1994). To date, there is no record about the half-life of IL-11R1. Therefore, in this study, the half-life of IL-6R and IL-11R1 was measured in Ba/F3-gp130-IL-6R and Ba/F3-gp130-IL-11R1 *via* internalization assay. Ba/F3 cells were chosen for this experiment because they are non-adherent cells and can be easily handled for internalization assays with low rate of cell death. MDCK cells are adherent cells which show high rate of cell death during the internalization assay as a result of several washing and incubation steps. Figure 3.1.4.A shows the decrease of cell surface IL-6R and IL-11R1 in 60 min intervals over a time period of 360 min. Ba/F3-gp130 cells served as negative control (NC) and were shown in black. Three independent internalization experiments were quantified and summarized in Figure 3.1.4.B. Cell surface half-life was calculated for IL-6R to be about 120 min and for IL-11R1 to be about 110 min.

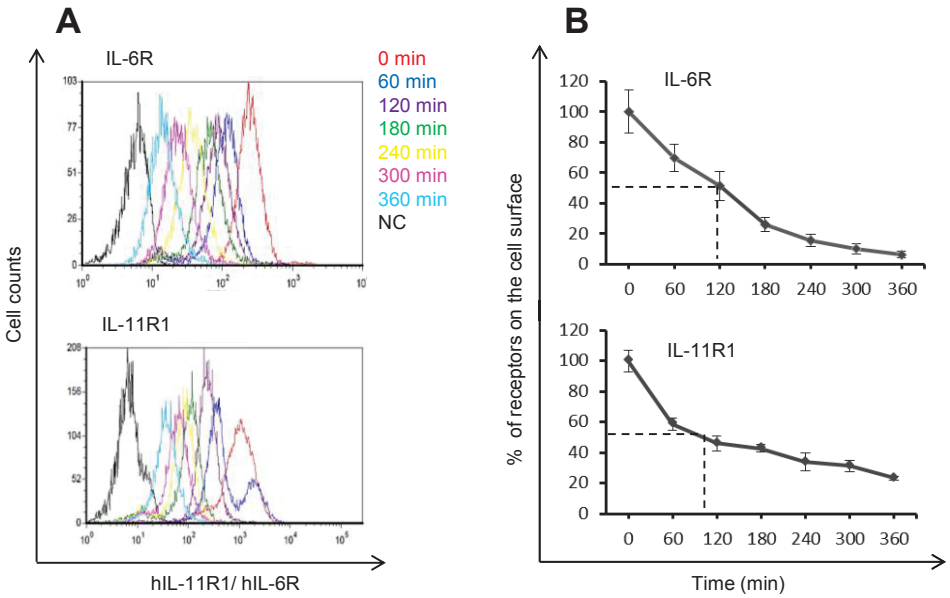

Figure 3.1.4: The half-life of IL-6R and IL-11R1 on the cell surface of Ba/f3-gp130-IL-6R and Ba/f3-gp130-IL-6R cells. Cells were washed with FACS buffer and incubated for 1 h on ice with primary antibody (for IL-6R 4-11 and for IL-11R myc 7D10 mAbs were used). The cells were washed and incubated for the indicated time points at 37°C. Then, the cells were incubated with secondary antibodies for 1 h on ice. The presence of the receptors was quantified by flow cytometry. A. Shows the internalization of IL-6R and IL-11R1

as measured by flow cytometry and analysed by FCS Express 4 Flow program. Ba/F3-gp130 served as a negative control and black. B. Shows the numerical calculation of IL-6R and IL-11R1 internalization and half-life via Microsoft Excel. This experiment was done 3 times.

3.1.5 Internalization of IL-6R and IL-11R1 is clathrin-dependent

Endocytosis pathways are used for internalization, signal transduction regulation, and modulation of plasma membrane composition. There are different internalization pathways. Well-studied endocytosis pathways are clathrin-dependent endocytosis (CDE) and clathrin-independent endocytosis (CIE) (Miaczynska and Stenmark, 2008). Clathrin-independent pathway is generally dependent on cholesterol-rich membrane domains (Sandvig *et al.*, 2011). Recently, it was reported that IL-6R internalization was dependent on clathrin (Fujimoto *et al.*, 2015), whereas the internalization pathway of IL-11R1 was unknown. In order to examine the IL-11R1 internalization pathway, inhibitors for CDE and CIE were applied in the internalization assay. Again, Ba/F3-gp130-IL-6R and Ba/F3-gp130-IL-11R1 cells were used. Before the start of the assay, cells were pre-incubated for 30 min with the specific inhibitors, Pitstop 2 (30 µM, from abcam) which was used as a clathrin-independent inhibitor (Dutta *et al.*, 2012) and Dynasore (100 µM, from abcam) which was used as an inhibitor of clathrin-dependent pathway (Macia *et al.*, 2006). The results revealed that in the absence of the inhibitors, about 90% of IL-6R and IL-11R were internalized within 360 min. However, in the presence of Dynasore but not Pitstop 2, internalization of receptors was drastically decreased. As shown in figure 3.1.5.1.1 A and B, preincubation of Ba/F3-gp130-IL-6R cells with Dynasore extended the cell surface half-life of IL-6R from 120 min to 340 min, whereas Pitstop 2 had no influence on the cell surface half-life of IL-6R. Interestingly, as shown in figure 3.1.5.1.2 A and B, preincubation of Ba/F3-gp130-IL-11R1 cells with Dynasore also extended the cell surface half-life of IL-11R1 from 110 min to 320 min, while Pitstop 2 application extended the cell surface half-life from 110 to 140 min. Ba/F3-gp130 served as negative control (NC) and was shown in black. These results indicated that internalization of IL-6R and IL-11R1 is mediated by clathrin-dependent endocytosis.

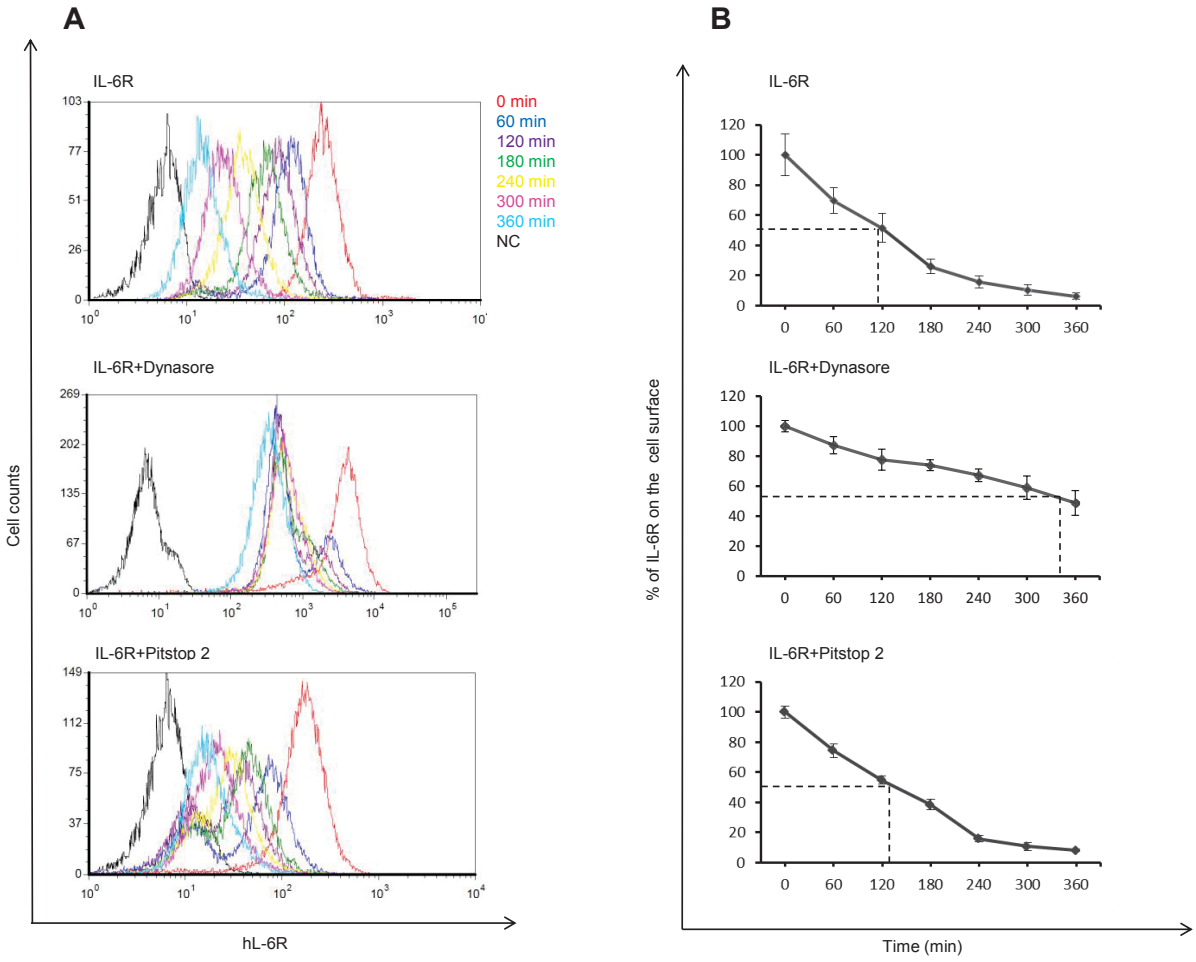

Figure 3.1.5.1.1: Internalization of IL-6R is dependent on clathrin-dependent endocytosis. A. shows the rate of internalization in the presence of Dynasore (clathrin-dependent endocytosis inhibitor) and Pitstop 2 (clathrin-independent endocytosis inhibitor). Ba/F3-gp130 served as negative control (NC) and was shown in black. Data were analysed *via* FCS express 4 Flow software. B. is quantitative data for the indicated time points. These experiments were done 2 times.

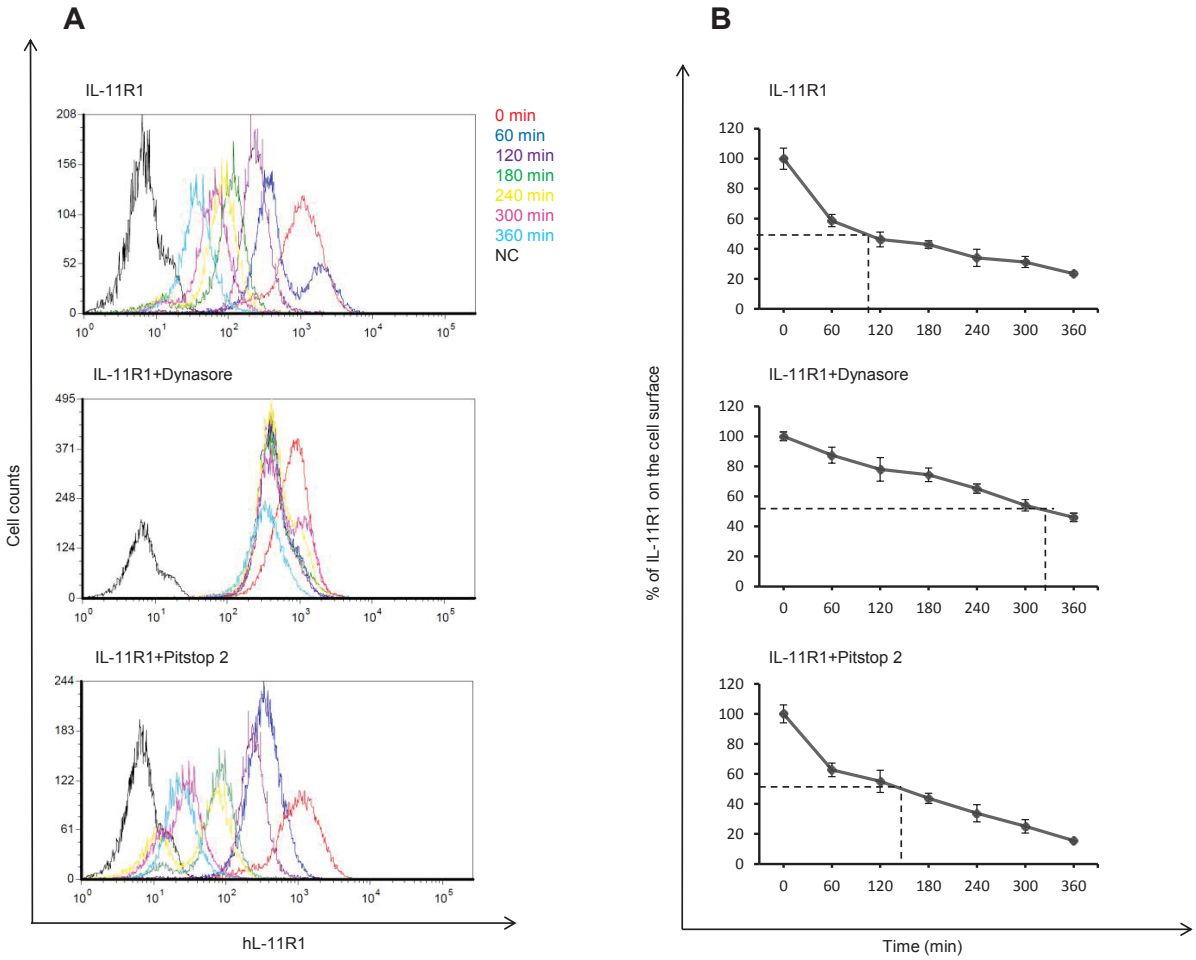

Figure 3.1.5.1.2: Internalization of IL-11R1 is dependent on clathrin-dependent endocytosis. A. shows the rate of internalization in the presence of Dynasore (clathrin-dependent endocytosis inhibitor) and Pitstop 2 (clathrin-independent endocytosis inhibitor). Ba/F3-gp130 served as negative control (NC) and was shown in black. Data were analysed *via* FCS express 4 Flow software. B. is quantitative data for the indicated time points. These experiments were done 2 times.

To confirm the result of the internalization assay, immunocytochemistry with HeLa cells was performed. HeLa cells were transiently transfected with cDNA coding for IL-6R and IL-11R1. Confocal images showed that in the absence of the inhibitors, almost all of the IL-6R and IL-11R were internalized within 360 min. However, in the presence of Dynasore but not Pitstop 2, internalization of receptors was inhibited. As shown in figure 3.1.5.2 A, preincubation of HeLa-IL-6R cells with Dynasore inhibited the internalization of IL-6R and

after 360 min, IL-6R was detactable in high number on the membrane, whereas Pitstop 2 had no influence on the internalization of IL-6R and all receptors were internalized after 360 min. Interestingly, as shown in figure 3.1.5.2 B, preincubation of HeLa-IL-11R1 cells with Dynasore inhibited the internalization of IL-11R1 and after 360 min, IL-11R1 was detectable in high number on the membrane, while Pitstop 2 did not influence the internalization of IL-11R1. These results indicated that internalization of IL-6R and IL-11R1 is mediated by clathrin-dependent endocytosis (Fig 3.1.5.1).

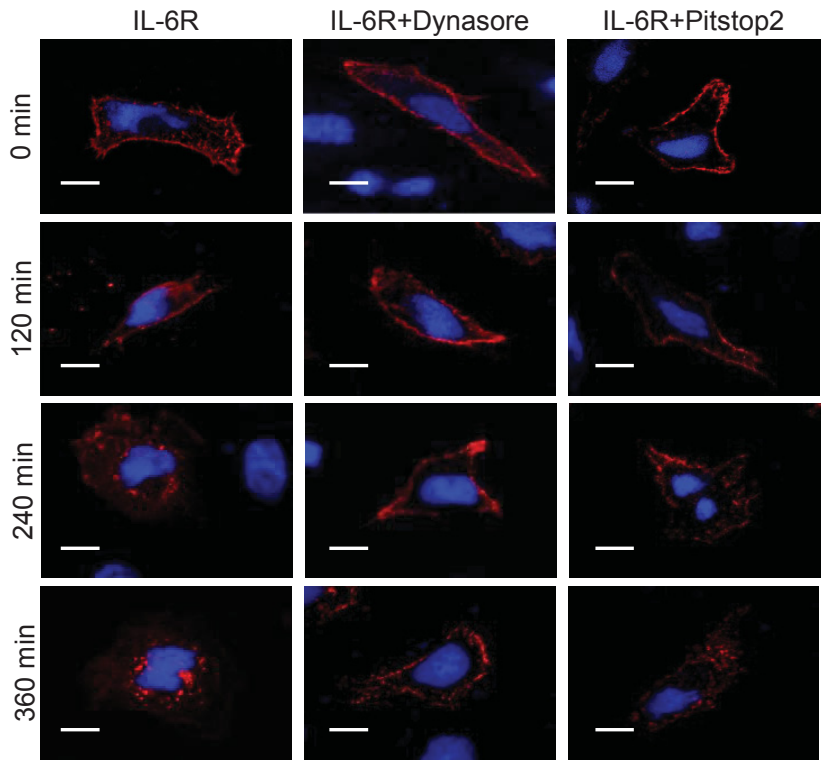

Figure 3.1.5.2.1: Dynasore inhibited the internalization of IL-6R. 1x10^4 HeLa cells were seeded on 15 mm coverslips in 12 well plates and transfected transiently with cDNAs coding for IL-6R. After 48 h, cells were pre-incubated with Dynasore, Pitstop 2 or DMSO for 30 min. At T0 cells were incubated with their specific antibodies (4-11 for IL-6R) on ice for 1 h and just the receptors were stained which were on the membrane. Then cells were washed and incubated at 37°C in the presence of inhibitors for the indicated time points. Thereafter, cells were washed, fixed, and exposed to the secondary antibody for 2 h at RT. Then, the cells were mounted on the microscopy slides by Prolong®Gold antifade reagent with DAPI. Images were taken with confocal microscopy and analysed *via* LSM Image Browser. Scale bars show 10 µm. This experiment was done 2 times.

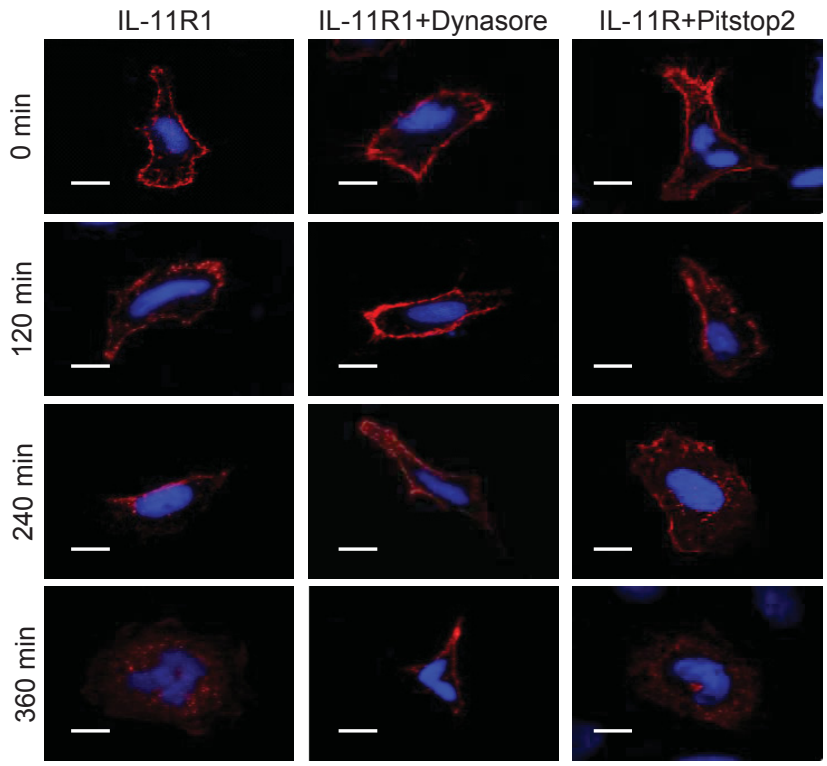

Figure 3.1.5.2.2: Dynasore inhibited the internalization of IL-11R1. $1x10^4$ HeLa cells were seeded on 15 mm coverslips in 12 well plates and transfected transiently with cDNAs coding for IL-11R1. After 48 h, cells were pre-incubated with Dynasore, Pitstop 2 or DMSO for 30 min. At T0 cells were incubated with their specific antibodies (N-20 from Santa Cruze) on ice for 1 h and just the receptors were stained which were on the membrane. Then cells were washed and incubated at 37°C in the presence of inhibitors for the indicated time points. Thereafter, cells were washed, fixed, and exposed to the secondary antibody for 2 h at RT. Then, the cells were mounted on the microscopy slides by Prolong®Gold antifade reagent with DAPI. Images were taken with confocal microscopy and analysed *via* LSM Image Browser. Scale bars show 10 µm. This experiment was done 2 times.

In order to examine the co-localization of IL-6R and IL-11R1 with clathrin, the co-localization of IL-6R and IL-11R1 with clathrin heavy chain was investigated. HeLa cells were applied and seeded on coverslips and transfected transiently with cDNAs coding for IL-6R and IL-11R1. After 48 h, cells were fixed and stained. IL-6R, IL-11R1, and endogenous clathrin heavy chain were stained and the localization was observed by confocal microscopy. The results demonstrated the co-localization of IL-6R and clathrin heavy chain as well as IL-

11R1 and clathrin heavy chain (Fig 3.1.5.3). The results proved that endocytosis of IL-6R and IL-11R1 was dependent on clathrin.

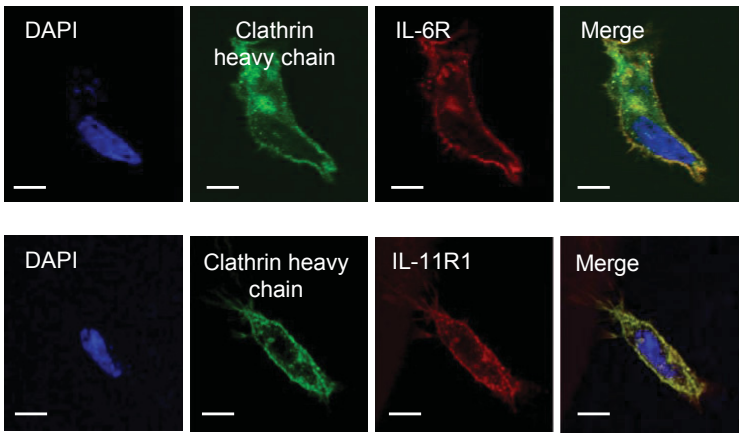

Figure 3.1.5.3: IL-6R and IL-11R1 are co-localized with clathrin heavy chain. $1x10^4$ HeLa cells were seeded on 15 mm coverslips in 12 well plates and transfected transiently with cDNAs coding for of IL-6R or IL-11R1. After 48 h, cells were fixed and stained according to the immunocytochemistry protocol. Blue is DAPI, green is clathrin heavy chain (4D12 Ab from Cell Signaling), red is IL-6R or IL-11R1 (4-11 for IL-6R and Santa Cruz 4D12 for IL-11R1), and yellow shows the co-localization. Images were taken by confocal microscopy and analysed *via* LSM Image Browser. Scale bars are 10 µm. This experiment was done 2 times.

3.1.6 Generation of IL-6R/IL-11R1 chimeras to determine the apical sorting motif within the IL-11R1

It was shown that IL-6R basolateral sorting motifs were located in the intracellular domain (Martens *et al.*, 2000). However, the domain which is responsible for the sorting of IL-11R1 was not investigated so far. Apical sorting signals could be localized in different regions of the apically sorted proteins such as extracellular, trans-membrane, and cytoplasmic domains (Weisz and Rodriguez-Boulan, 2009). IL-6R/IL-11R1 chimeras were used to determine which part of IL-11R1 contained the sorting motif. In IL-$6R_{cbECD}$/IL-$11R1_{S,TM,ICD}$ the cytokine

binding domain of IL-6R was transferred to IL-11R1 and in IL-$6R_{ECD}$/IL-$11R1_{ICD}$ the extracellular domain of IL-11R1 was replaced with IL-6R extracellular domain. In IL-$11R1_{cbECD}$/IL-$6R_{S,TM,ICD}$ the cytokine binding domain of IL-11R1 was transferred to IL-6R and in IL-$11R1_{ECD}$/IL-$6R_{ICD}$ the extracellular domain of IL-6R was replaced with IL-11R1 extracellular domain. These chimeras were designed and generated by Rebecca Nitz (Nitz *et al.*, 2015) (Fig 3.1.6 A). All chimeras were stably transfected into MDCK cells. The expression of receptors was shown by Western blotting (Fig 3.1.6 B). The glycosylation of IL-6R and IL-11R are not determined very well so far, therefore, we calculated the molecular weight of chimeras approximately without post-translational modifications. Calculated molecular weight of IL-6R was 49.8 kDa and of IL-$6R_{cbECD}$/IL-$11R1_{S,TM,ICD}$ and IL-$6R_{ECD}$/IL-$11R1_{ICD}$ were 43.68 and 46.91 kDa, respectively. IL-11R molecular weight is 43.1 kDa the calculated molecular weight for IL-$11R1_{cbECD}$/IL-$6R_{S,TM,ICD}$ and IL-$11R1_{ECD}$/IL-$6R_{ICD}$ were 46.13 and 44.52, respectively.

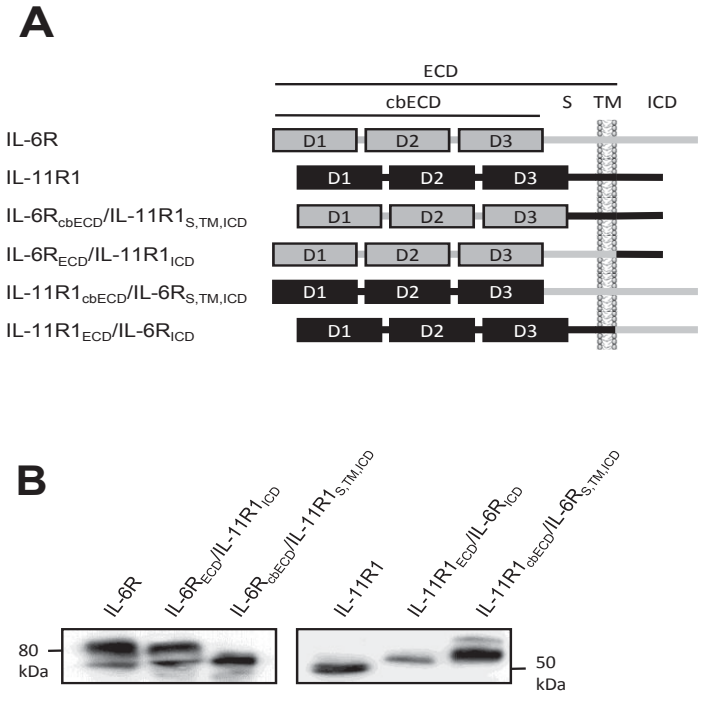

Figure 3.1.6: Expression of IL-6R/IL-11R1 chimeric proteins in MDCK cells. A. Schematic illustration of IL-6R/IL-11R1 chimeras. B. Expression of the IL-6R/IL-11R1 chimeras in stably transfected MDCK cells was examined by Western blotting. 4-11 and 7D10 myc mAbs were applied for IL-6R and IL-11R1, respectively.

cbECD: cytokine binding extracellular domain (D1-D3). ECD: extracellular domain. S: stalk. TM: trans membrane. ICD: intracellular domain. Calculated molecular weight of IL-6R was 49.8 kDa and of IL-$6R_{cbECD}$/IL-$11R1_{S,TM,ICD}$ and IL-$6R_{ECD}$/IL-$11R1_{ICD}$ were 43.68 and 46.91 kDa, respectively. IL-11R molecular weight is 43.1 kDa the calculated molecular weight for IL-$11R1_{cbECD}$/IL-$6R_{S,TM,ICD}$ and IL-$11R1_{ECD}$/IL-$6R_{ICD}$ were 46.13 and 44.52, respectively. Calculation of the receptors molecular weight (without post-translational modification) was done by sciencegateway.org online program.

3.1.7 Apical sorting signal is located in the intracellular domain of IL-11R1

Basolateral sorting signals are basically located in the intracellular domain of the proteins whereas the apical sorting signal could be localized in different regions of the apically sorted proteins such as extracellular, transmembrane, and cytoplasmic domains (Weisz and Rodriguez-Boulan, 2009). MDCK cells which were stably transfected with IL-6R/IL-11R1 chimeras, were polarized and stained for immunocytochemistry analysis. Again, Na^+-K^+ ATPase staining was done to determine the basolateral borders (Shoshani *et al.*, 2005). As shown in figure 3.1.7.1 A, IL-$6R_{cbECD}$/IL-$11R1_{S,TM,ICD}$ chimera which contained the extracellular domain of IL-6R but the stalk, transmembrane parts and intracellular domain of IL-11R1 was sorted apically and basolaterally and demonstrated the co-localization on basolateral surface with Na^+-K^+ ATPase. Figure 3.1.7.1 B showed IL-$6R_{ECD}$/IL-$11R1_{ICD}$ chimera which contained the extracellular domain, stalk, and transmembrane parts of IL-6R but the intracellular domain of IL-11R1 was sorted to apical and basolateral membranes and co-localized with Na^+-K^+ ATPase on basolateral surface. In figure 3.1.7.1 C, IL-$11R1_{cbECD}$/IL-$6R_{S,TM,ICD}$ chimera which contained the extracellular domain of IL-11R1 but the stalk, transmembrane part, and intracellular domain of IL-6R was localized on the basolateral surface of cells and showed the co-localization with Na^+-K^+ ATPase on the basolateral membrane. Figure 3.1.7. D showed the basolateral localization of IL-$11R1_{ECD}$/IL-$6R_{ICD}$ receptors which consisted of the extracellular domain of IL-11R but the stalk, transmembrane part, and intracellular domain of IL-6R. The results showed that the sorting signal of IL-11R1 was located on the intracellular domain of the receptor (Fig 3.1.7.1).

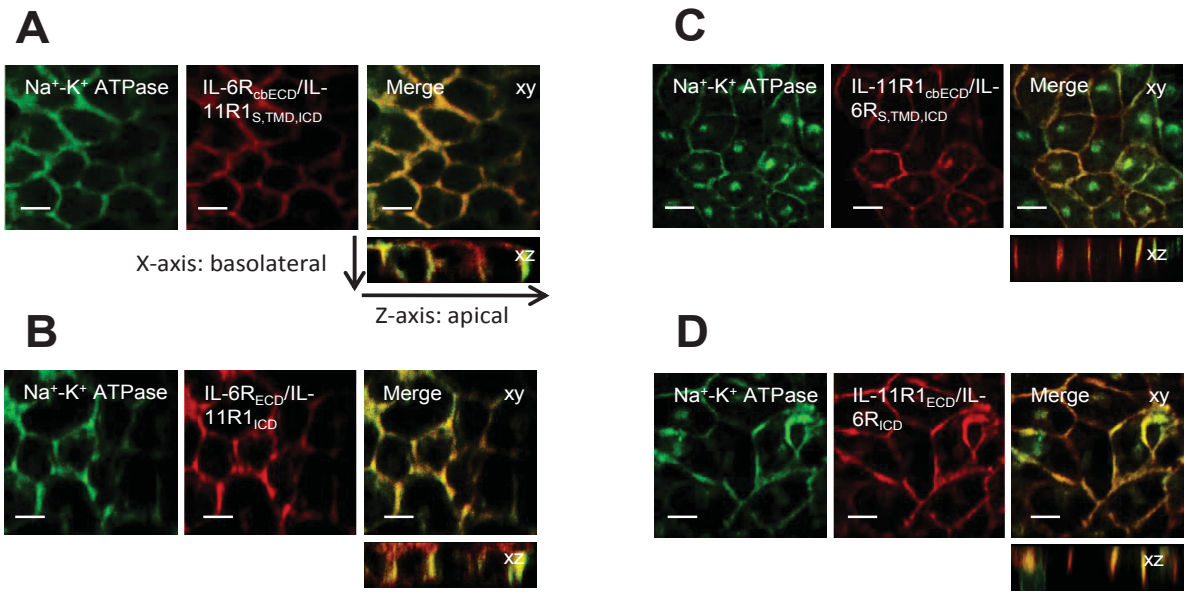

Figure 3.1.7.1: Apical sorting signal is located in the intracellular domain of the IL-11R1. Stably transfected MDCK cells were polarized on transwell inserts for 5 days and then fixed with 4% PFA. According to the chimera, cells were stained with IL-6R or IL-11R antibodies (4-11 for IL-6R and 4D12 Santa Cruz for IL-11R) and Na^+-K^+ ATPase (H-300 from Santa Cruz). A: Sorting of IL-$6R_{cbECD}$/IL-$11R1_{S,TM,ICD}$ chimera. B: Sorting of IL-$6R_{ECD}$/IL-$11R1_{ICD}$.chimera. C: Sorting of IL-$11R1_{cbECD}$/IL-$6R_{S,TM,ICD}$ chimera. D: Sorting of IL-$11R1_{ECD}$/IL-$6R_{ICD}$.chimera. Images were taken with confocal microscopy and analysed *via* LSM Image Browser. Scale bars show 10 µm. This experiment was done 3 times.

To prove that the sorting motif is located in the intracellular domain of IL-11R1, the isoform 2 of IL-11R (IL-11R2) was analysed. The IL-11R1 gene contains 13 exons and is located on chromosome 9q13. IL-11R2 results from differential splicing. The mRNA of IL-11R2 lacks exon 12, which codes for the 32 amino acids of the intracellular domain. Due to a frame-shift, IL-11R2 lacks all 32 amino acids of IL-11R1-intracellular domain and instead, consists of four alternative intracellular amino acid residues (LGLW) (Cherel *et al.*, 1995) (Fig 3.1.7.2 A&B). MDCK cells were stably transfected with a cDNA coding for IL-11R2. MDCK- IL-11R2 cells were polarized and localization of IL-11R2 was analysed. The co-localization of IL-11R2 with Na^+-K^+ ATPase (basolateral marker) on the basolateral membrane indicated that IL-11R2 sorting was limited to the basolateral surface (Fig 3.1.7.2

C). This result was supporting our finding that the apical sorting motif is located in the intracellular domain of IL-11R1.

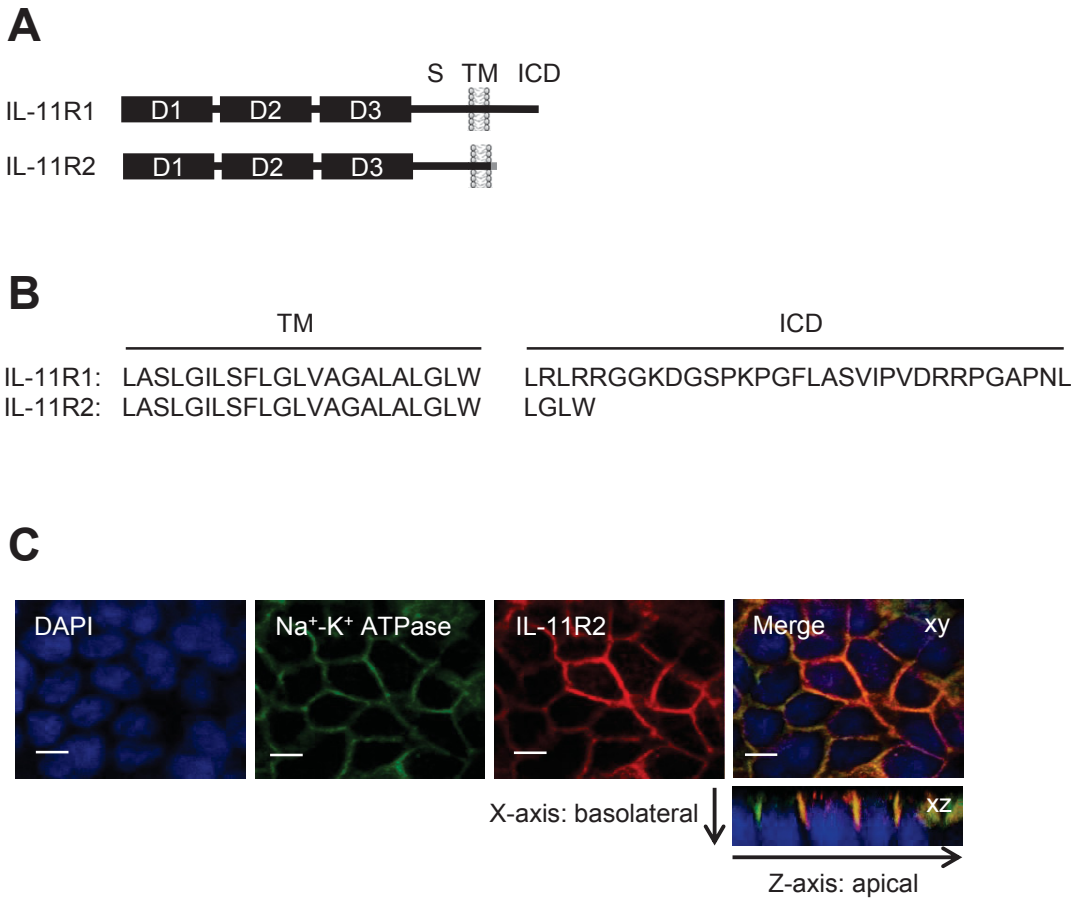

Figure 3.1.7.2: IL-11R2 is mainly localized on the basolateral surface of polarized cells. A. Schematic illustration of IL-11R2 in comparison to IL-11R1. A. Comparison of the overall composition of the transmembrane and intracellular amino acids sequence of human IL-11R1 and IL-11R2. B. Alignment of sequences of intracellular domain of IL-11R1 and IL-11R2. C. MDCK-IL-11R2 cells were seeded on transwell filters to be polarized. Cells were fixed, permeablized, and blocked. Afterwards, cells were incubated with primary antibodies (4D12 from Santa Cruz for IL-11R and H-300 from Santa Cruz for Na^+-K^+ ATPase) overnight at 4°C. Then, cells were washed 3 times and incubated with secondary antibodies for 2 h at RT. The cells were mounted on microscopy slides by Prolong®Gold antifade reagent with DAPI. Images were taken with confocal microscopy and analysed *via* LSM Image Browser. Scale bars are 10 µm. This experiment was done 2 times.

3.1.8 Apical sorting of IL-11R1 forced the typically basolateral-restricted gp130 to the apical membrane and enabled IL-11 classic signaling and IL-6 trans-signaling

The IL-6/IL-11 signal transducing chain, gp130 is ubiquitously expressed on all cells of the body. It was shown that the di-leucin motif (L^{786} L^{787}) in the cytoplasmic domain of gp130 was responsible for the internalization of the receptor (Dittrich *et al.*, 1996). Later, it was shown that the same motif is also responsible for basolateral sorting of gp130 in polarized MDCK cells (Doumanov *et al.*, 2006). Therefore, we decided to analyse gp130 on the apical and basolateral surface of polarized cells by the examination of STAT3 activation in stimulated polarized MDCK cells. Stably transfected MDCK cells were polarized and stimulated from apical and basolateral parts. MDCK-IL-6R, MDCK-IL-6R_{ECD} /IL-11$R1_{ICD,}$ and MDCK-IL-6R_{cbECD}/IL-11$R1_{S,TM,ICD}$ cells were stimulated with 10 ng/ml recombinant IL-6 for 30 min from apical and basolateral side. MDCK-IL-11R, MDCK-IL-11R_{ECD} /IL-6$R_{ICD,}$ and MDCK-IL-11R_{cbECD}/IL-6$R_{S,TM,ICD}$ cells were stimulated with 20 ng/ml IL-11 for 30 min from apical and basolateral side. To determine the presence and biological activity of receptors on apical and basolateral surface of cells, STAT3 phosphorylation was examined by Western blotting. As shown in Figure 3.1.8.1, stimulation of MDCK cells expressing IL-6R, IL-11R_{ECD}/IL-6R_{ICD},and IL-11R_{cbECD}/IL-6$R_{S,TM,ICD}$ resulted in phosphorylation of STAT3 from the basolateral but not the apical side, whereas STAT3 phosphorylation of MDCK cells expressing IL-11R, IL-6R_{ECD}/IL-11R_{ICD}, and IL-6R_{cbECD}/IL-11$R_{S,TM,ICD}$ was inducible from the both apical and basolateral sides. Non-polarized MDCK-IL-6R cells served as stimulation control. Our results suggested that since gp130 was previously found to be located on the basolateral membrane (Doumanov *et al.*, 2006), expression of IL-11R1 and chimeras containing the intracellular domain of IL-11R1 resulted in redirection of gp130 to the apical membrane (Fig 3.1.8.1).

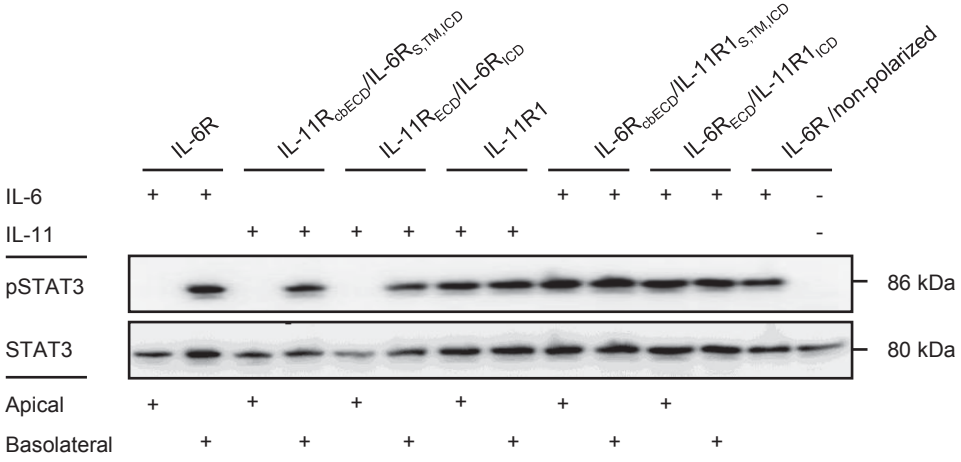

Figure 3.1.8.1: Intracellular domain of IL-11R1 redirected gp130 to the apical membrane. Stably transfected MDCK cells with IL-6R, IL-11R1 and IL-6R/IL-11R chimeras were polarized. MDCK-IL-6R, MDCK-IL-6R$_{cbECD}$/IL-11R1$_{ICD,}$ and MDCK-IL-6R$_{ECD}$/IL-11R1$_{S,TM,ICD}$ cells were stimulated with recombinant IL-6 (10 ng/ml) and MDCK-IL-11R1, MDCK-IL-11R$_{ECD}$/IL-6R$_{ICD}$ and MDCK-IL-11R$_{cbECD}$/IL-6R$_{S,TM,ICD}$ cells were stimulated with recombinant IL-11 (20 ng/ml) from the apical and basolateral side for 30 min. STAT3 phosphorylation was examined by Western blotting. STAT3 served as loading control. 124H6 and D3A7 antibodies from Cell Signaling Biotechnology were used for pSTAT3 and STAT3, respectively. This experiment was done 3 times.

In continue, MDCK-IL-11R1 and MDCK-IL-11R2 cells were stimulated with IL-11 (20 ng/ml) and MDCK-IL-6R and MDCK-IL-6RΔICD cells were stimulated with IL-6 (10 ng/ml) from apical and basolateral side for 30 min. Phosphorylation of STAT3 was examined by Western blotting. As shown in figure 3.1.8.2, IL-11-stimulation of MDCK-IL-11R1 resulted in the induction of STAT3 phosphorylation from the both apical and basolateral sides, whereas phosphorylation of STAT3 in MDCK-IL-11R2 cells from the apical side was much weaker than from the basolateral side. Interestingly, IL-6-stimulation of MDCK-IL-6R cells resulted in basolateral phosphorylation of STAT3, while in MDCK-IL-6DΔICD cells phosphorylation of STAT3 was strongly inducible from the apical side. The results supported our previous data that IL-11R2 was localized mainly on basolateral side and only to a lesser extent on the apical side which resulted in stronger induction of STAT3 phosphorylation from

the basolateral side compared to the apical side. Moreover, the results of Western blotting elucidated that the presence of α-receptors determined the localization of gp130 in polarized cells (Fig 3.1.8.2).

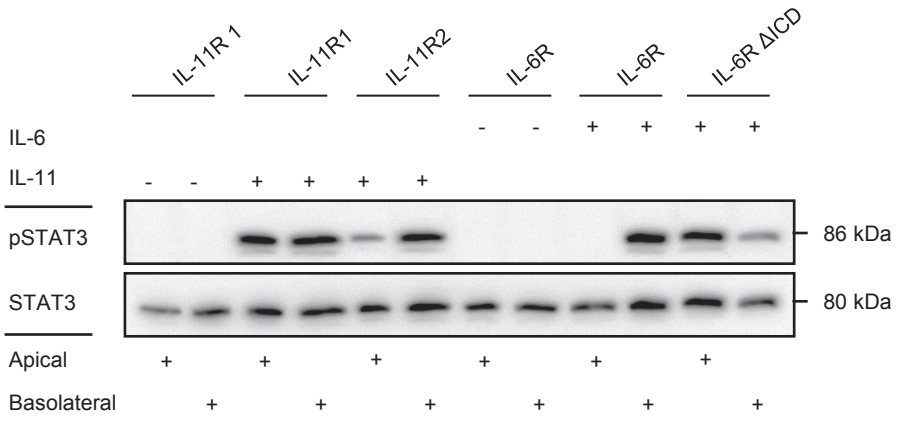

Figure 3.1.8.2: Low expression of IL-11R2 on the apical membrane facilitated apical delivery of gp130. Polarized MDCK-IL-11R1 and MDCK-IL-11R2 cells were stimulated with 20 ng/ml recombinant IL-11 and polarized MDCK-IL-6R and MDCK-IL-6RΔICD cells were stimulated with 10 ng/ml recombinant IL-6 from apical and basolateral sides for 30 min. Western blotting for STAT3 and pSTAT3 was done. 124H6 and D3A7 antibodies from Cell Signaling Biotechnology for pSTAT3 and STAT3, respectively, were applied as primary antibodies. This experiment was done 3 times.

Hyper IL-6 (HIL-6) is a synthetic fusion protein consisting of IL-6 and the soluble IL-6R connected by a flexible linker peptide, while specifically induces IL-6-trans-signaling (Rose-John and Heinrich, 1994). Phosphorylation of STAT3 under the treatment of HIL-6 is just due to the presence of gp130 as the signal transducing receptor. To confirm that apically delivery of gp130 is due to the presence of α-receptors on the apical side, polarized MDCK-IL-6R and MDCK-IL-11R1 cells were stimulated with HIL-6 (10 ng/ml) from apical or basolateral side. Then, cells were lysed and phosphorylation of STAT3 was assessed by Western blotting. In MDCK-IL-11R1 cells, HIL-6-induced STAT3 phosphorylation was detected from both apical and basolateral membranes, whereas in MDCK-IL-6R cells, HIL-6-induced STAT3 phosphorylation was detectable only from the basolateral side (Fig 8.1.8.3). As shown in figure 3.1.8.3, apical and basolateral HIL-6-stimulation of MDCK-IL-11R1 induced the

phosphorylation of STAT3 from both sides, whereas in MDCK-IL-6R resulted in the basolateral induction of STAT3 phosphorylation. Interestingly, HIL-6-stimulation of non-transfected MDCK cells led to the phosphorylation of STAT3 from basolateral but not apical side which supported the previous report showing basolaterally sorting of gp130 in polarized MDCK cells (Doumanov *et al.*, 2006). The results demonstrated that HIL-6 was not able to induce STAT3 phosphorylation on apical side of MDCK-IL-6R cells. However, apically sorted IL-11R1 rendered the delivery of gp130 to the apical surface which results in the phosphorylation of STAT3 in apically-HIL-6 stimulated MDCK-IL-11R1 cells (Fig 3.1.8.3).

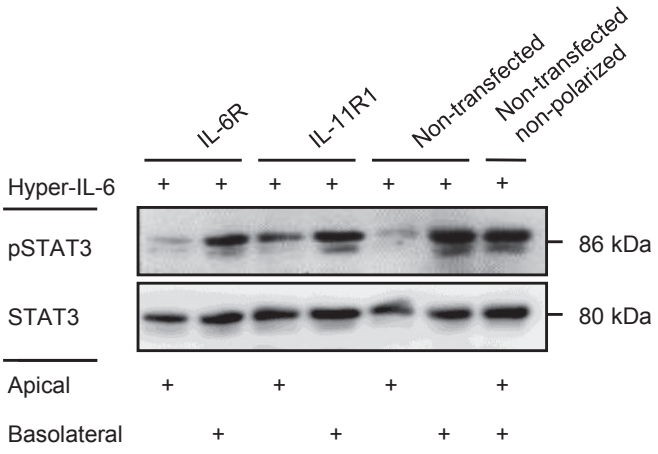

Figure 3.1.8.3: IL-11R1 but not IL-6R rendered the apical delivery of gp130. Polarized MDCK, MDCK-IL-6R, MDCK-IL-11R, and non-polarized MDCK cells were stimulated with 10 ng/ml HIL-6. STAT3 and pSTAT3 was examined by Western blotting. 124H6 mAb and D3A7 mAb from Cell Signaling Biotechnology for pSTAT3 and STAT3, respectively, were applied as primary antibodies. This experiment was done 2 times.

3.1.9 Detection of gp130 via confocal microscopy on the apical surface of MDCK-gp130-IL-11R1 cells

Endogenous gp130 could not be detected *via* confocal microscopy; therefore a cDNA coding for gp130 was sub-cloned into pcDNA-3.1-puro vector. Afterwards, MDCK-IL-6R

and MDCK-IL-11R1 cells were stably transfected with pcDNA-3.1-puro-gp130-myc and positive cells (MDCK-gp130-IL-6R and MDCK-gp130-IL-11R1 cells) were selected using puromycin (1.5 µg/ml). Cells were polarized and gp130, IL-6R and IL-11R1 were stained by immunocytochemistry. According to the secondary antibodies for IL-6R and IL-11R, different antibodies were applied for gp130 staining. In MDCK-gp130-IL-6R cells, IL-6R was stained via 4-11 mAb and gp130 was stained by myc 71D19 mAb from Cell Signaling. In MDCK-gp130-IL-11R1 cells, IL-11R1 was stained via 4D12 mAb from Santa Cruz and gp130 was stained via B-T2 mAb from Thermo Scientific. The results demonstrated that in MDCK-gp130-IL-6R cells, the presence of gp130 was restricted to the basolateral side, whereas, in MDCK-IL-11R1-gp130 cells, gp130 was observed on the apical and basolateral membranes. Our data suggested that the presence of IL-11R1 on the apical side shifted gp130 to the apical surface, whereas sorting of IL-6R on the basolateral side resulted in the basolateral-restricted sorting of gp130 (Fig 3.1.9).

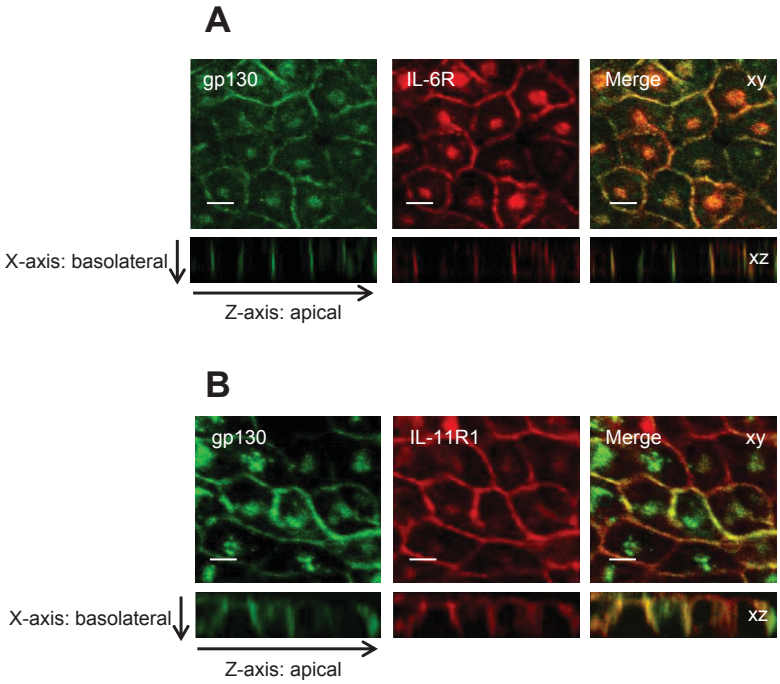

Fig 3.1.9: Basolateral and apical co-localization of gp130 with IL-11R1 in polarized MDCK-gp130-IL-11R1 cells. A. In MDCK-gp130-IL-6R cells IL-6R and gp130 were stained with 4-11 and 71D10 mAb from cell signaling, respectively. B. In MDCK-gp130-IL-11R1 cells, IL-11R1 and gp130 were stained with 4D12 mAb from Santa Cruz and B-T2 mAb from Thermo Scientific, respectively. Cells were mounted on the microscopy slides by Prolong®Gold antifade reagent with DAPI. Images were taken with confocal microscopy and analysed *via* LSM Image Browser. Scale bars are 10 µm. This experiment was done 2 times.

3.1.10 IL-11R1 is a cytokine transcytosis receptor

To establish and maintain the asymmetry of polarized cells, newly synthetic plasma membrane proteins are sorted in the trans-Golgi network (TNG) for directing to apical or basolateral surfaces (Griffiths and Simons, 1986). All transmembrane proteins carry a signal which determined the final destiny of the protein. Transcytosis is a critical process to transfer macro-molecules through the cell to the opposite cell surface. This mechanisms is responsible for sorting of receptors which are localized first in the basolateral membrane and then according to the endo/transcytosis be transported to the apical surface (Orzech *et al.*, 2000). Due to the presence of IL-11R1 on basolateral and apical surface of polarized MDCK cells, we hypothesised that IL-11R1 served as transcytosis receptor for transportation of IL-11 across polarized cells. Therefore, polarized MDCK, MDCK-IL-11R1, and MDCK-IL-11R2 cells were stimulated for 0 h, 1 h, and 24 h with 50 ng/ml recombinant IL-11 from the basolateral side. After the indicated time points, the concentration of IL-11 was quantified by ELISA in the apical and basolateral media as well as in the lysate of cells. As shown in figure 3.1.10 A, in all cell types at 0 h, the concentration of IL-11R1 at the basolateral side is about 50 ng/ml and there is no IL-11 in the lysate of cells and the media from the apical side. Interestingly, in MDCK-IL-11R1 cells after 1 h and 24 h, the concentration of IL-11 in the basolateral medium was decreased about one fifth of the initial used amount of IL-11, whereas about 5 ng/ml and 10 ng/ml IL-11 was measured in the apical media after 1 h and 24 h, respectively. However, in MDCK and MDCK-IL-11R2 cells after 1 h and 24 h, the concentration of IL-11 in the basolateral medium was only slightly decreased due to the endocytosis and instability of the cytokine, and importantly IL-11 was not detected in the apical media. In the lysate of all cell types after 1 h and 24 h, IL-11 was detectable because of endocytosis of the cytokine, although the concentration of IL-11 in the lysate of MDCK-IL-11R1, and MDCK-IL-11R2 cells was higher than MDCK cells. Intriguingly, in MDCK-IL-11R1 cells after 24 h, about 20 ng/ml decease of IL-11 concentration in the basolateral medium was comparable to the appeared concentration of IL-11 in the apical (about 10 ng/ml) and lysate (about 5 ng/ml) (Fig 3.1.10 A). Our data suggested that IL-11R1 is a transcytosis receptor of IL-11.

Next, polarized MDCK, MDCK-IL-6R, MDCK-IL-6RΔICD and MDCK-IL-6R_{ECD}/IL-11R_{ICD} cells ($1x10^4$ cells) were stimulated basolaterally with 50 ng/ml recombinant IL-6 for 0 h and 24 h. After 24 h, the concentration of IL-6 was examined by Nevox IL-6 ELISA kit in the apical and basolateral media as well as in the lysate of the cells (Fig 3.1.10 B). As shown in the figure 3.1.10 B, in MDCK-IL-6R and MDCK-IL-6R_{ECD}/IL-11R1$_{ICD}$ cells, the concentration of IL-6 was decreased in the basolateral medium as compared to MDCK-IL-6RΔICD and MDCK-cells. The decrease of IL-6 in the basolateral media of MDCK-IL-6R was due to the endocytosis and also instability of cytokine in the media, whereas the decreased concentration of IL-6 in the basolateral media of MDCK-IL-6R_{ECD}/IL-11R1$_{ICD}$ cells was also because of the endocytosis and importantly transcytosis of IL-6 to the apical side of the cells. Interestingly, about 10 ng/ml IL-6 was transported to the apical side of MDCK-IL-6R_{ECD}/IL-11R_{ICD} cells. After 24 h the concentration of IL-6 in the basolateral media of MDCK-IL-6RΔICD cells was similar to that in MDCK cells and showed a slight decrease due to the instability of the cytokine compared to the initially amount of used IL-6. The results showed that transcytosis of IL-6 is mediated by IL-6R_{ECD}/IL-11R1$_{ICD}$ in MDCK-IL-6R_{ECD}/IL-11R_{ICD} cells in which the receptors contained the intracellular domain of IL-11R1 (Fig 3.1.10 B).

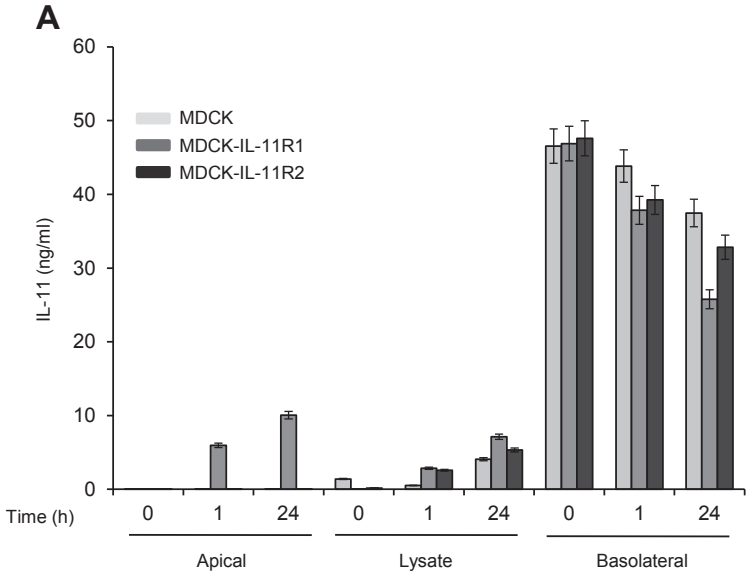

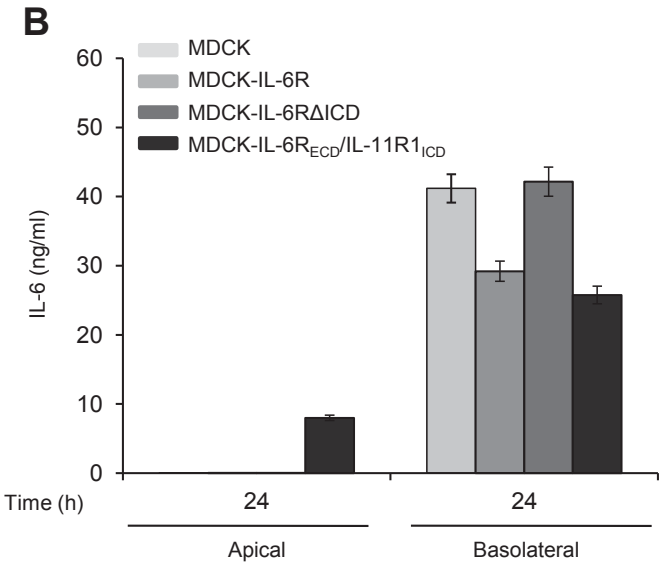

Fig 3.1.10: IL-11R1 is a cytokine transcytosis receptor. A. Polarized MDCK, MDCK-IL-11R1, and MDCK-IL-11R2 cells were stimulated with 50 ng/ml recombinant IL-11 from the basolateral side for 0 h, 1 h, and 24 h. To measure the concentration of IL-11 in the apical and basolateral media as well as the lysate of cells IL-11 R&D ELISA kit was applied. B. Polarized MDCK, MDCK-IL-6R, MDCK-IL-6RΔICD, and MDCK-IL-6R$_{ECD}$/IL-11R1$_{ICD}$ cells were basolaterally stimulated with 50 ng/ml IL-6 for 0 h and 24 h. The concentration of IL-6 in the apical and basolateral media was assessed with Novex IL-6 Elisa kit. These experiments were done 2 times.

3.1.11 Transcytosed IL-6 and IL-11 were biologically active

According to the data from the transcytosis experiments, it was shown that IL-11R1 was transcytosed and the IL-11R1 intracellular domain carried the transcytosis signal. Transcytosis of IL-11R1 and IL-6R$_{ECD}$/IL-11R1$_{ICD}$ receptors resulted in transfer of IL-11 and IL-6, respectively, from basolateral side of polarized cells to the apical side. To test the biological activity of transcytosed IL-6 and IL-11, non-polarized MDCK-IL-6R and MDCK-IL-11R1 cells were stimulated with the apical media from MDCK-IL-6R$_{ECD}$/IL-11R1$_{ICD}$ and MDCK-IL-11R2, respectively, for 30 min, and STAT3 phosphorylation was examined by Western blotting. As shown in figure 3.1.11 A, induction of STAT3 phosphorylation in non-

polarized MDCK-IL-11R1 cells *via* the apical media of MDCK-IL-11R cells was comparable to 10 ng/ml IL-11 stimulation. Stimulation of the non-polarized MDCK-IL-11R1 cells with apical media of MDCK and MDCK-IL-11R2 cells did not lead to the phosphorylation of STAT3. Moreover, as it was shown in figure 3.1.11 B, induction of STAT3 phosphorylation in non-polarized MDCK-IL-6R cells *via* the apical media of MDCK-IL-6R$_{ECD}$/IL-11R1$_{ICD}$ cells was comparable to 10 ng/ml IL-6 stimulation. Stimulation of the non-polarized MDCK-IL-6R cell with apical media of MDCK, MDCK-IL-6R, and MDCK-IL-6RΔICD cells did not lead to the phosphorylation of STAT3. Our results showed that transcytosed IL-6 and IL-11 are biologically active (Fig 3.1.11 A&B).

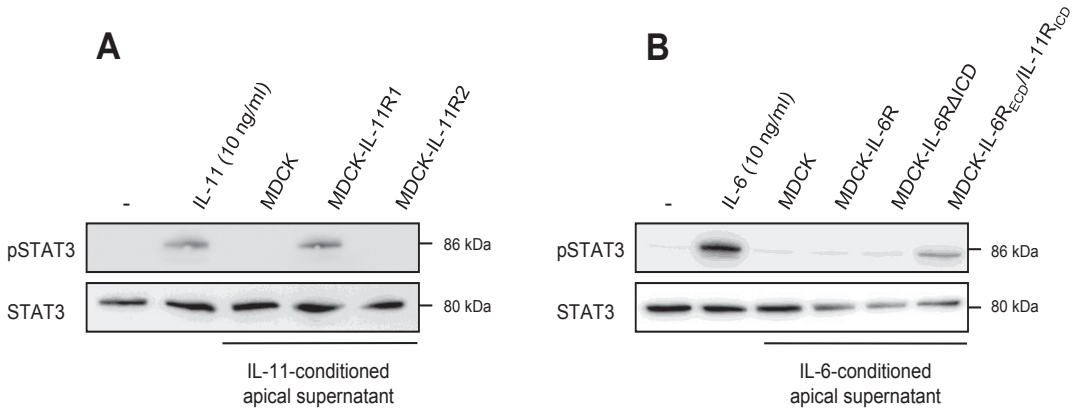

Fig 3.1.11: Transcytosed IL-6 and IL-11 were biologically active. A. Non-polarized MDCK-IL-11R1 cells were starved for 2 h and were stimulated with the apical media of transcytosis experiment for 30 min; MDCK, MDCK-IL-11R1, MDCK-IL-11R2 cells; and 10 ng/ml recombinant IL-11. B. Non-polarized MDCK-IL-6R cells were stimulated with the apical media of transcytosed experiment; MDCK, MDCK-IL-6R, MDCK-IL-6RΔICD and MDCK-IL-6R$_{ECD}$/IL-11R1$_{ICD}$ cells; and 10 ng/ml recombinant IL-6. Conditional apical supernatants were obtained from the transcytosis assay in 3.1.10 part. Apical supernatant was collected after 24 h of the transcytosis assays. 124H6 mAb and D3A7 mAb from Cell Signaling Biotechnology were used for pSTAT3 and STAT3, respectively. This experiment was done 2 times.

3.1.12 No transcytosis of IL-11R1 from the apical to basolateral side of polarized MDCK cells

It is known that transcytosis resulted in transfer of receptor and/or ligand from basolateral to apical side of polarized cells and not in the opposite direction (Weisz and Rodriguez-Boulan, 2009). To analyse the transcytosis from apical to basolateral side, polarized MDCK, MDCK-IL-11R1 and MDCK-IL-11R2 cells were stimulated from the apical side with 50 ng/ml recombinant IL-11. At time point 0 and after 24 h, the concentration of IL-11 in the apical and basolateral media and also in lysate of cells was measured by ELISA. As shown in figure 3.1.12, there was no IL-11 in the basolateral media of all cell types analysed after 24 h. However, there was a slight reduction in the concentration of IL-11 in the apical media of MDCK and MDCK-IL-11R2 cells likely because of instability of the cytokine. Interestingly, the apical media of MDCK-IL-11R1 showed about 8 ng/ml decrease of IL-11 concentration, which was not only due to instability of cytokine but also because of apical endocytosis of IL-11. Therefore, about 4 ng/ml IL-11 was detectable in the lysate of MDCK-IL-11R1. Our results showed no transcytosis from the apical to basolateral side of polarized MDCK cells.

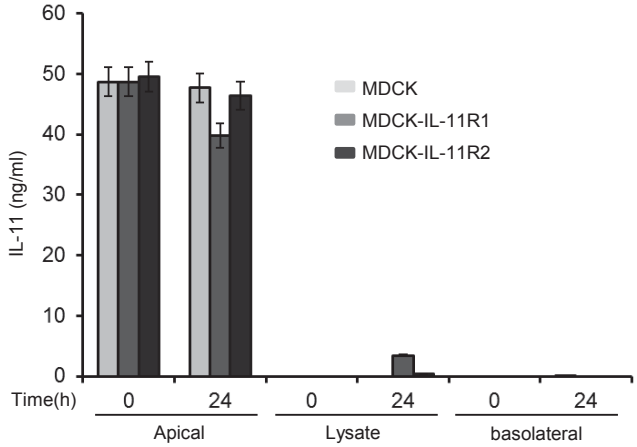

Fig 3.1.12: No transcytosis of IL-11R1 from apical to basolateral side of polarized cells. Polarized MDCK, MDCK-IL-11R1, and MDCK-IL-11R2 cells were stimulated for 24 h from the apical side with 50 ng/ml recombinant IL-11. After 24 h the concentration of IL-11 in the media from the apical and basolateral side and also in lysate was assessed. IL-11 R&D Elisa kit was used. This experiment was done 2 times.

3.1.13 gp130 is transcytosed by IL-11R1

In polarized MDCK cells, gp130 is localized preferentially to the basolateral surface of cells (Doumanov *et al.*, 2006). Stimulation of polarized MDCK-IL-6RΔICD and MDCK-IL-$6R_{ECD}$/IL-$11R1_{ICD}$ with recombinant IL-6 and MDCK-IL-11R1 with recombinant IL-11 from apical side resulted in the phosphorylation of STAT3 which approved the transduction of signals *via* gp130 (Fig 3.1.8.2). Gp130 might be directly transported to the apical side or first be sorted to the basolateral side and then transcytosed to the apical membrane. To examine the mechanism of gp130 sorting to the apical side of polarized cells, we used HIL-6, because it binds to gp130 without the need to bind to the other α-receptors, IL-6R or IL-11R. Therefore, applying HIL-6 was a suitable approach to analyse the transcytosis of gp130. Polarized MDCK-IL-6R, MDCK-IL-6RΔICD, MDCK-IL-$6R_{ECD}$/IL-$11R1_{ICD}$, MDCK-IL-11R1, and MDCK-IL-11R2 cells were stimulated from the basolateral side with 50 ng/ml HIL-6 and then incubated for 24 h at 37°C. After 24 h, the concentration of HIL-6 in the apical media of cells was measured by HIL-6 ELISA. As it was shown in figure 3.1.13, after 24 h, in MDCK-IL-11R1 cell about 1800 pg/ml HIL-6 and in MDCK-IL-$6R_{ECD}$/IL-$11R_{ICD}$ cells about 1500 pg/ml HIL-6 was detected in the apical media. However, almost no HIL-6 was detected in the apical media of MDCK, MDCK-IL-6R, and MDCK-IL-11R2 cells. The result showed that HIL-6 was transcytosed in MDCK-IL-11R1 and MDCK-IL-$6R_{ECD}$/IL-$11R1_{ICD}$ cells which revealed that gp130 was first sorted to the basolateral side and subsequently transcytosed to the apical membrane. It does, however, not exclude that some gp130 molecules are also transported directly to the apical membrane together with IL-11R1. Our results suggested that sorting of gp130 to the apical side is dependent on IL-11R1 *via* transcytosis.

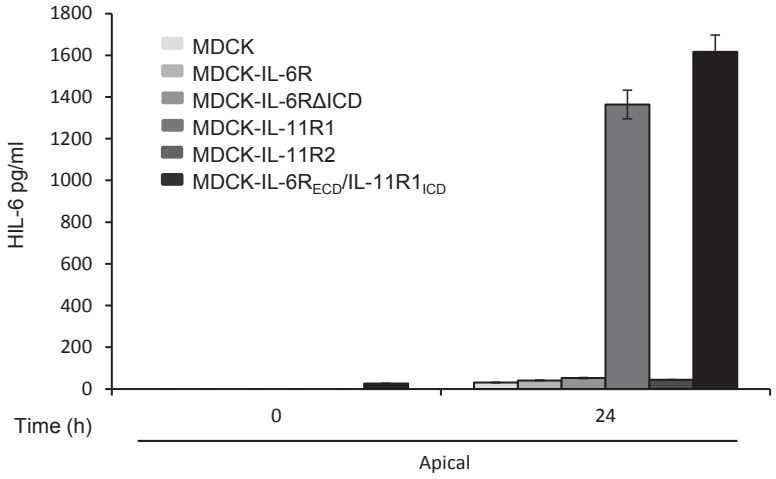

Fig 3.1.13: gp130 is transcytosed along with IL-11R1. Polarized MDCK-IL-6R, MDCK-IL-6RΔICD, MDCK-IL-6R$_{ECD}$/IL-11R1$_{ICD}$, MDCK-IL-11R1, and MDCK-IL-11R2 cells were stimulated from basolateral side with 50 ng/ml HIL-6. After 24 h the concentration of HIL-6 was measured in the apical media using HIL-6 ELISA. This experiment was done 2 times.

3.2 Identification of MAD2B as a novel regulatory protein of IL-6 classic signaling

Several studies investigated the structure and modification of IL-6R extracellular domain, but less attention was spend on the intracellular domain of the receptor. The intracellular domain of IL-6R consists of 82 amino acids and two dis-continuous motifs which are responsible for internalization and basolateral sorting of the receptor (Martens *et al.*, 2000). In order to identify potential binding partners of IL-6R intracellular domain, a yeast-two-hybrid assay was designed by Prof. Dr. Jürgen Scheller and was done by Dr. Christoph Garbers from the Institute of Biochemistry at Christian-Albrechts-University Kiel in the cooperation with Dr. Micheal Winkler from the Institute of Infection Medicine, Christian-Albrechts-University Kiel. MAD2B was one of the identified binding partners of the intracellular domain of IL-6R.

3.2.1 OOxPxxxpP is the binding motif of MAD2B in the IL-6R intracellular domain

Hanafusa et al. have introduced "OOxPxxxpP" as the binding motif of MAD2B to REV7. REV3 is one of the subunit of Polξ. Polξ is a DNA polymerase specialized for translesion DNA synthesis and comprised of two subunits, the REV3 catalytic subunit and the REV7 accessory subunit. The binding motif is "OOxPxxxpP"; O is aliphatic amino acid, P is proline, and x can be any amino acid (Hanafusa *et al.*, 2010). We found a similar motif within the intracellular domain of the IL-6R. To determine the binding site of MAD2B in the intracellular domain of IL-6R, we generated deletion variants within the intracellular domain

of the IL-6R. In each cDNA the intracellular domain of IL-6R was shortened by stepwise deletion of 10 C-terminal amino acids (Fig 3.2.1.1).

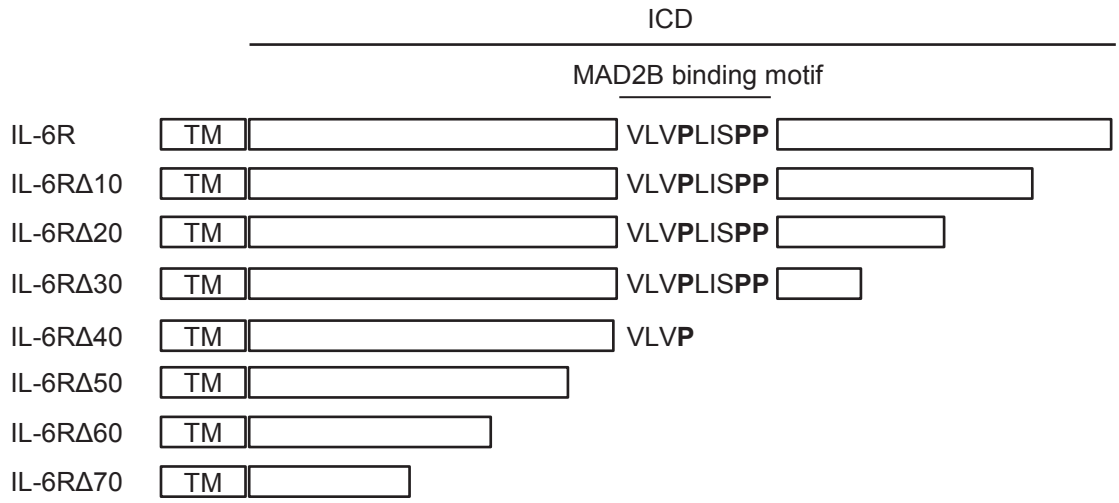

Figure 3.2.1.1: Schematic illustration of deletion variants within the intracellular domain of the IL-6R. The intracellular domain of IL-6R was shorted by stepwise deletion of the 10 aa from the C-terminus. TM: transmembrane domain. ICD: intracellular domain. $VLVP_{426}LISP_{430}P_{431}$ was the potential binding motif of MAD2B.

HEK293 cells were transiently transfected with the cDNAs coding for the IL-6R deletion variants and MAD2B-GFP and a Nanotrap assay was done. The Nanotrap assay was carried out according to the protocol of Nanotrap. Nanotrap is a powerful tool for capturing of GFP-fusion proteins. In this assay, sepharose beads were coupled with GFP-nanobodies which were used to precipitate GFP-tagged proteins including interaction proteins (Rothbauer *et al.*, 2008). In our experiment MAD2B was GFP-tagged and precipitated *via* sepharose-GFP-Nano beads and IL-6R bound to the precipitated MAD2B-GFP. As shown in figure 3.2.1.2 A, MAD2B and IL-6R wild type binding was clearly shown by coprecipitation in the bound fraction. Binding of MAD2B and IL-6RΔ10 was still detectable but not as strong as the binding of MAD2B to IL-6R. However, from IL-6RΔ20 to IL-6RΔ70 the IL-6R protein in the bound fraction were faint and revealed almost no binding between MAD2B and the IL-6R deletion variants. The result of the Nanotrap co-precipitation showed that MAD2B needs

almost the entire intracellular domain of IL-6R for efficient binding, however, MAD2B was still binding to IL-6RΔ10 albeit to a lesser extent (Fig 3.2.1.2 A).

To confirm the results of Nanotrap, immunocytochemistry assay was performed. $3x10^4$ HeLa cells were seeded on 15 mm coverslips in a 12 well plate. Cells were transfected transiently with cDNAs coding for IL-6R, IL-6RΔ10, IL-6RΔ20, IL-6RΔ30, IL-6RΔ40, IL-6RΔ50, IL-6RΔ60, IL-6RΔ70 together with MAD2B-GFP. 48 h after transfection, cells were fixed and stained according to the immunocytochemistry protocol. The co-localization of MAD2B and IL-6R was examined in HeLa cells. As shown in figure 3.2.1.2 B, IL-6R was mainly localized on plasma-membrane and in intracellular vesicular structure of HeLa cells and MAD2B was localized in the nucleus and cytoplasm. However, the result in figure 3.2.1.2 C. showed the co-localization of MAD2B with IL-6R, IL-6RΔ10, IL-6RΔ20, and IL-6RΔ30 on the plasma-membrane but not with IL-6RΔ40, IL-6RΔ50, IL-6RΔ60 and IL-6RΔ70. IL-6RΔ40, IL-6RΔ50, IL-6RΔ60 and IL-6RΔ70 were the variants which lack the proposed binding site of MAD2B to IL-6R and had no co-localization with MAD2B on the membrane of HeLa cells (Fig 3.2.1.2.1 B). According to the Nanotrap assay, there was almost no binding between MAD2B with IL-6RΔ20 and IL-6RΔ30 (fig 3.2.1.2.1 A), however, the immunocytochemistry assay showed the co-localization of them in HeLa cells. Our results suggested that MAD2B needed the full length of IL-6R for the efficient binding (fig 3.2.1.2.1 A), however, under the deletion of last 30 amino acids from the C-terminus of IL-6R, they still could bind to each other with lower affinity in the cells (fig 3.2.1.2.2.). Intriguingly, binding of MAD2B to IL-6R resulted in the presence of MAD2B on the membrane, whereas, in the absence of IL-6R or lack of binding site of MAD2B within IL-6R, MAD2B localization is restricted to the nucleus and cytoplasm (fig 3.2.1.2.1&2).

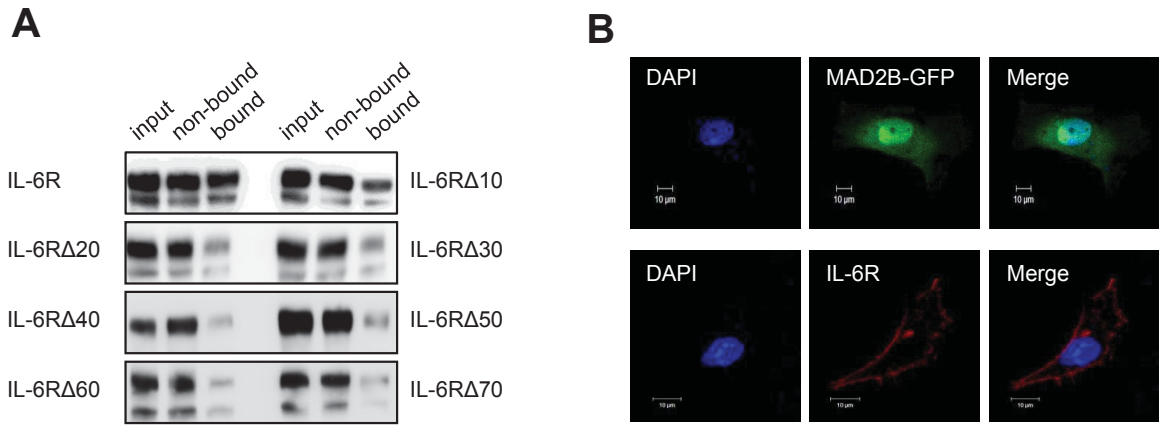

Figure 3.2.1.2.1: MAD2B needs the complete IL-6R intracellular domain for efficient binding. A. $2x10^6$ HEK293 cells were transiently transfected by TurboFect with the deletion variants of IL-6R and MAD2B-GFP and Nanotrap assay was carried out. MAD2B was GFP-tagged and 4-11 mAb was applied for IL-6R detection. Input: the cell lysate, non-bound: the supernatant of the lysate and beads mixture after precipitation, bound: the precipitated fraction shows the presence or absence of the binding between MAD2B and IL-6R. B. $3x10^4$ HeLa cells were seeded on 15 mm coverslips in a 12 well plate. Cells were transiently transfected and after 48 h cells were fixed and stained according to the immunocytochemistry protocol. Antibody for IL-6R was 4-11 and MAD2B was detected by GFP. For the detection of DAPI the mounting solution Prolong®Gold antifade reagent with DAPI was used. Images were made by confocal microscopy and analysed *via* LSM Image Browser. These experiments were done 3 times.

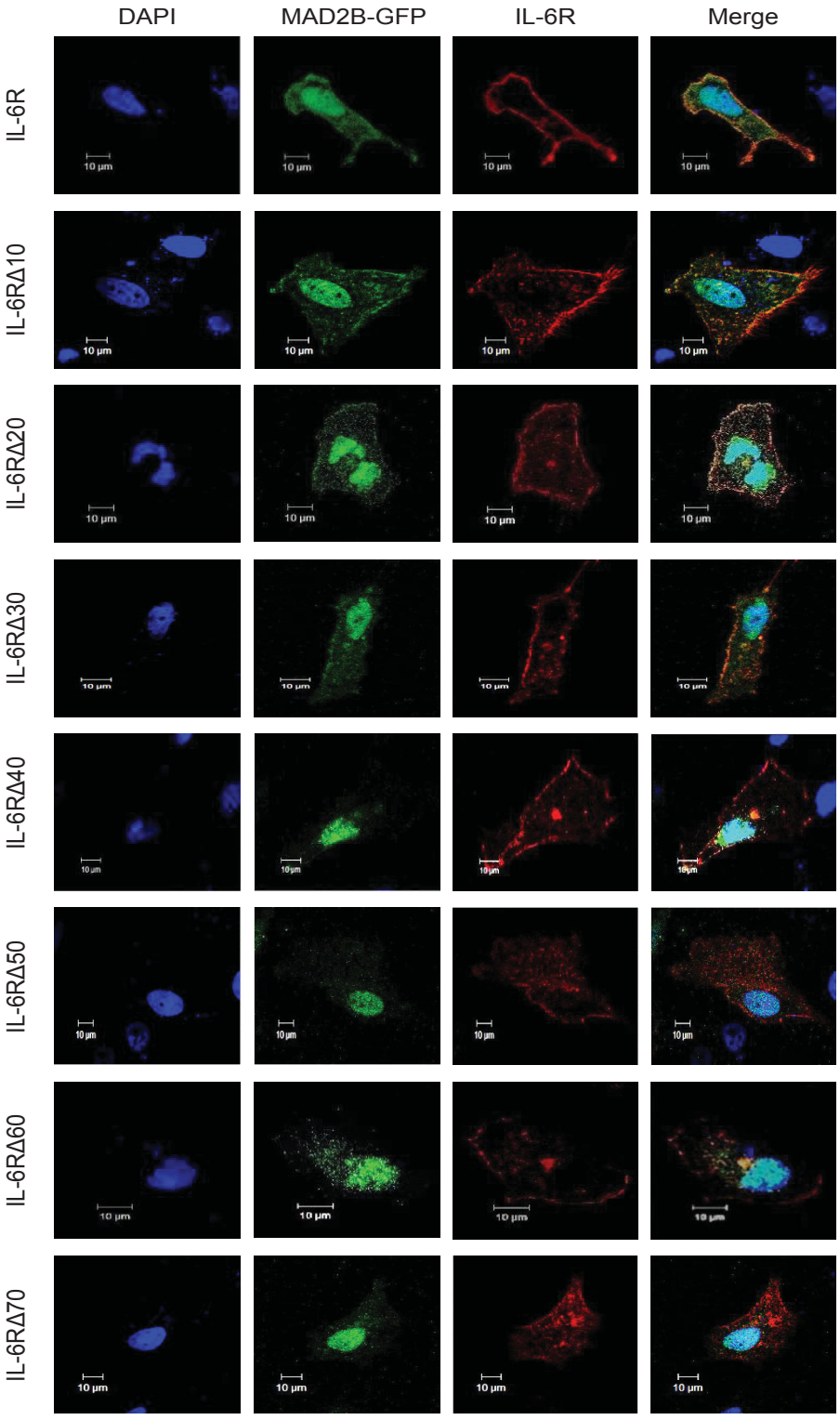

Figure 3.2.1.2: MAD2B needs the complete IL-6R intracellular domain for efficient binding. A. $2x10^6$ HEK293 cells were transiently transfected by TurboFect with the deletion variants of IL-6R and MAD2B-GFP and Nanotrap assay was carried out. MAD2B was GFP-tagged and 4-11 mAb was applied for IL-6R detection. Input: the cell lysate, non-bound: the supernatant of the lysate and beads mixture after precipitation, bound: the

precipitated fraction shows the presence or absence of the binding between MAD2B and IL-6R. B. & C. $3x10^4$ HeLa cells were seeded on 15 mm coverslips in a 12 well plate. Cells were transiently transfected and after 48 h cells were fixed and stained according to the immunocytochemistry protocol. Antibody for IL-6R was 4-11 and MAD2B was detected by GFP. For the detection of DAPI the mounting solution Prolong®Gold antifade reagent with DAPI was used. Images were made by confocal microscopy and analysed *via* LSM Image Browser. These experiment were done 3 times.

According to the introduced binding motif of MAD2B "OOxPxxxpP", Dr. Garbers found the similar motif in the intracellular domain of IL-6R and generated a cDNA in which these three prolines of IL-6R were replaced by three alanines (IL-6R3P-A). These three prolines are the amino acid numbers 426, 430 and 431. This motif is present in IL-6RΔ10, IL-6RΔ20, and IL-6RΔ30 deletion variants of IL-6R but the other deletion variants lack this motif (Fig 3.2.1.1). To examine the protein binding motif of MAD2B in IL-6R, the Nanotrap assay was performed. HEK293 cells were transiently transfected with cDNAs coding for IL-6R+MAD2B-GFP, IL-6R3P-A+MAD2B-GFP, and IL-6R+GFP. The results of the Nanotrap assay revealed the binding between MAD2B and IL-6R, whereas there was no binding between IL-6R3P-A and MAD2B. This result supported the result of the Nanotrap and immunocytochemistry experiments in part 3.2.2 which showed that there was no binding between MAD2B and IL-6RΔ40, IL-6RΔ50, IL-6RΔ60 and IL-6RΔ70 which lacked "OOxPxxxpP" motif. In conclusion, the binding motif of MAD2B in IL-6R is as the same as the previously introduced binding motif "OOxPxxxpP" (Fig 3.2.1.3 A) (Hanafusa *et al.*, 2010). To prove the results of Nanotrap, an immunocytochemistry assay was performed. $3x10^4$ HeLa cells were seeded on 15 mm coverslips in a 12 well plate. Cells were transfected transiently and after 48 h cells were fixed and stained according to the immunocytochemistry protocol. MAD2B was GFP-tagged and IL-6R3P-A was stained by 4-11 mAb. The images showed that mutation on three prolines to alanines prevented the binding of MAD2B to IL-6R3P-A. In addition, in the absence of the MAD2B binding motif in the IL-6R, MAD2B was not co-localized with IL-6R on the plasma-membrane (Fig 3.2.1.3.B). Sequences of IL-6R and IL-6R3P-A revealed that there is an overlapping between the binding motif of MAD2B and the di-leucine motif which is important for the internalization of IL-6R (Fig 3.2.1.3 C) (Martens *et al.*, 2000).

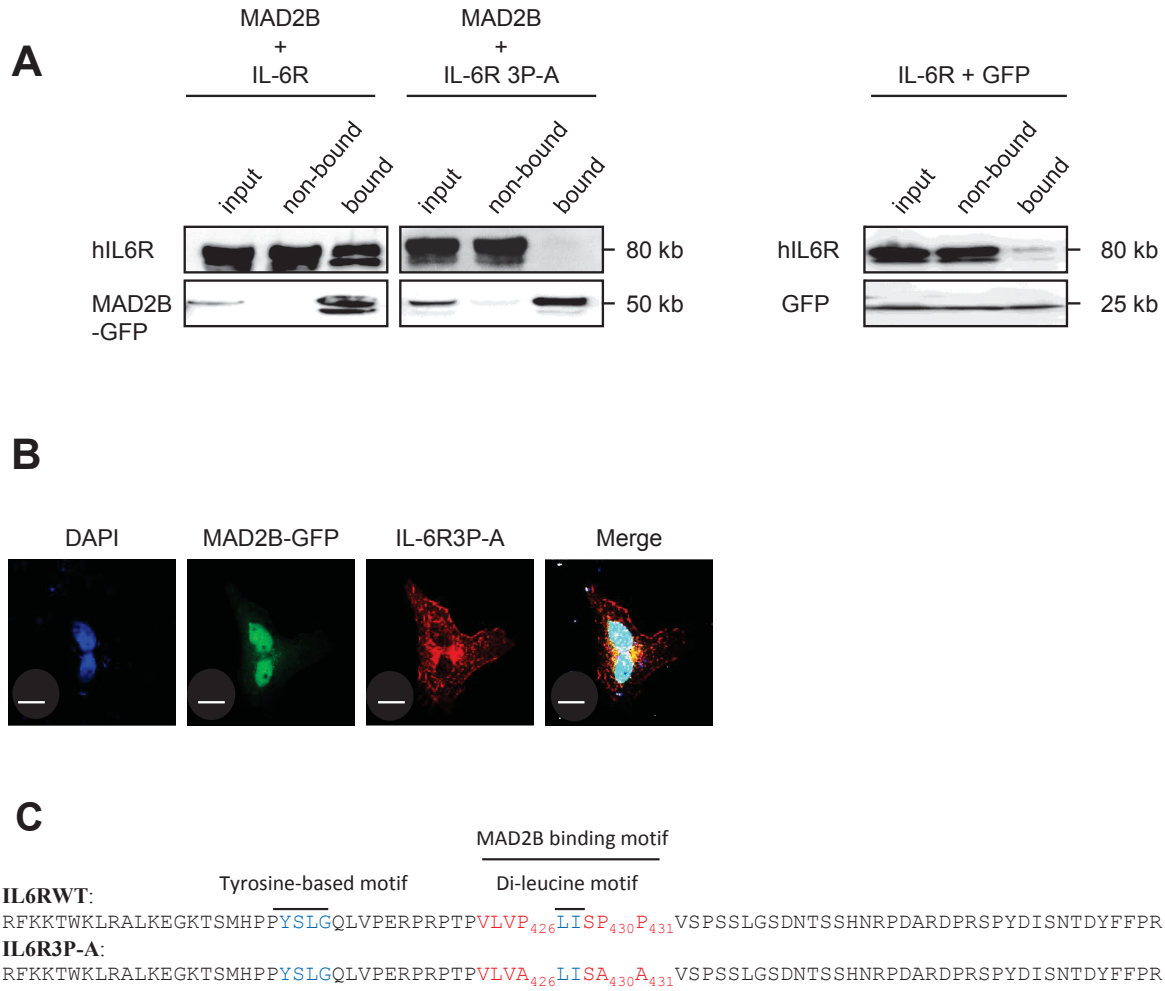

Figure 3.2.1.3: "OOxPxxxpP" is the binding motif of MAD2B in the intracellular domain of IL-6R. A. $2x10^6$ HEK293 cells were transiently transfected with cDNAs coding for MAD2B-GFP+IL-6R, MAD2B-GFP+IL-6R3P-A, and IL-6R+GFP and Nanotrap was done. MAD2B was detected via anti-GFP mAb from Roche and IL-6R was detected via 4-11 mAb. GFP served as the control. Input: the cell lysate, non-bound: the supernatant of the lysate and beads mixture after precipitation, bound: the precipitated fraction showed the presence or absence of the binding between two proteins. B. $3x10^4$ HeLa cells were seeded on 15 mm coverslips in a 12 well plate and were transiently transfected with the cDNAs coding for IL-6R and MAD2B-GFP. 48 h after transfection, cells were fixed with 4% PFA and stained according to the immunocytochemistry protocol. MAD2B was GFP-tagged and IL-6R was stained with 4-11 mAb. For the detection of the nucleus, the mounting solution Prolong®Gold antifade reagent with DAPI was used. Images were made by confocal microscopy and analysed *via* LSM Image Browser. C. Sequences of IL-6R and IL-6R3P-A intracellular domain. "VLVPLISPP" was recognized as the binding motif of MAD2B in IL-6R intracellular domain. O is aliphatic amino acid, P is proline, and x can be any amino acid. These experiments were done 3 times.

3.2.2 MAD2B and IL-6R interaction has no influence on the cell cycle progression

MAD2B is one of the proteins which regulates the cell cycle progression by inhibition of CDH1 and CDC20 molecules and subsequently inhibition of anaphase promoting complex (APC/C). The most important function of CDH1 and CDC20 is to activate APC/C, a large 11-13 subunit complex that initiates chromatid separation and entry into anaphase (Chen and Fang, 2001; Pfleger *et al.*, 2001). In order to examine if the interaction of IL-6R and MAD2B affected the cell cycle, HEK293 cells were transiently transfected with cDNAs coding for IL-6R and MAD2B and a double thymidine block assay was accomplished. According to the double thymidine block protocol, cell cycle progression was controlled for 7 indicated time points. On day 1, $2x10^6$ HEK293 cells were seeded for each time points. On the day 2, at 8 am cells were transiently transfected with cDNAs coding for IL-6R and MAD2B by TurboFect and at 5 pm, cells were exposed to 200 mM thymidine. On day 3, at 8 am cells were washed with PBS and exposed to the fresh DMEM (+/+) and at 5 pm, cells were again exposed to 200 mM thymidine. On day 5, at 8 am cells were washed with PBS and fresh DMEM (+/+) was added to the plates. Every 2 h, one plate was taken out of incubator, cells were fixed and stored at -20°C. Before the measurement, the cells were stained with Nicoletti. The cell cycle was synchronized and at time point 0 the cells were arrested at G1, but by removing the thymidine, the cells were permitted to go back to the normal cell cycle. According to the DNA concentration, the cell cycle stage was determined for each group *via* flow cytometry (Figure 3.2.2). Figure 3.2.2 A. showed the cell cycle progression of HEK293 and HEK293+IL-6R+MAD2B cells over 12 h. G1 gate stands for G1 stage in cell cycle in which cells increase in size and prepare for DNA replication. S gate stands for S stage in which DNA replication is done. G2/M gate stands for G2 in which cells continue to grow and prepare for the cell division and M (mitosis) phase in which cells divide into two daughter cells (Harashima *et al.*, 2013). At time point 0, the cell cycle of all cells was synchronized at G1. As shown in figure 3.2.2 A, every 2 h cells progressed through the cell cycle from G1 to S, S to G2/M, and G2/M to G1. Interestingly, in both groups cell cycle progression was comparable. No arrest was detected and after 12 h, the high population of cells in both groups were at G1. As shown in figure 3.2.2 B, the percentage of each cell cycle stage at each time

point in both HEK293 and HEK293+IL-6R+MAD2B cells was similar and no significant difference was detected. Figure 3.2.2 C, showed the comparison between the percentage of cells in each time point in the two groups of HEK293 and HEK293+IL-6R+MAD2B cells.

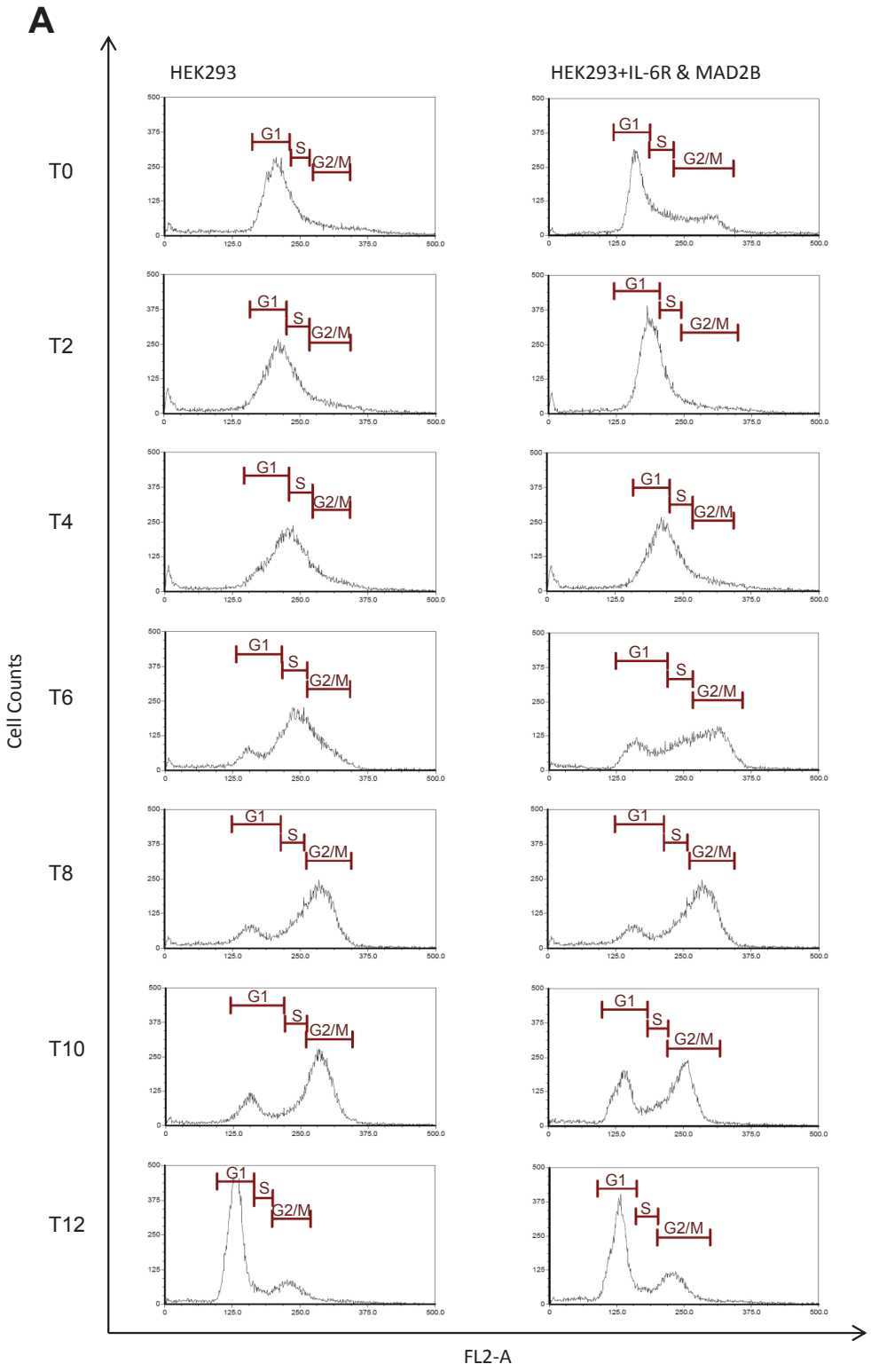

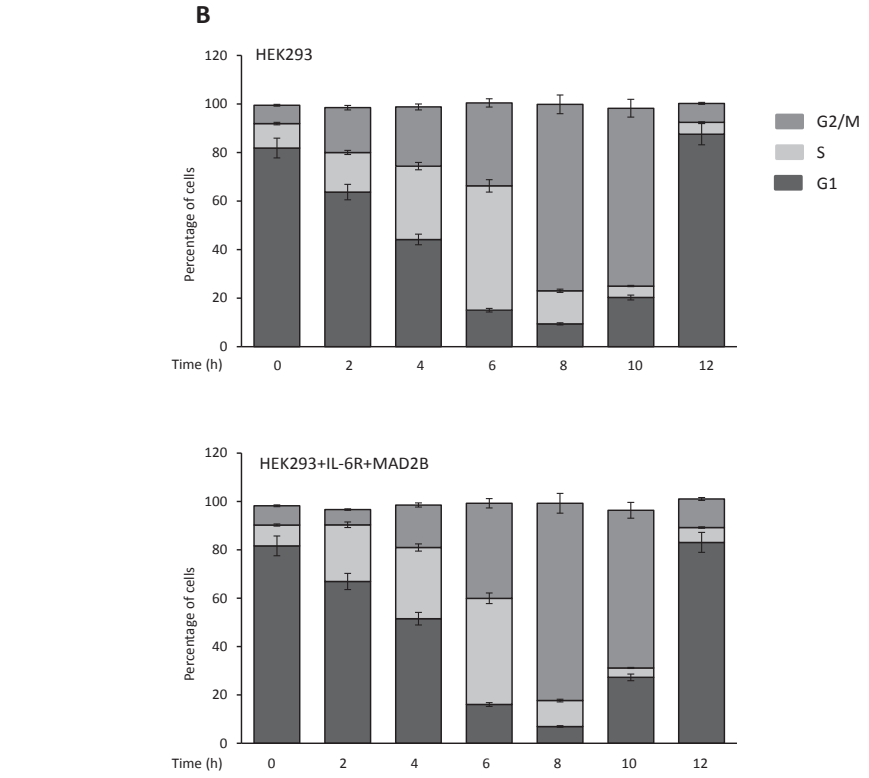
B
HEK293
HEK293+IL-6R+MAD2B
Percentage of cells
Time (h)
0
2
4
6
8
10
12
20
40
60
80
100
120
G2/M
S
G1

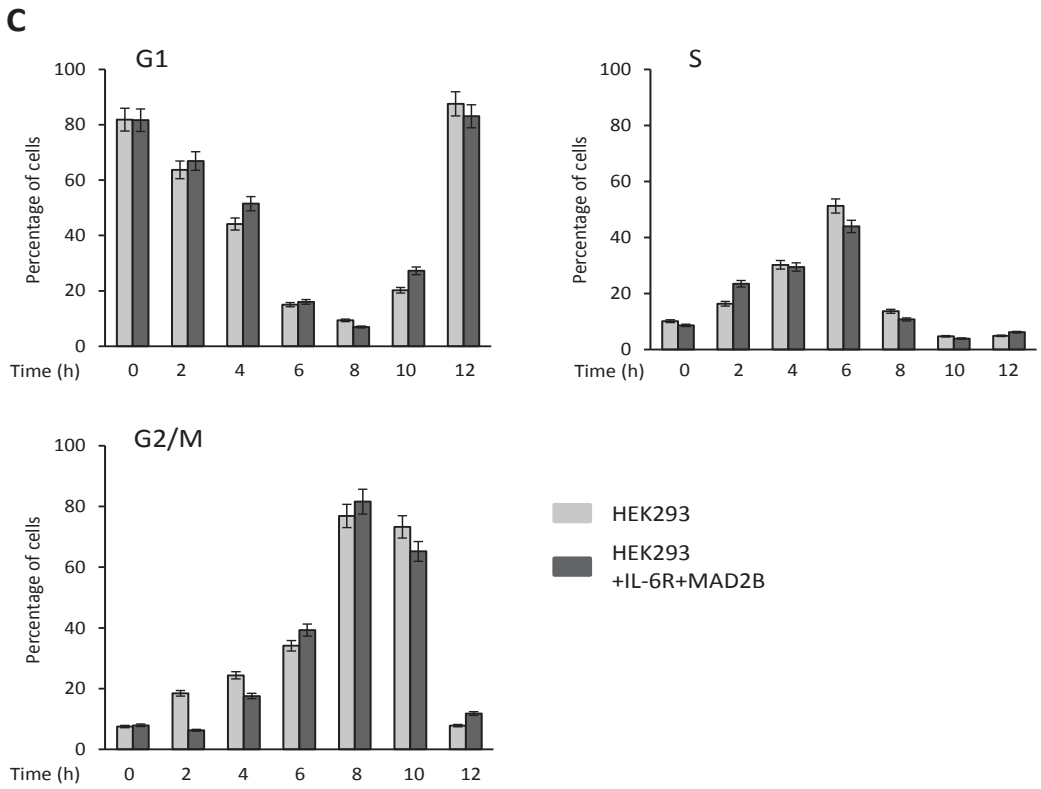
C
G1
S
G2/M
Percentage of cells
Time (h)
0
2
4
6
8
10
12
20
40
60
80
100
HEK293
HEK293
+IL-6R+MAD2B

Figure 3.2.2: Interaction of MAD2B and IL-6R has no influence on the cell cycle. In one group, HEK293 cells were transiently transfected with IL-6R and MAD2B and in another group non-transfected HEK293 cells were seeded in 10 cm dishes. For each group, 7 plates of cells were needed for 7 time points. Cells were synchronized *via* double thymidine block and arrested in G1 stage of the cell cycle. Cells were released every 2 h, fixed with 100% ethanol, stained with Nicoletti, and examined by flow cytometry. The graphs were drawn using FACS EXPRESS 4 Flow program. G1: G1 stage in the cell cycle. S: DNA replication stage in the cell cycle. G2/M: G2 and mitosis in the cell cycle. A. showed the cell cycle progression. B. showed the percentage of cells in each stage of the cell cycle at each time point. C. comparison between the percentage of HEK293 and HEK293+IL-6R+MAD2B cells in different stages of the cell cycle at each time point. These experiments were done 3 times.

3.2.3 Interaction of MAD2B and IL-6R led to an increased number of IL-6R and gp130 molecules on the surface of HepG2 cells

Due to the critical pro- and anti-inflammatory roles of IL-6, the formation, stability, and degradation of the receptor complex is tightly controlled. IL-6 stimulation induces lysosome-dependent degradation of gp130, which associates with K63-linked polyubiquitination of gp130 and c-CbI is the E3 ligase which mediates the ubiquitination of gp130. Following ubiquitination, gp130 undergoes hepatocyte growth factor regulated tyrosine kinase substrate (Hrs)-dependent endosomal sorting and lysosomal degradation, which is essential for termination of IL-6 signaling (Tanaka *et al.*, 2008). Hrs interacts with ubiquitylated cargos through its ubiquitin-interacting-motif domain (UIM domain), and plays an essential early role in endosomal sorting (Raiborg *et al.*, 2002). Specificity in the ubiquitination (Ub) process is mediated by the E3 ligase (d'Azzo *et al.*, 2005). The Cbl family of Ub ligases plays pivotal roles in polyubiquitination of EGFR (Huang *et al.*, 2006). MAD2B can bind to CDH1 and CDC20 which are known as the activators of anaphase promoting complex/cyclosome (APC/C), therefore, MAD2B can affect the cell cycle progression by inhibiting the activity of APC/C *via* the inhibition of ubiquitin ligase CDH1-APC and CDC20-APC (Chen and Fang, 2001; Pfleger *et al.*, 2001; Sudakin *et al.*, 2001). Therefore, it could be hypothesised that the specific interaction of IL-6R and MAD2B might affect the ubiquitination and subsequently degradation of gp130. In the first step, we examined the presence of endogenous IL-6R and

gp130 in HepG2 cells after the overexpression of MAD2B. HepG2 cells have a low endogenous expression of IL-6R HepG2 cells were transiently transfected with cDNA coding for MAD2B. 48 h after transfection, expression of gp130 and IL-6R on the cell surface was quantified by flow cytometry. As shown in the figure 3.2.3 A, there was a low endogenous expression of IL-6R on the cell surface of HepG2 cells. However, overexpression of MAD2B clearly increased the number of IL-6R molecules on the membrane of HepG2 cells. The faint line determined the increased cell surface expression of IL-6R in HepG2+MAD2B cells in figure 3.2.3 A. Moreover, as shown in figure 3.2.3 B, overexpression of MAD2B resulted also in a slight increase in the number of gp130 molecules on the cell surface of HepG2 cells. The faint line highlighted the increased cell surface expression of gp130 in HepG2+MAD2B cells. In the control group, because of the absence of any FITC or APC signal the population of cells were located in Q3. In HepG2 cells, due to the endogenous expression of IL-6R and gp130, the APC signal was detected and the population of cells were placed in Q1 region. In HepG2-MAD2B cells, according to the high expression of MAD2B and endogenous expression of IL-6R and gp130, the population of cells were located in Q2 region in which both signals were detected. Our data showed that in the presence of MAD2B, the number of gp130 and IL-6R on the cell surface was increased (Fig 3.2.3). The obtained data from the P2 gate in which all the cells were expressing MAD2B elucidated that the more MAD2B expression resulted in more gp130 and IL-6R on the membrane.

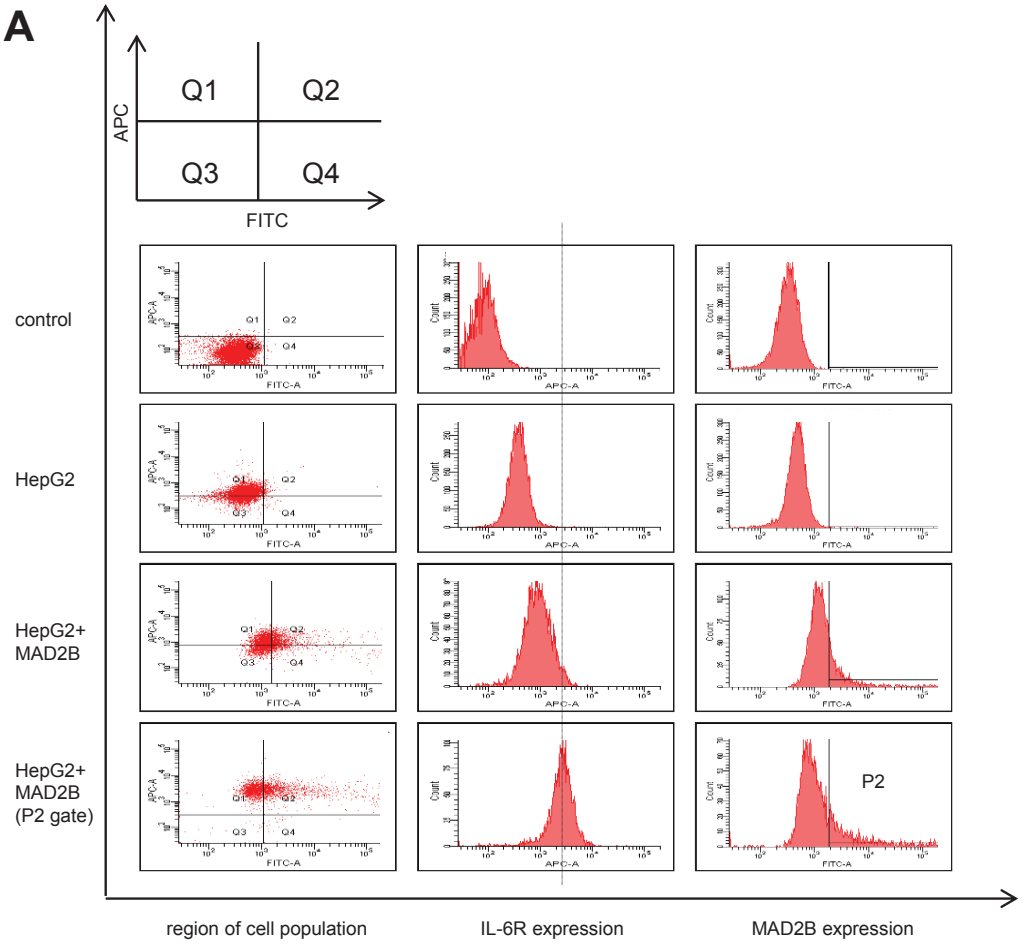
A
APC
Q1
Q2
Q3
Q4
FITC
control
HepG2
HepG2+
MAD2B
HepG2+
MAD2B
(P2 gate)
P2
region of cell population
IL-6R expression
MAD2B expression

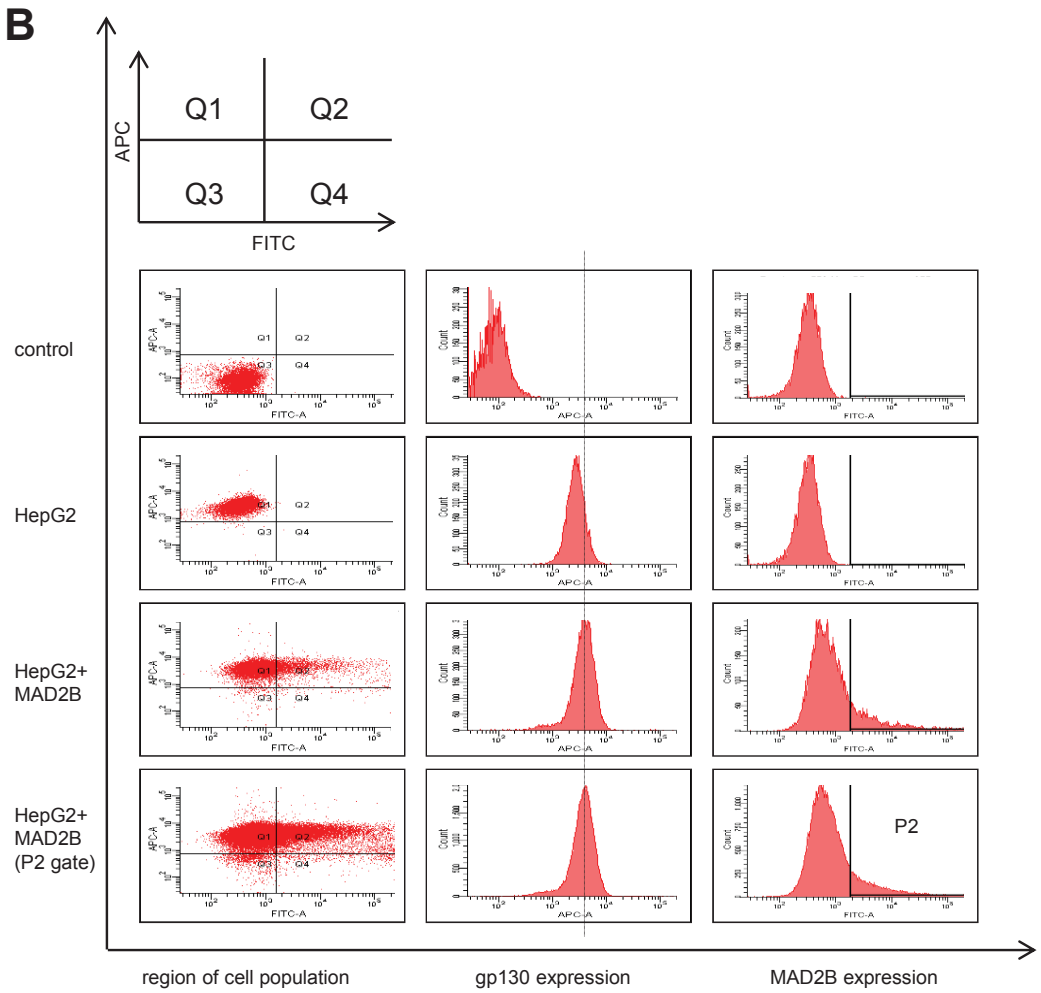

Figure 3.2.3 Interaction of MAD2B and IL-6R led to an increased number of IL-6R and gp130 molecules on the surface of HepG2 cells. HepG2 cells were transiently transfected with a cDNA coding for MAD2B. After 48 h, presence of gp130 and IL-6R was examined by flow cytometry. A. Showed the expression of gp130 and B. Showed the expression of IL-6R on the surface of HepG2 cells. Region of cell population showed the group of cells which were examined in the assay. P2 gate referred to the population of cells which were highly expressing MAD2B. The faint line outlined the increased presence of receptors. MAD2B was GFP-tagged and was detected via FITC. 4-11 mAb for IL-6R and B-S12 from abcam for gp130 labelling was applied and APC-conjugated secondary antibodies were used. The data was analysed by FCS Express 4 Flow program. These experiments were done 3 times.

3.2.4 Interaction of MAD2B and IL-6R led to an increased number of IL-6R and gp130 on the surface of Ba/F3-gp130-IL-6R cells

To confirm that the increased number of IL-6R and gp130 on the cell surface is due to the interaction of IL-6R and gp130, Ba/F3-gp130-IL-6R cells were applied. The cDNA coding for MAD2B was sub-cloned in pMOWS vector which carried the hygromycin resistant gene. Ba/F3-gp130-IL-6R cells were transduced with pMOWS-hygro-MAD2B-GFP. After selection of stably transduced cells by application of hygromycin, the expression of gp130 and IL-6R on the cell surface was examined using flow cytometry. As shown in figure 3.2.4 A and B, Ba/F3-gp130-IL-6R cells expressed IL-6R and gp130 on the cell surface, however, overexpression of MAD2B resulted in an increased expression of IL-6R and gp130 on the membrane of Ba/F3-gp130-IL-6R cells. Ba/F3-gp130 cell did not express IL-6R and MAD2B and cell population detected in Q3 region in which no APC or FITC signal was detected. High expression of IL-6R and gp130 was detected in Ba/F3-gp130-IL-6R cells and the examined group of the cells were located in Q1 in which APC signal was detected but there was no FITC signal. Ba/F3-gp130-IL-6R-MAD2B cells were present in Q2 region in which both FITC and APC signals were detectable and increase number of IL-6R and gp130 on the membrane of cells was clearly shown. Our results elucidated an increased number of gp130 and IL-6R molecules on the membrane of Ba/F3-gp130-IL-6R-MAD2B cells as compared to Ba/F3-gp130-IL-6R cells (Fig3.2.4).

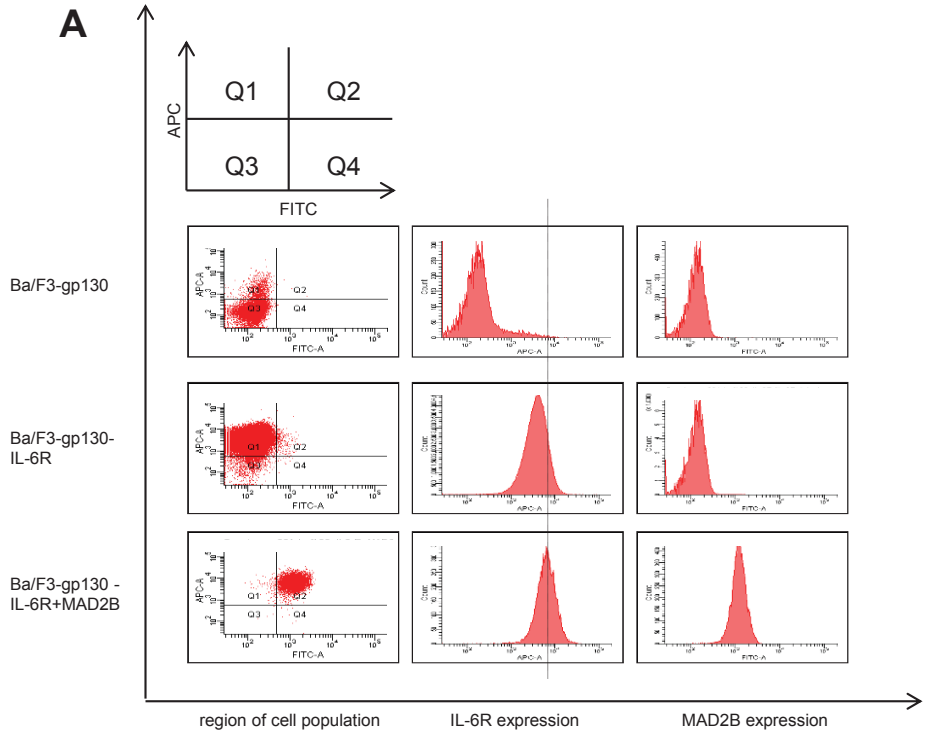
A
Q1
Q2
Q3
Q4
APC
FITC
Ba/F3-gp130
Ba/F3-gp130-IL-6R
Ba/F3-gp130 - IL-6R+MAD2B
region of cell population
IL-6R expression
MAD2B expression

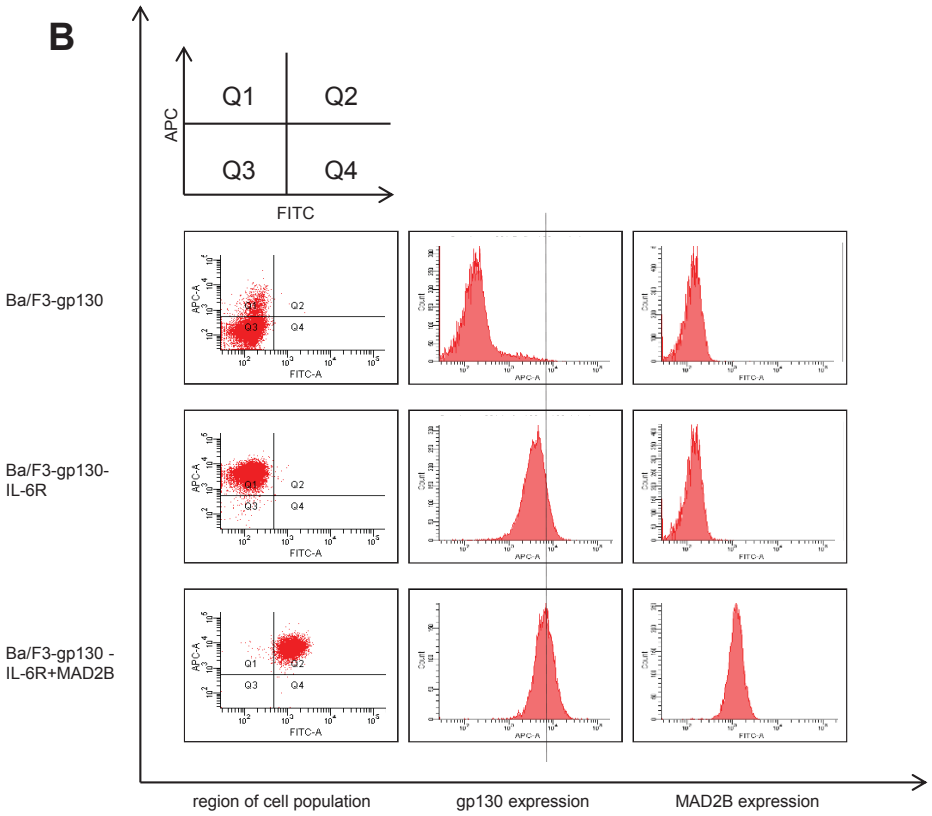
B
Q1
Q2
Q3
Q4
APC
FITC
Ba/F3-gp130
Ba/F3-gp130-IL-6R
Ba/F3-gp130 - IL-6R+MAD2B
region of cell population
gp130 expression
MAD2B expression

Figure 3.2.4: Interaction of MAD2B and IL-6R led to an increased number of IL-6R and gp130 molecules on the surface of Ba/F3-gp130-IL-6R cells. $1x10^6$ Ba/F3-gp130-IL-6R, Ba/F3-gp130-IL-6R-MAD2B, and Ba/F3-gp130 cells were counted and washed with FACS buffer. Afterwards, cells were incubated for 1 h on ice with 4-11 mAb and BS-12 from abcam for IL-6R and gp130 labelling, respectively. Next, cells were washed 3 times with FACS buffer and incubated on ice for 1 h with the secondary antibodies. A. Examination of the presence of IL-6R on the membrane of cells. B. Examination of the presence of gp130 on the cell surface. MAD2B was GFP-tagged and examined *via* FITC and for IL-6R and gp130 APC-conjugated secondary antibody was applied and were detected *via* APC. The data were analysed by FACS Express 4 Flow software. These experiments were done 3 times.

3.2.5 Expression of MAD2B resulted in the stronger phosphorylation of STAT3 through classic IL-6 signaling

The signal transduction of IL-6 is induced by binding of IL-6 to its specific α-receptor (IL-6R). The complex of IL-6/IL-6R activates a homodimer of the signal transducing β-receptor gp130. For signal transduction, IL-6R can either be membrane-bound or soluble and the signaling process is accordingly named classic or trans-signaling (Garbers *et al.*, 2015). MAD2B interacts with the C-terminus of transmembrane IL-6R. We decided to examine if IL-6R and MAD2B interaction which resulted in an increased presence of IL-6R and gp130 on the cell surface resulted in changes in the classic signaling pathway. HEK293 cells were transiently transfected with cDNAs coding for IL-6R, IL-6R3P-A, MAB2B, IL-6R + MAD2B, and IL-6R3P-A + MAD2B. 48 h after transfection, cells were starved for 2 h and then stimulated with 10 ng/ml recombinant IL-6 for 30 min and STAT3 phosphorylation was examined by Western blotting. The activation of STAT3 at time point 0 was used as a control. According to the Western blotting results, phosphorylation of STAT3 was increased after co-expression of MAD2B and IL-6R as compared to HEK293-IL-6R cells. As shown in figure 3.2.5.1 A, in the absence of MAD2B, activation of STAT3 in HEK293-IL-6R and HEK293-IL-6R3P-A cells was similar. However, in the presence of MAD2B, stimulation of HEK293-IL-6R-MAD2B cells resulted in stronger phosphorylation of STAT3 as compared to HEK293-IL-6R3P-A-MAD2B cells in which IL-6R3P-A had no interaction with MAD2B (Fig 3.2.5.1 A). The quantification of 3 independent Western blots showed about 40%

increase in the IL-6-induced phosphorylation of STAT3 in HEK293+IL-6R+MAD2B cells compared to HEK293+IL-6R, HEK293+IL-6R3P-A, and HEK293+IL-6R3P-A+MAD2B cells (Fig 3.2.5.1 B).

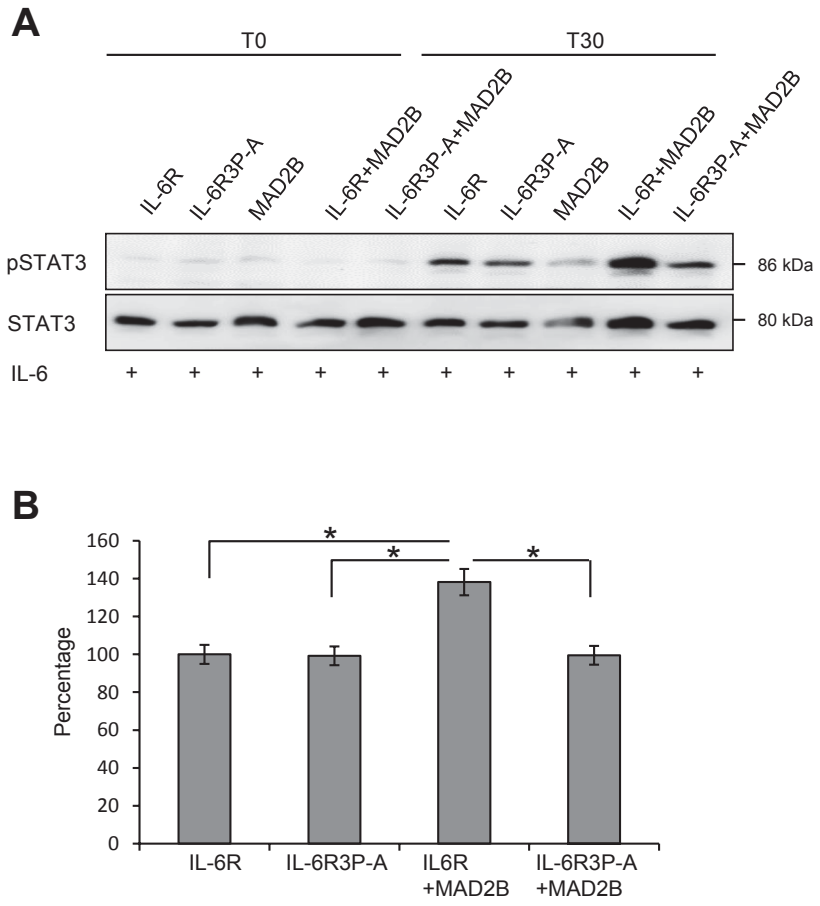

Figure 3.2.5.1: Interaction of MAD2B and IL-6R resulted in stronger phosphorylation of STAT3 after IL-6 stimulation. A. HEK293 cells were transiently transfected with cDNAs coding for IL-6R, IL-6R3P-A, MAD2B, IL-6R+MAD2B, and IL-6R3P-A+MAD2B. After 48 h, the cells were starved and stimulated with 10 ng/ml recombinant IL-6 for 30 min and STAT3 phosphorylation was detected by Western blotting. STAT3 served as the loading control. 124H6 and D3A7 mAbs from Cell Signaling Biotechnology were used for pSTAT3 and STAT3, respectively. This experiment were done 3 times. B. IL-6-induced STAT3 activation was quantified by Image J software. The calculated amount of STAT3 phosphorylation in HEK293-IL-6R was set to 100% and all other values were calculated accordingly.

In order to investigate if the interaction of MAD2B and IL-6R influenced the IL-6-induced STAT3 phosphorylation in cells with endogenous IL-6R/gp130 expression, HepG2 cells were selected. HepG2 cells endogenously express IL-6R and IL-11R. MAD2B cDNA was transiently transfected in HepG2 cells and 48 h after transfection, cells were starved for 2 h, then stimulated for 30 min with recombinant IL-6 (10 ng/ml) and IL-11 (200 ng/ml). pSTAT3/STAT3 was examined by Western blotting. As shown in figure 3.2.5.2 A, IL-6-induced STAT3 activation led to the stronger phosphorylation of STAT3 in cells which expressed MAD2B, whereas IL-11-induced STAT3 phosphorylation was not changed by expression of MAD2B. The quantification of 3 independent Western blots demonstrated that IL-6-induced STAT3 phosphorylation was increased about 20% by overexpression of MAD2B in HEK293 cells (Fig 3.2.5.2 B). Our results demonstrated that heterologous expression of MAD2B and endogenous expression of IL-6R resulted in increased IL-6-induced STAT3 phosphorylation (Fig 3.2.5.2).

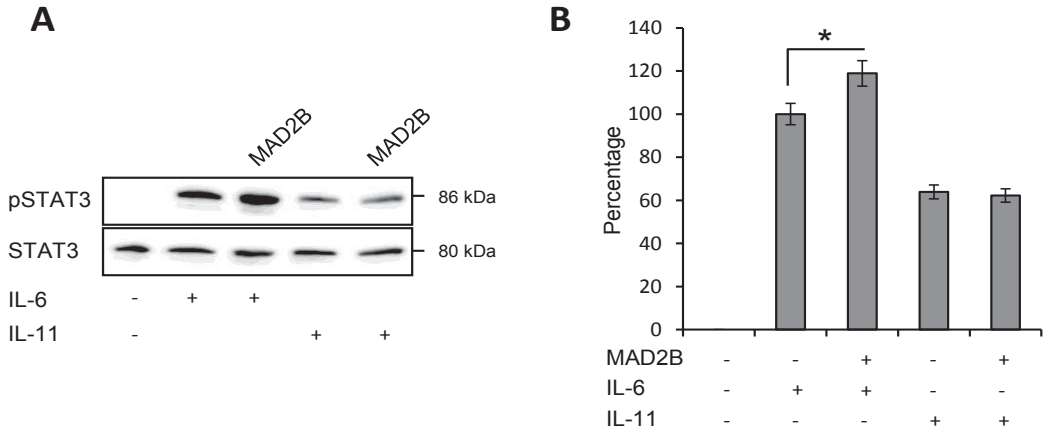

Figure 3.2.5.2: Co-expression of MAD2B and IL-6R affected the STAT3 signaling pathway. A. $5x10^5$ HepG2 cells were seeded and transiently transfected with cDNA coding for MAD2B. 48 h after transfection, cells were starved for 2 h and then stimulated with 10 ng/ml recombinant IL-6 or 200 ng/ml recombinant IL-11. Cells were lysed and Western blotting for pSTAT3/STAT3 was done. STAT3 served as the loading control. 124H6 mAb and D3A7 mAb from Cell Signaling Biotechnology were used for pSTAT3 and STAT3, respectively. This experiment was done 3 times. B. IL-6 induced STAT3 phosphorylation was quantified with Image J software. The calculated amount of STAT3 phosphorylation in HepG2 cells under the stimulation of IL-6 was set to 100% and all other values were calculated accordingly.

3.2.6 Co-expression of MAD2B and IL-6R has no effect on IL-6 trans-signaling

In order to examine the effect of MAD2B and IL-6R interaction on IL-6 trans-signaling, HEK293 cells were transiently transfected with cDNAs coding for IL-6R, IL-6R3P-A, MAD2B, IL-6R+MAD2B, IL-6R3P-A+MAD2B, IL-11R, and IL-11R+MAD2B. Two days after transfection, cells were starved for 2 h and then were stimulated with 10 ng/ml Hyper IL-6 (HIL-6) for 30 min. We used HIL-6, because it binds to gp130 without the need to bind to membrane bound IL-6R and triggers trans-signaling pathway. As shown in figure 3.2.6.1, HIL-6-induction of STAT3 phosphorylation in HEK293-IL-6R, HEK293-IL-6R3P-A, and HEK293-IL-11R with or without expression of MAD2B was similar. Our result revealed that the interaction of MAD2B and IL-6R had no effect on the trans-signaling pathway (Fig 3.2.6.1).

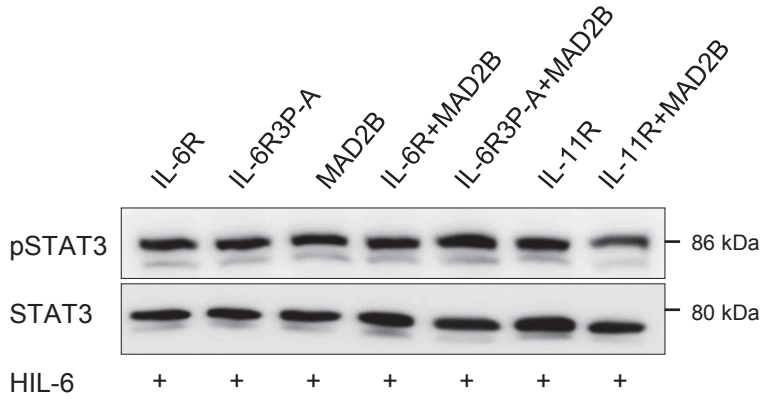

Figure 3.2.6.1: Co-expression of MAD2B and IL-6R has no effect on IL-6 trans-signaling. HEK293 cells were transiently transfected with cDNAs coding for IL-6R, IL-6R3P-A, MAD2B, IL-6R+MAD2B, IL-6R3P-A+MAD2B, IL-11R, and IL-11R+MAD2B. 48 h after transfection, the cells were starved and stimulated with 10 ng/ml HIL-6 for 30 min. Western blotting was done for detection of pSTAT3/STAT3. STAT3 served as loading control. 124H6 mAb and D3A7 mAb from Cell Signaling Biotechnology were used for pSTAT3 and STAT3, respectively. This experiment was done 2 times.

Next, we investigated if the concentration of HIL-6 has any effect on the activation of STAT3. HEK293 cells were transiently transfected with cDNAs coding for MAD2B+IL-6R, MAD2B+IL-6R3P-A, and MAD2B. 48 h after transfection, cells were starved for 2 h and then stimulated for 30 min with HIL-6. Concentration gradients of Hyper IL-6 from 100 to 0 ng/ml was applied. Phosphorylation of STAT3 was analysed by Western blotting. As shown in figure 3.2.6.2, phosphorylation of STAT3 was comparable in HEK293, HEK293+MAD2B+IL-6R, HEK293+MAD2B+IL-6R3P-A, and HEK293+MAD2B cells after stimulation with different HIL-6 concentrations. Our results revealed that the effect of MAD2B on the STAT3 signaling pathway was not dependent on the concentration of HIL-6 (Fig 3.2.6.2)

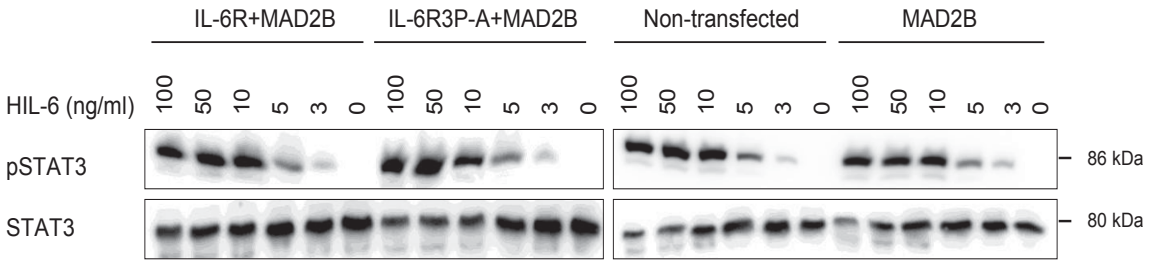

Figure 3.2.6.2: Co-expression of MAD2B and IL-6R did not influence IL-6 trans-signaling. Transiently transfected HEK293 cells with cDNAs coding for IL-6R+MAD2B, IL-6R3P-A+MAD2B, MAD2B, and non-transfected cells were starved for 2 h and then stimulated with different concentrations of HIL-6 for 30 min. Afterwards, cells were lysed and phosphorylation of STAT3 was evaluated by Western blotting. STAT3 served as the loading control. 124H6 mAb and D3A7 mAb from Cell Signaling Biotechnology were used for pSTAT3 and STAT3, respectively. This experiment was done 3 times.

4 Discussion

4.1 Transcytosis of Interleukin (IL-)11 and apical redirection of gp130 is mediated by IL-11 α-receptor

4.1.1 IL-11R1 is sorted to apical and basolateral membranes of polarized MDCK cells

IL-6 and IL-11 are two members of IL-6 cytokine family which share similarities in signal transduction and function. Binding of IL-6 and IL-11 to their specific α-receptors (IL-6R and IL-11R, respectively) induces the homo-dimerization of gp130 and consequently resulted in triggering of downstream signaling pathways. In general, IL-6 is known as a pro- and anti-inflammatory cytokine, whereas IL-11 is involved in proliferation and regeneration of epithelial cells. Albeit IL-11 is less important for the hematopoietic system, it has potent anti-apoptotic and anti-necrotic properties on the intestinal mucosa (Putoczki and Ernst, 2010). Importantly, IL-11R expression on different types of polarized epithelial cells might be assumed as a critical role of IL-11 signaling in these cell types. IL-11R1 is widely expressed and found in the lung, liver, thymus, spleen, kidney, intestinal epithelial cells, bone marrow, and uterus. Intestinal wound-healing critically depends on polarized intestinal epithelial cells and hematopoietic cells-derived IL-11 and both processes are severely impaired in IL-11R1 deficient mice. Administration of IL-11 is protective in several disease states, among them colitis, renal ischemia and reperfusion injury, experimental autoimmune encephalomyelitis, acute liver injury and cardiac fibrosis after myocardial infarction (Gurfein *et al.*, 2009; Lee *et*

al., 2012; Nishina *et al.*, 2012a; Obana M *et al.*, 2010; Qiu *et al.*, 1996). In gastric tumors, IL-11R1 deficient mice displayed a delayed onset and reduced overall tumor formation (Putoczki *et al.*, 2014).

To generate the asymmetric cell surface in polarized epithelial cells, recently synthetized proteins and lipids should be sorted differentially to apical or basolateral sides. IL-6R and gp130 are localized in the basolateral membrane of polarized MDCK cells (Martens *et al.*, 2000; Doumanov *et al.*, 2006). However, the localization of IL-11R1 in polarized cells was not studied so far. Analysing the intracellular domain of IL-11R1 revealed the absence of well-known basolateral sorting signals. Examination of IL-11R1 sorting in polarized MDCK-IL-11R1 cells demonstrated that IL-11R1 was localized on both basolateral and apical membranes. Co-localization of IL-11R1 with Na^+-K^+ ATPase on the basolateral but not apical surface of polarized MDCK cells confirmed the apical and basolateral sorting pattern of IL-11R1. Interestingly, our data revealed that stimulation of polarized MDCK-IL-11R1 with IL-11 did not change the localization of IL-11R1 which suggested that IL-11R1 was sorted independent on the cytokine stimulation. Presence of ligand in the media is one of the important factors which might change the localization of receptors in polarized cells (Orlando and Guo, 2009). For instance, polymeric immunoglobulin receptor (pIgR) is mainly located in the basolateral surface of polarized cells, but under the stimulation with pIg, pIgR is detoured to the apical membranes (Mostov, 1994). In accordance to the sorting pattern of IL-11R1, IL-11 stimulation of polarized MDCK-IL-11R1 cells from the apical and basolateral sides resulted in the phosphorylation of STAT3 from the both sides. IL-11-induction of STAT3 phosphorylation from the apical and basolateral sides of polarized MDCK-IL-11R1 cells elucidated that the apically transported IL-11R1 was biologically active. However, IL-6 stimulation of polarized MDCK-IL-6R cells resulted in the phosphorylation of STAT3 from just basolateral side which revealed that IL-6R sorting was restricted to the basolateral surface of polarized MDCK cells. Our data suggested that IL-11R1 was sorted to the apical and basolateral membrane of polarized MDCK cells independent on the presence of IL-11.

4.1.2 The apical sorting signal of IL-11R1 is located on the intracellular domain

Basolateral sorting signals are mainly located in the cytoplasmic domain of transmembrane receptors. There are two main basolateral sorting signals, di-Leucine and tyrosine-based motifs (Mellman and Nelson, 2008). However, apical signals can be localized throughout the apically sorted proteins. IL-6R is mainly localized on the basolateral surface of epithelial polarized cells and contains two discontinues basolateral signaling motifs, the membrane-proximal tyrosin-based motif (YSLG) and the membrane-distal di-leucine-type motif (LI). Interestingly, deletion of the intracellular domain of the IL-6R led to the apical delivery of IL-6R in polarized MDCK cells (Martens *et al.*, 2000). gp130 is also located on the basolateral surface of polarized MDCK cells (Doumanov *et al.*, 2006). Generation of IL-11R2 and IL-6R/IL-11R1 chimeras demonstrated that the IL-11R1 intracellular domain contained the apical sorting signal. IL-11R2 lacks the 32 amino acids of IL-11R1 c-terminus as a result of differential splicing (Cherel *et al.*, 1995). Interestingly, our study showed that IL-11R2 is mainly sorted to the basolateral surface of polarized MDCK cells. In addition, localization of receptors in polarized MDCK-IL-6R$_{ECD}$/IL-11R1$_{S,TM,ICD}$ and MDCK-IL-6R$_{ECD,S,TM}$/IL-11R1$_{ICD}$ cells on apical and basolateral surfaces and in MDCK-IL-11R$_{ECD}$/IL-6R$_{S,TM,ICD}$, MDCK-IL-11R$_{ECD,S,TM}$/IL-6R$_{ICD}$, and MDCK-IL-11R2 cells on just the basolateral membrane revealed that IL-11R1 intracellular domain is the critical domain which determines the sorting pattern of IL-11R and IL-11R/IL-6R chimeras. Intriguingly, IL-6-induced phosphorylation of STAT3 in polarized MDCK-IL-6R$_{ECD}$/IL-11R1$_{S,TM,ICD}$ and MDCK-IL-6R$_{ECD,S,TM}$/IL-11R1$_{ICD}$ cells from apical and basolateral membranes confirmed that receptors were not only localized on the apical and basolateral sides, but they were also biologically active and functional. However, in MDCK-IL-11R$_{ECD}$/IL-6R$_{S,TM,ICD}$, MDCK-IL-11R$_{ECD,S,TM}$/IL-6R$_{ICD}$, and MDCK-IL-11R2 cells, IL-11 stimulation from apical and basolateral sides resulted in the phosphorylation of STAT3 only from the basolateral side. Our data elucidated that IL-11R1 intracellular domain is the prominent domain which governs the sorting pattern of the IL-11R1 in polarized MDCK cells. Intriguingly, replacement of the intracellular domain of IL-11R1 with IL-6R intracellular domain resulted in the alteration of receptor sorting pattern in polarized MDCK cells from apical and basolateral to only basolateral surface.

4.1.3 IL-11R1 is a cytokine transcytosis receptor

Transcytosis is a critical process to transfer macro molecules through a cell to the opposite cell surface. It is a strategy used by multicellular organisms to selectively move material between two different environments while maintaining the distinct compositions of those environments (Tuma and Hubbard, 2003). This mechanisms is responsible for sorting of receptors which are localized first in the basolateral membrane and then according to the endocytosis process be directed to the apical surface (Orzech *et al.*, 2000). Our data identified that the intracellular domain of IL-11R1 is carrying the transcytosis signal. The result of transcytosis assay showed that IL-11R1 first was transported to the basolateral surface of polarized cells and then independent on presence of cytokines was shipped to the apical side. IL-11R2 was mainly located in the basolateral side of polarized cells because of the lack of the intracellular domain (transcytosis signal). IL-11R1 transcytosis resulted transportation of IL-11 from the basolateral to the apical side. Stimulation of polarized MDCK-IL-11R1, MDCK-IL-6R_{ECD}/IL-11$R_{S,TM,ICD}$ and MDCK-IL-6$R_{ECD,S,TM}$/IL-11R_{ICD} with IL-11 or IL-6 led to transcytosis of biologically active cytokine to the apical side. Intriguingly, IL-11R1 deficient mice demonstrated the overall importance of IL-11 signaling in regeneration and tumor development, including polarized epithelial cells. Selective deletion of the intracellular domain in knockout mice will reveal if polarized expression of IL-11R1 and transcytosis of IL-11 has an important (patho-) physiological role in regeneration and tumor development. However, in polarized MDCK-IL-11R_{ECD}/IL-6$R_{S,TM,ICD}$, MDCK-IL-11$R_{ECD,S,TM}$/IL-6R_{ICD}, and MDCK-IL-11R2 cells, presence of IL-11 in the basolateral media did not lead to transcytosis of IL-11 to the apical side which supported our previous data regarding to the critical role of the intracellular domain of IL-11R1 in transcytosis of the receptors and ligands. Interestingly, our results showed that the stimulation of polarized MDCK-IL-11R1 cells from apical side did not result in transcytosis of IL-11 to the basolateral side. Our data revealed that the transcytosis of IL-11R1 happened just from basolateral to apical side but not in the reverse direction. Endocytosis pathways are used for internalization of nutrients, signal transduction regulation, and modulation of plasma membrane composition. There are different internalization pathways. Well-studied endocytosis pathways are Clathrin-dependent endocytosis (CDE) which is dependent on clathrin molecule and Clathrin-independent

endocytosis that generally is dependent on cholesterol-rich membrane domains (Orzech *et al.*, 2000; Orlando and Guo, 2009). The endocytosis of IL-6R is dependent on the clathrin pathway (Fujimoto *et al.*, 2015). Intriguingly, our data demonstrated that IL-11R1 endocytosis is clathrin-dependent. The half-life of IL-6R and IL-11R was comparable and were about 120 and 110 min, respectively. Inhibition of IL-6R and IL-11R1 endocytosis by Dynasore (clathrin-dependent endocytosis inhibitor) but not with Pitstop 2 (clathrin-independent endocytosis inhibitor) demonstrated that both receptors were internalized *via* clathrin-dependent endocytosis. Transcytosis is based on the clathrin-dependent endocytosis pathway (Orlando and Guo, 2009). Dependency of IL-11R1 endocytosis to clathrin, reveals the outstanding role of clathrin-dependent endocytosis pathway in the transcytosis of IL-11R1.

4.1.4 gp130 is transcytosed by IL-11R1

The IL-6/IL-11 signal transducing chain gp130 is ubiquitously expressed on all cells of the body. It was shown that the di-leucine motif (L^{786} L^{787}) in the cytoplasmic domain of gp130 was responsible for the internalization of the receptor (Dittrich *et al.*, 1996). In addition, these di-leucine motif has been identified as the prominent motif for basolateral sorting of receptors in polarized cells (Doumanov *et al.*, 2006). Our data demonstrated that gp130 was localized on the basolateral and apical membranes in MDCK-IL-11R1 cells and in MDCK-IL-6R cells only on basolateral side. Intriguingly, apically delivered IL-11R1 and 2 were responsive to the stimulation of IL-11, which suggested apical sorting of gp130 in these groups of cells. gp130 might be directly transported to the apical membrane or first be sorted to the basolateral surface and then transported to the apical membrane. Apical localization of gp130 was, however, suggested previously for heterodimeric gp130/LIFR-signaling. LIFR is expressed in an un-polarized fashion in polarized MDCK cells, albeit an apical expression was not shown directly (Buk *et al.*, 2004). Glycosylphosphatidylinositol (GPI)-anchored CNTFR is the α-receptor for CNTF-induced signaling *via* CNTF:CNTFR:gp130:LIFR-complexes. CNTFR was specifically found on the apical site of polarized MDCK cells (Buk *et al.*, 2004), because GPI-anchorage of membrane proteins promote their apical sorting (Simons and Ikonen,

1997). In accordance with our findings, expression of CNTFR renders polarized MDCK cells also responsive to CNTF from the apical site *via* CNTF:CNTFR:gp130:LIFR complexes (Buk *et al.*, 2004), suggesting that gp130 was tagged along by CNTFR and LIFR to the apical membrane. Interestingly, stimulation of polarized cells with Hyper IL-6 which just bind to gp130 without the need of other α-receptors (IL-6R or IL-11R) revealed that gp130 was transcytosed along with IL-11R1. These results, however, do not exclude the direct transportation of gp130 to the apical side.

In this study, we clarified that IL-11R1 was located on the basolateral and apical surface of polarized MDCK cells, whereas IL-11R2 was located mainly on the basolateral side. In addition, examination of the sorting pattern analysis of IL-6/IL-11R chimeras revealed that the apical sorting signal of IL-11R1 was located on the intracellular domain of IL-11R1. Interestingly, IL-11R1 in the apical surface was biologically active. Stimulation of polarized MDCK-IL-11R1 cells with IL-11 from apical side resulted in the activation of STAT3. Moreover, the comparison between the IL-6R and IL-11R internalization pathways elucidated that both of them were internalized *via* the clathrin-dependent pathway and the half-life of IL-6R and IL-11R on the membrane was comparable. Intriguingly, herein, we reported IL-11R1 as the first transcytosed cytokine receptors. Our data demonstrated that IL-11R1 was primarily sorted on basolateral surface of polarized cells and then with or without binding to the cytokine was transcytosed to the apical surface. Consequently, transcytosis of the receptor led to the transfer of IL-11 to the apical side of polarized cells. Moreover, we discovered that gp130 was also transcytosed along with IL-11R to the apical side (Fig 4.1).

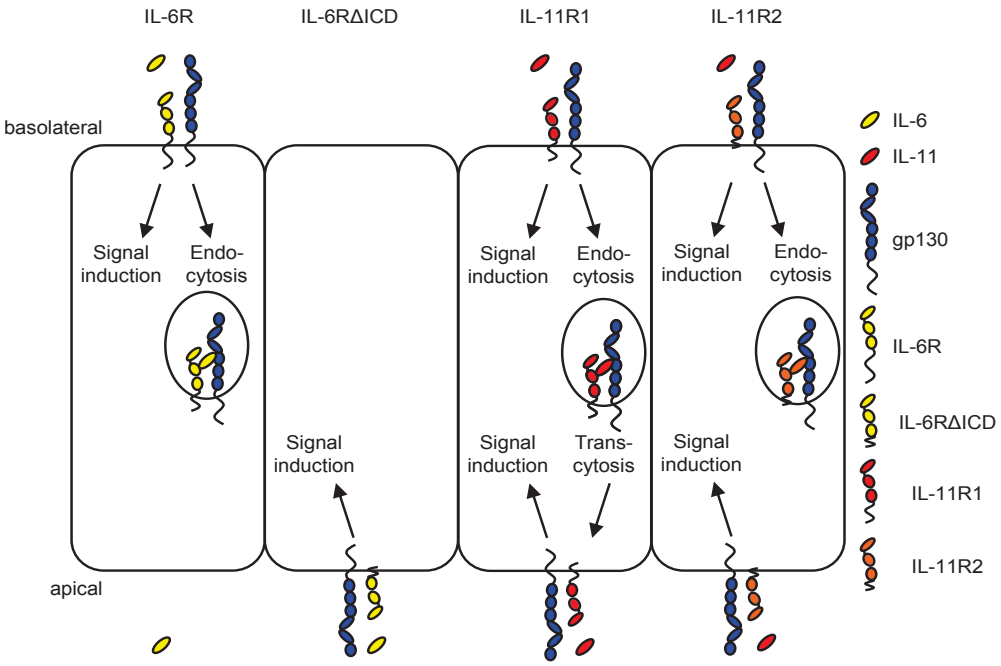

Fig 4.1: Schematic overview of apical/basolateral sorting and mode of activation in polarized MDCK cells expressing IL-6R, IL-6RΔICD, IL-11R1 and IL-11R2. Left: IL-6R expressing cell; middle left: IL-6RΔICD expressing cell; middle right: IL-11R1 expressing cell; right: IL-11R2 expressing cell.

4.2 Identification of MAD2B as a novel regulatory protein of IL-6 classic signaling

4.2.1 "OOxPxxxpP" is the binding motif of MAD2B in the IL-6R intracellular domain

IL-6 is one of the members of IL-6 type cytokine family with wide varieties of functions. IL-6 needs a complex of receptors for triggering of the signaling pathways. The receptor complex consists of binding type I transmembrane glycoprotein termed IL-6R and the type I transmembrane signal transducer protein gp130. Transmembrane IL-6R is expressed only on a few cell types such as macrophages, neutrophils, some types of T-cells and hepatocytes, while gp130 is ubiquitously expressed (Oberg *et al.*, 2006; Scheller and Rose-John, 2006). IL-6R consists of three main domains, extracellular, transmembrane and intracellular domain. The intracellular domain of IL-6R consists of 83 amino acids which are not involved in signaling but has role in internalization and basolateral sorting of the receptor (Martens *et al.*, 2000). Using yeast two-hybrid-based interaction trap with intracellular domain of IL-6R as a bait, we identified MAD2B as a novel partner of IL-6R intracellular domain. The mitotic arrest deficient protein MAD2B (MAD2L2) is a member of MAD family (Cahill *et al.*, 1999). MAD2B is a chromatin binding protein and is critically involved in both cell cycle regulation and DNA repair (Aravind and Koonin, 1998; Pfleger *et al.*, 2001). MAD2B contains a HORMA structure domain, which is involved in protein-protein interactions, protein oligomerization, and chromatin state recognition (Hanafusa *et al.*, 2010). Interestingly, MAD2B is known as the binding protein of T cell factor 4 (TCF4) and their interaction abolished the DNA binding ability of TCF4. Moreover, knock-down of MAD2B in SW480 colorectal cancer led to the conversion of epithelial cell to a mesenchymal fibroblastoid, because of blockade of E-cadherin expression and induction of mesenchymal markers (Hong *et al.*, 2009). Intriguingly, MAD2 interacted with c-terminus of insulin receptors (IR) and represented a novel binding partner for IR, however, the role of MAD2 in insulin signaling was not elucidated (O'Neill *et al.*, 1997). We have shown by Nanotrap assay that MAD2B bound to the intracellular domain of IL-6R; "OOxP_{426}xxx$p_{430}P_{431}$" is the binding motif.

Mutation on these three prolines resulted in the loss of MAD2B binding to the IL-6R. The result of Nanotrap assay showed that MAD2B needed almost the full length of IL-6R C-terminal for efficient binding. However, the results of immunocytochemistry assay demonstrated co-localization of MAD2B and IL-6RΔ10, IL-6R-Δ20, and IL-6R-Δ30 but not IL-6R3P-A deletion variants in HeLa cells. Revealed that the "OOxP_{426}xxx$p_{430}P_{431}$" motif was necessary for IL-6R and MAD2B binding in cells. Interestingly, the localization of MAD2B was changed according to the presence or absence of IL-6R binding motif. In HeLa cells, overexpression of MAD2B and IL-6R resulted in co-localization of MAD2B with IL-6R on the membrane of cells, whereas MAD2B localization in the absence of IL-6R was restricted to nucleus and cytoplasm. Interestingly, in accordance to our finding, it was shown that interaction of Sim2 protein with MAD2B affected the distribution and localization of MAD2B in primary culture neurons. Sim2 plays a critical role in development of CNS (Meng *et al.*, 2012). Our data demonstrated that MAD2B is a binding partner of IL-6R and co-expression of MAD2B and IL-6R resulted in the alteration of MAD2B localization.

4.2.2 Co-expression of MAD2B and IL-6R has no influence on the cell cycle progression

MAD2B is a chromatin binding protein and is critically involved in both cell cycle regulation and DNA repair (Aravind and Koonin, 1998; Pfleger *et al.*, 2001). MAD2B can affect APC/C by binding to CDH1 and/or CDC20. CDH1 and CDC20 are activators of APC the complex which is involved in the delivery of cells from G2 to M phase of the cell cycle (Chen and Fang, 2001). Furthermore, MAD2B was described as an accessory, non-catalytic subunit of the translation DNA polymerase yeta (δ), and knockdown of MAD2B resulted in hypersensitivity to DNA damage (Zhang *et al.*, 2007). Interestingly, it was shown that MAD2B is essential for the development of primordial germ cells (PGCs) by regulation of cell cycle. Knocking out of MAD2B in PGCs cells resulted in failure of G2 arrest and elimination of cells by apoptosis due to the deficient cell cycle progression (Cheung *et al.*, 2006; Gan *et al.*, 2008). However, the results of double thymidine block assay revealed that

transient co-expression of MAD2B and IL-6R in HEK293 did not influence the cell cycle progression. Intriguingly, in accordance to our results, interaction of small GTPase RAN, a well-known cell cycle regulator, with MAD2B did not affect the cell cycle as well. Interaction of small GTPase and MAD2B control the spindle checkpoint mitosis and regulated the nocleocytoplasm (Medendorp *et al.*, 2010). Our study demonstrated that interaction of MAD2B and IL-6R did not change the cell cycle progression.

4.2.3 Interaction of MAD2B and IL-6R resulted in an increased number of IL-6R and gp130 molecules on the surface of HepG2 cells and stronger STAT3 phosphorylation via classic signaling

MAD2B interacts with clathrin light chain and is acting as an inhibitor of ubiquitin ligases (Medendorp *et al.*, 2010; Pfleger *et al.*, 2001). MAD2B can be assumed as a part of the scaffold protein complexes due to the interaction with clathrin light chain (Medendorp *et al.*, 2010). MAD2B and IL-6R interaction might act as a regulator of gp130 degradation. gp130 is degraded *via* ubiquitination pathway and c-CbI is the ubiquitin ligase of gp130 (Tanaka *et al.*, 2008). Our study revealed that overexpressing of MAD2B in HepG2 and Ba/F3-gp130-IL-6R cells, resulted in an increased number of IL-6R and gp130 molecules on the cell surface. High number of IL-6R and gp130 as a result of MAD2B overexpression might counted by an alteration in the internalization process of IL-6R and gp130. Moreover, MAD2B might affect the ubiquitination, endocytosis, and degradation of gp130 and IL-6R which needs to be investigated.

In this study we have shown that overexpression of MAD2B in HepG2 cells resulted in increased numbers of IL-6R and gp130 on the cells surface. In addition, our investigation revealed that expression of MAD2B resulted in an increased number of IL-6R and gp130 molecules on the cell surface of Ba/F3gp-130-IL-6R-MAD2B cells compared to Ba/F3gp-130-IL-6R cells. In accordance to this finding, we revealed that co-expression of MAD2B and IL-6R resulted in stronger IL-6-induced phosphorylation of STAT3. Stimulation of HepG2 cells with recombinant IL-11 and IL-6, showed the stronger IL-6-induced phosphorylation of

STAT3 in HepG2+MAD2B cells, while IL-11 stimulation did not affect STAT3 phosphorylation. Moreover, stimulation of HEK293 cells with recombinant IL-6 showed that HEK293-IL-6R+MAD2B cells displayed stronger STAT3 phosphorylation as compared to HEK293-IL-6R3P-A+MAD2B cells. Interestingly, our data suggested that MAD2B and IL-6R interaction was specifically affect the IL-6 classic signaling. Stimulation of HEK293 cells in the presence or absence of MAD2B and IL-6R with Hyper IL-6 did not change the phosphorylation of STAT3. Our results suggested that the effect of MAD2B on IL-6 signalling pathway was dependent on the binding of cytokine to the transmembrane IL-6R. Collectively, MAD2B and IL-6R interaction is specific and influence the phosphorylation of STAT3. Our study showed the high number of gp130 and IL-6R on the surface of the cells as well as stronger phosphprylation of STAT3 as a result of MAD2B and IL-6R interaction.

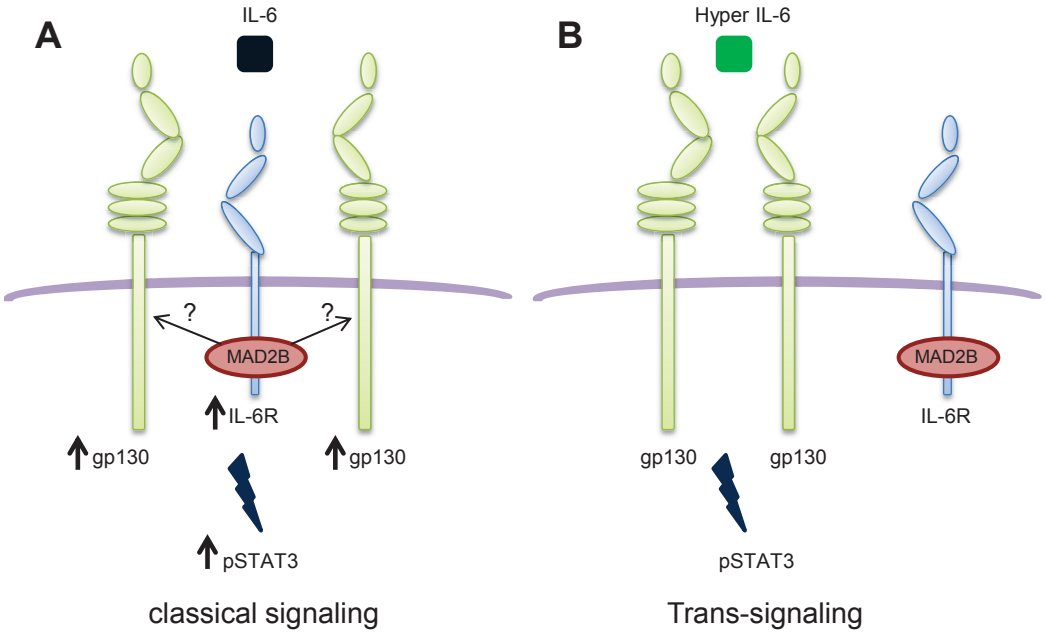

Fig 4.1: Co-expression of IL-6R and MAD2B affect the classic signaling of IL-6. A. Co-expression of MAD2B and IL-6R results in an increased number of IL-6R and gp130 on the surface of cells and subsequently, lead to the strong phosphorylation of STAT3. B. Co-expression of MAD2B and IL-6R has no effect on trans-signaling of IL-6R.

Summary

Interleukin (IL-)11 is involved in various processes, including intestinal and cardial regeneration and tumor progression. IL-11 signaling *via* one of the individual IL-11 α-receptor splice variants IL-11R1 or IL-11R2 and the signal-transducing β-receptor gp130 is frequently conducted at cellular barriers. The results of this thesis show that biologically active IL-11R1/2:gp130 receptor complexes were localized on apical and basolateral membranes of polarized cells, whereas IL-6 signaling *via* IL-6R:gp130 complexes was restricted to the basolateral side. Consequently, IL-11R1/2 forced apical redirection of gp130. Moreover, basolaterally supplied IL-11 was transported and released to the apical extracellular space by transcytosis exclusively mediated by IL-11R1, whereas the IL-6R and IL-11R2 had no transcytosis activity. Transcytosis of IL-11 was dependent on the intracellular domain of IL-11R1, and synthetic transfer of the intracellular domain of IL-11R1 to IL-6R facilitates transcytosis of IL-6. Finally, expression of IL-11R1 renders gp130 into a transcytosis receptor of IL-6:sIL-6R complexes, specifically inducing IL-6 trans-signaling. Our data define the IL-11R as the first cytokine receptor with full transcytotic activity by which IL-11 and IL-6/sIL-6R are transported across cellular barriers.

IL-6 is a multifunctional cytokine with outstanding pro- and anti-inflammatory properties. IL-6 activates cells by binding to the soluble or membrane-bound forms of IL-6R, which recruits a gp130 homodimer. In order to discover the cytoplasmic binding partners of the IL-6R a yeast-two-hybrid assay was performed. The results identified MAD2B as one of the binding partners of IL-6R intracellular domain. Our study identified the binding motif of MAD2B in the intracellular domain of IL-6R, "$OOxP_{426}xxxp_{430}$ P_{431}". Interestingly, co-expression of MAD2B and IL-6R did not affect the cell cycle, although MAD2B has a critical role in cell cycle regulation. However, the interaction of MAD2B and IL-6R modulated the localization of MAD2B and resulted in the presence of MAD2B on the plasma membrane of HeLa cells. Moreover, MAD2B and IL-6R interaction resulted in stronger phosphorylation of STAT3 *via* classic signaling. Intriguingly, overexpression of MAD2B resulted in an increased number of IL-6R and gp130 molecules on the cell-surface of HepG2 and Ba/F3-gp130-IL-6R cells. Our study identified MAD2B as a binding partner of IL-6R and outlined the effect of MAD2B on IL-6-induced activation of the STAT3 signalling pathway.

Zusammenfassung

Interleukin (IL)-11 ist in verschiedenste Prozesse involviert, wie die Regeneration des Darmepithels, des Herzens und auch in die Tumorprogression. Die Signaltransduktion von IL-11 nach Bindung an eine der beiden Spleißvarianten des α-Rezeptors (IL-11R1 und IL-11R2) über den β-Rezeptor gp130 findet ständig an zellulären Grenzflächen statt. In dieser Arbeit konnte gezeigt werden, dass der biologisch aktive Signaltransduktionskomplex IL-11R1/2:gp130 sowohl in der apikalen, als auch in der basolateralen Membran von polarisierten Zellen lokalisiert war, wohingegen die IL-6-Signaltransduktion über den IL-6R:gp130 Komplex auf die basolaterale Membran begrenzt war. Die Expression des IL-11R1/2 induzierte dabei die apikale Sortierung von gp130. Außerdem wurde basolateral appliziertes IL-11 per Transzytose auf der apikalen Seite in den Überstand abgegeben, wobei dies ausschließlich durch den IL-11R1 vermittelt wurde, während der IL-6R und der IL-11R2 keine Transzytose zeigten. Für die Transzytose war die intrazelluläre Domäne des IL-11R1 verantwortlich, welche durch gentechnischen Transfer in den IL-6R auch zur Transzytose von IL-6 führte. Schließlich führte auch die Expression vom IL-11R1 dazu, dass gp130 in der Lage war, IL-6 in Komplex mit dem löslichen IL-6R auf die apikale Seite zu transportieren, also zu einer Transzytose, die spezifisch Transsignaltransduktion induzierte. Diese Ergebnisse identifizieren den IL-11R als den ersten Zytokinrezeptor mit Transzytose-Aktivität, wodurch IL-11 und IL-6/sIL-6R-Komplexe über zelluläre Grenzflächen transportiert werden können.

IL-6 ist ein multifunktionelles Zytokin mit herausragenden pro- und anti-entzündlichen Eigenschaften. Der signaltransduzierende Rezeptorkomplex für IL-6 besteht aus dem IL-6R in membrangebundener oder löslicher Form und einem gp130-Homodimer. Ein detailliertes Wissen über die Struktur des IL-6R, seine Lokalisation und seine Bindungspartner ist von zentraler Bedeutung, um die Regulation der Signaltransduktion zu verstehen und zu beeinflussen. Die Ergebnisse eines *yeast-two-hybrid* Experiments zeigten, dass MAD2B ein Interaktionspartner des IL-6R ist. Das *Mitotic arrest deficient protein* (MAD2B) ist ein Mitglied der MAD Familie, deren Mitglieder verschiedene physiologische Funktionen haben. MAD2B fungiert als Inhibitor von Ubiquitin-Ligasen wie CDC20 und CDH1 und ist an der Bildung des Anaphase-fördernden Komplexes (APC) beteiligt. Die Interaktion mit der leichten Kette von Clathrin deutet außerdem auf eine Funktion von MAD2B für das Zytoskelett hin. Unsere Ergebnisse zeigen, dass die intrazelluläre Domäne des IL-6R Sequenz (OOxPxxxpP) enthält, welche ein Bindemotiv für MAD2B darstellt. Eine Überexpression von

MAD2B und dem IL-6R hatte trotz der prominenten Rolle von MAD2B im Zellzyklus auf diesen keinen Einfluss. Allerdings änderte die gleichzeitige Überexpression und damit einhergehende Interaktion die Lokalisation von MAD2B, das dadurch verstärkt an der Zellmembran auftrat. Außerdem führte eine Überexpression von MAD2B zu einer stärkeren Aktivierung des STAT3-Signalweges und interessanterweise zu einer verstärkten Oberflächenexpression der Rezeptoren gp130 und IL-6R auf HepG2- und Ba/F3-gp130-IL-6R-Zellen. Unsere Ergebnisse weisen eine Interaktion von MAD2B mit dem IL-6R nach und belegen eine Rolle von MAD2B bei der IL-6-vermittelten Signaltransduktion.

Literature

Aitsebaomo, J., Srivastava, S., Zhang, H., Jha, S., Wang, Z., Winnik, S., Veleva, A. N., Pi, X., Lockyer, P., Faber, J. E. & Patterson, C. (2011). Recombinant human interleukin-11 treatment enhances collateral vessel growth after femoral artery ligation. *Arterioscler Thromb Vasc Biol* 31(2): 306-312.

Alfalah, M., Jacob, R. & Naim, H. Y. (2002). Intestinal dipeptidyl peptidase IV is efficiently sorted to the apical membrane through the concerted action of N- and O-glycans as well as association with lipid microdomains. *J Biol Chem* 277(12): 10683-10690.

Andoh, A., Zhang, Z., Inatomi, O., Fujino, S., Deguchi, Y., Araki, Y., Tsujikawa, T., Kitoh, K., Kim-Mitsuyama, S., Takayanagi, A., Shimizu, N. & Fujiyama, Y. (2005). Interleukin-22, a member of the IL-10 subfamily, induces inflammatory responses in colonic subepithelial myofibroblasts. *Gastro* 129(3): 969-984.

Angel, P., Imagawa, M., Chiu, R., Stein, B., Imbra, R. J., Rahmsdorf, H. J., Jonat, C., Herrlich, P. & Karin, M. (1987). Phorbol ester-inducible genes contain a common cis element recognized by a TPA-modulated trans-acting factor. *Cell* 49(6): 729-739.

Aravind, L. & Koonin, E. V. (1998). The HORMA domain: a common structural denominator in mitotic checkpoints, chromosome synapsis and DNA repair. *Trends Biochem Sci* 23(8): 284-286.

Balcarova-Ständer, J., Pfeiffer, S. E., Fuller, S. D. & Simons, K. (1984). Development of cell surface polarity in the epithelial Madin-Darby canine kidney (MDCK) cell line. *EMBO J* 3(11): 2687-2694.

Bamba, S., Andoh, A., Yasui, H., Makino, J., Kim, S. & Fujiyama, Y. (2003). Regulation of IL-11 expression in intestinal myofibroblasts: role of c-Jun AP-1- and MAPK-dependent pathways. *Am J Physiol Gastrointest Liver Physiol* 285(3): G529-538.

Baran, P., Nitz, R., Grötzinger, J., Scheller, J. & Garbers, C. (2013). Minimal interleukin 6 (IL-6) receptor stalk composition for IL-6 receptor shedding and IL-6 classic signaling. *J Biol Chem* 288(21): 14756-14768.

Barrett, E., Brothers, S., Wahlestedt, C. & Beurel, E. (2014). I-BET151 selectively regulates IL-6 production. *Biochim Biophys Acta* 1842(9): 1549-1555.

Baumann, H., Wang, Y., Morella, K. K., Lai, C. F., Dams, H., Hilton, D. J., Hawley, R. G. & Mackiewicz, A. (1996). Complex of the soluble IL-11 receptor and IL-11 acts as IL-6-type cytokine in hepatic and nonhepatic cells. *J Immunol* 157(1): 284-290.

Bazan, J. F. (1989). A novel family of growth factor receptors: a common binding domain in the growth hormone, prolactin, erythropoietin and IL-6 receptors, and the p75 IL-2 receptor beta-chain. *Biochem Biophys Res Commun* 164(2): 788-795.

Bazan, J. F. (1990).Structural design and molecular evolution of a cytosine receptor superfamily. *Proc Natl Acad Sci U S A* 87(18): 6934-6938.

Bettelli, E., Carrier, Y., Gao, W., Korn, T., Strom, T. B., Oukka, M., Weiner, H. L. & Kuchroo, V. K. (2006). Reciprocal developmental pathways for the generation of pathogenic effector TH17 and regulatory T cells. *Nature* 441(7090): 235-238.

Bharadwaj, R. & Yu, H. (2004). The spindle checkpoint, aneuploidy, and cancer. *Oncogene* 23(11): 2016-2027.

Boulanger, M. J., Bankovich, A. J., Kortemme, T., Baker, D. & Garcia, K. C. (2003). Convergent mechanisms for recognition of divergent cytokines by the shared signaling receptor gp130. *Mol Cell* 12(3): 577-589.

Boulanger, M. J. & Garcia, K. C. (2004). Shared cytokine signaling receptors: structural insights from the gp130 system. *Adv Protein Chem* 68 (10): 107-146.

Buk, D. M., Waibel, M., Braig, C., Martens, A. S., Heinrich, P. C. & Graeve, L. (2004). Polarity and lipid raft association of the components of the ciliary neurotrophic factor receptor complex in Madin-Darby canine kidney cells. *J Cell Sci* 117: 2063-2075.

Burnett, A. F., Biju, P. G., Lui, H. & Hauer-Jensen, M. (2013). Oral interleukin 11 as a countermeasure to lethal total-body irradiation in a murine model. *Radiat Res* 180(6): 595-602.

Cahill, D. P., da Costa, L. T., Carson-Walter, E. B., Kinzler, K. W., Vogelstein, B. & Lengauer, C. (1999). Characterization of MAD2B and other mitotic spindle checkpoint genes. *Genomics* 58(2): 181-187.

Camporeale, A., Marino, F., Papageorgiou, A., Carai, P., Fornero, S., Fletcher, S., Page, B. D., Gunning, P., Forni, M., Chiarle, R., Morello, M., Jensen, O., Levi, R., Heymans, S. & Poli, V. (2013). STAT3 activity is necessary and sufficient for the development of immune-mediated myocarditis in mice and promotes progression to dilated cardiomyopathy. *EMBO Mol Med* 5(4): 572-590.

Castell, J. V., Geiger, T., Gross, V., Andus, T., Walter, E., Hirano, T., Kishimoto, T. & Heinrich, P. C. (1988). Plasma clearance, organ distribution and target cells of interleukin-6/hepatocyte-stimulating factor in the rat. *Eur J Biochem* 177(2): 357-361.

Chang, Q., Daly, L. & Bromberg, J. (2014). The IL-6 feed-forward loop: a driver of tumorigenesis. *Sem Immunol* 26(1): 48-53.

Chen, J. & Fang, G. (2001). MAD2B is an inhibitor of the anaphase-promoting complex. *Genes Dev* 15(14): 1765-1770.

Cherel, M., Sorel, M., Lebeau, B., Dubois, S., Moreau, J. F., Bataille, R., Minvielle, S. & Jacques, Y. (1995). Molecular cloning of two isoforms of a receptor for the human hematopoietic cytokine interleukin-11. *Blood* 86(7): 2534-2540.

Cheung, H. W., Chun, A. C., Wang, Q., Deng, W., Hu, L., Guan, X. Y., Nicholls, J. M., Ling, M. T., Chuan Wong, Y., Tsao, S. W., Jin, D. Y. & Wang, X. (2006). Inactivation of human MAD2B in nasopharyngeal carcinoma cells leads to chemosensitization to DNA-damaging agents. *Cancer Res* 66(8): 4357-4367.

Chomarat, P., Banchereau, J., Davoust, J. & Palucka, A. K. (2000). IL-6 switches the differentiation of monocytes from dendritic cells to macrophages. *Nat Immunol*1(6): 510-514.

Coles, B., Fielding, C. A., Rose-John, S., Scheller, J., Jones, S. A. & O'Donnell, V. B. (2007). Classic interleukin-6 receptor signaling and interleukin-6 trans-signaling differentially control angiotensin II-dependent hypertension, cardiac signal transducer and activator of transcription-3 activation, and vascular hypertrophy in vivo. *Am J Pathol* 171(1): 315-325.

Cornelissen, C., Luscher-Firzlaff, J., Baron, J. M. & Luscher, B. (2012). Signaling by IL-31 and functional consequences. *Eur J Cell Biol* 91(6-7): 552-566.

Curtis, D. J., Hilton, D. J., Roberts, B., Murray, L., Nicola, N. & Begley, C. G. (1997). Recombinant soluble interleukin-11 (IL-11) receptor alpha-chain can act as an IL-11 antagonist. *Blood* 90(11): 4403-4412.

d'Azzo, A., Bongiovanni, A. & Nastasi, T. (2005). E3 ubiquitin ligases as regulators of membrane protein trafficking and degradation. *Traffic* 6(6): 429-441.

Davidson, A. J., Freeman, S. A., Crosier, K. E., Wood, C. R. & Crosier, P. S. (1997). Expression of murine interleukin 11 and its receptor alpha-chain in adult and embryonic tissues. *Stem Cells* 15(2): 119-124.

Dawn, B., Xuan, Y. T., Guo, Y., Rezazadeh, A., Stein, A. B., Hunt, G., Wu, W. J., Tan, W. & Bolli, R. (2004). IL-6 plays an obligatory role in late preconditioning via JAK-STAT signaling and upregulation of iNOS and COX-2. *Cardiovasc Res* 64(1): 61-71.

de Haan, G., Dontje, B., Engel, C., Loeffler, M. & Nijhof, W. (1995). In vivo effects of interleukin-11 and stem cell factor in combination with erythropoietin in the regulation of erythropoiesis. *Br J Haematol* 90(4): 783-790.

Diehl, S. & Rincon, M. (2002). The two faces of IL-6 on Th1/Th2 differentiation. *Mol Immunol* 39(9): 531-536.

Dittrich, E., Haft, C. R., Muys, L., Heinrich, P. C. & Graeve, L. (1996). A di-leucine motif and an upstream serine in the interleukin-6 (IL-6) signal transducer gp130 mediate ligand-induced endocytosis and down-regulation of the IL-6 receptor. *J Biol Chem* 271(10): 5487-5494.

Dominitzki, S., Fantini, M. C., Neufert, C., Nikolaev, A., Galle, P. R., Scheller, J., Monteleone, G., Rose-John, S., Neurath, M. F. & Becker, C. (2007). Cutting edge: trans-signaling via the soluble IL-6R abrogates the induction of FoxP3 in naive CD4+CD25 T cells. *J Immunol* 179(4): 2041-2045.

Doumanov, J. A., Daubrawa, M., Unden, H. & Graeve, L. (2006). Identification of a basolateral sorting signal within the cytoplasmic domain of the interleukin-6 signal transducer gp130. *Cell Signal* 18(8): 1140-1146.

Du, X., Everett, E. T., Wang, G., Lee, W. H., Yang, Z. & Williams, D. A. (1996). Murine interleukin-11 (IL-11) is expressed at high levels in the hippocampus and expression is developmentally regulated in the testis. *J Cell Physiol* 168(2): 362-372.

Düsterhöft, S., Hobel, K., Oldefest, M., Lokau, J., Waetzig, G. H., Chalaris, A., Garbers, C., Scheller, J., Rose-John, S., Lorenzen, I. & Grotzinger, J. (2014). A disintegrin and metalloprotease 17 dynamic interaction sequence, the sweet tooth for the human interleukin 6 receptor. *J Biol Chem* 289(23): 16336-16348.

Dutta, D., Williamson, C. D., Cole, N. B. & Donaldson, J. G. (2012). Pitstop 2 is a potent inhibitor of clathrin-independent endocytosis. *PloS one* 7(9): e45799.

Edwards, D. R., Handsley, M. M. & Pennington, C. J. (2008). The ADAM metalloproteinases. *Mol Aspects Med* 29(5): 258-289.

Fiedler, K. & Simons, K. (1995). The role of N-glycans in the secretory pathway. *Cell* 81(3): 309-312.

Fong, Y., Moldawer, L. L., Marano, M., Wei, H., Tatter, S. B., Clarick, R. H., Santhanam, U., Sherris, D., May, L. T., Sehgal, P. B. & et al. (1989). Endotoxemia elicits increased circulating beta 2-IFN/IL-6 in man. *J Immunol* 142(7): 2321-2324.

Fujimoto, K., Ida, H., Hirota, Y., Ishigai, M., Amano, J. &Tanaka, Y. (2015). Intracellular Dynamics and Fate of a Humanized Anti-Interleukin-6 Receptor Monoclonal Antibody, Tocilizumab (TCZ). *Mol Pharmacol* 88(4): 660-675.

Furugaki, K., Moriya, Y., Iwai, T., Yorozu, K., Yanagisawa, M., Kondoh, K., Fujimoto-Ohuchi, K. & Mori, K. (2011). Erlotinib inhibits osteolytic bone invasion of human non-small-cell lung cancer cell line NCI-H292. *Clin Exp Metastasis* 28(7): 649-659.

Galicia, J. C., Tai, H., Komatsu, Y., Shimada, Y., Akazawa, K. & Yoshie, H. (2004). Polymorphisms in the IL-6 receptor (IL-6R) gene: strong evidence that serum levels of soluble IL-6R are genetically influenced. *Genes Immun* 5(6): 513-516.

Gan, G. N., Wittschieben, J. P., Wittschieben, B. O. & Wood, R. D. (2008). DNA polymerase zeta (pol zeta) in higher eukaryotes. *Cell Res* 18(1): 174-183.

Garbers, C., Aparicio-Siegmund, S. & Rose-John, S. (2015). The IL-6/gp130/STAT3 signaling axis: recent advances towards specific inhibition. *Curr Opin Immunol* 34(10): 75-82.

Garbers, C., Hermanns, H. M., Schaper, F., Müller-Newen, G., Grötzinger, J., Rose-John, S. & Scheller, J. (2012). Plasticity and cross-talk of interleukin 6-type cytokines. *Cytokine Growth Factor Rev* 23(3): 85-97.

Garbers, C., Monhasery, N., Aparicio-Siegmund, S., Lokau, J., Baran, P., Nowell, M. A., Jones, S. A., Rose-John, S. & Scheller, J. (2014). The interleukin-6 receptor Asp358Ala single nucleotide polymorphism rs2228145 confers increased proteolytic conversion rates by ADAM proteases. *Biochim Biophys Acta* 1842(9): 1485-1494.

Garbers, C. & Scheller, J. (2013). Interleukin-6 and interleukin-11: same same but different. *Biol Chem* 394(9): 1145-1161.

Gerhartz, C., Dittrich, E., Stoyan, T., Rose-John, S., Yasukawa, K., Heinrich, P. C. & Graeve, L. (1994). Biosynthesis and half-life of the interleukin-6 receptor and its signal transducer gp130. *Eur J Biochem* 223(1): 265-274.

Gordon, M. S. (1996). Thrombopoietic activity of recombinant human interleukin 11 in cancer patients receiving chemotherapy. *Cancer Chemother Pharmacol* 38(1): 96-98.

Gordon, M. S., McCaskill-Stevens, W. J., Battiato, L. A., Loewy, J., Loesch, D., Breeden, E., Hoffman, R., Beach, K. J., Kuca, B., Kaye, J. & Sledge, G. W., Jr. (1996). A phase I trial of recombinant human interleukin-11 (neumega rhIL-11 growth factor) in women with breast cancer receiving chemotherapy. *Blood* 87(9): 3615-3624.

Griffiths, G. & Simons, K. (1986). The trans Golgi network: sorting at the exit site of the Golgi complex. *Science* 234(4775): 438-443.

Grötzinger, J., Kurapkat, G., Wollmer, A., Kalai, M. & Rose-John, S. (1997). The family of the IL-6-type cytokines: specificity and promiscuity of the receptor complexes. *Proteins* 27(1): 96-109.

Gurfein, B., Zhang, Y., López, C., Argaw, A., Zameer, A., Moran, T. & John, G. (2009). IL-11 regulates autoimmune demyelination. *J Immunol* 183(7): 4229-4240.

Hanafusa, T., Habu, T., Tomida, J., Ohashi, E., Murakumo, Y. & Ohmori, H. (2010). Overlapping in short motif sequences for binding to human REV7 and MAD2 proteins. *Genes Cells* 15(3): 281-296.

Harashima, H., Dissmeyer, N. & Schnittger, A. (2013). Cell cycle control across the eukaryotic kingdom. *Trends Cell Biol* 23(7): 345-356.

Hashizume, M., Hayakawa, N. & Mihara, M. (2008). IL-6 trans-signalling directly induces RANKL on fibroblast-like synovial cells and is involved in RANKL induction by TNF-alpha and IL-17. *Rheumatology* 47(11): 1635-1640.

Heinrich, P. C., Behrmann, I., Haan, S., Hermanns, H. M., Müller-Newen, G. & Schaper, F. (2003). Principles of interleukin (IL)-6-type cytokine signalling and its regulation. *Biochem J* 374(1): 1-20.

Heinrich, P. C., Behrmann, I., Müller-Newen, G., Schaper, F. & Graeve, L. (1998). Interleukin-6-type cytokine signalling through the gp130/Jak/STAT pathway. *Biochem J* 334 (2): 297-314.

Hill, G. R., Cooke, K. R., Teshima, T., Crawford, J. M., Keith, J. C., Jr., Brinson, Y. S., Bungard, D. & Ferrara, J. L. (1998). Interleukin-11 promotes T cell polarization and prevents acute graft-versus-host disease after allogeneic bone marrow transplantation. *J Clin Invest* 102(1): 115-123.

Hong, C. F., Chou, Y. T., Lin, Y. S. & Wu, C. W. (2009). MAD2B, a novel TCF4-binding protein, modulates TCF4-mediated epithelial-mesenchymal transdifferentiation. *J Biol Chem* 284(29): 19613-19622.

Hotamisligil, G. S. (2006). Inflammation and metabolic disorders. *Nature* 444(7121): 860-867.

Huang, F., Kirkpatrick, D., Jiang, X., Gygi, S. & Sorkin, A. (2006). Differential regulation of EGF receptor internalization and degradation by multiubiquitination within the kinase domain. *Mol Cell* 21(6): 737-748.

Iwasaki, H., Takeuchi, O., Teraguchi, S., Matsushita, K., Uehata, T., Kuniyoshi, K., Satoh, T., Saitoh, T., Matsushita, M., Standley, D. M. & Akira, S. (2011). The IkappaB kinase complex regulates the stability of cytokine-encoding mRNA induced by TLR-IL-1R by controlling degradation of regnase-1. *Nature Immunol* 12(12): 1167-1175.

Jacob, R., Alfalah, M., Grunberg, J., Obendorf, M. & Naim, H. Y. (2000). Structural determinants required for apical sorting of an intestinal brush-border membrane protein. *J Biol Chem* 275(9): 6566-6572.

Jones, S. A. (2005). Directing transition from innate to acquired immunity: defining a role for IL-6. *J Immunol* 175(6): 3463-3468.

Karow, J., Hudson, K. R., Hall, M. A., Vernallis, A. B., Taylor, J. A., Gossler, A. & Heath, J. K. (1996). Mediation of interleukin-11-dependent biological responses by a soluble form of the interleukin-11 receptor. *Biochem J* 318 (2): 489-495.

Keith, J. C., Jr., Albert, L., Sonis, S. T., Pfeiffer, C. J. & Schaub, R. G. (1994). IL-11, a pleiotropic cytokine: exciting new effects of IL-11 on gastrointestinal mucosal biology. *Stem Cells* 12(1): 79-90.

Kershaw, N. J., Murphy, J. M., Liau, N. P., Varghese, L. N., Laktyushin, A., Whitlock, E. L., Lucet, I. S., Nicola, N. A. & Babon, J. J. (2013). SOCS3 binds specific receptor-JAK complexes to control cytokine signaling by direct kinase inhibition. *Nat Struct Mol Biol* 20(4): 469-476.

Kohase, M., Henriksen-DeStefano, D., May, L. T., Vilcek, J. & Sehgal, P. B. (1986). Induction of beta 2-interferon by tumor necrosis factor: a homeostatic mechanism in the control of cell proliferation. *Cell* 45(5): 659-666.

Kohase, M., May, L. T., Tamm, I., Vilcek, J. & Sehgal, P. B. (1987). A cytokine network in human diploid fibroblasts: interactions of beta-interferons, tumor necrosis factor, platelet-derived growth factor, and interleukin-1. *Mol Cellular Biol* 7(1): 273-280.

Koivisto, U. M., Hubbard, A. L. & Mellman, I. (2001). A novel cellular phenotype for familial hypercholesterolemia due to a defect in polarized targeting of LDL receptor. *Cell* 105(5): 575-585.

Lamas, J. R., Rodriguez-Rodriguez, L., Tornero-Esteban, P., Villafuertes, E., Hoyas, J., Abasolo, L., Varade, J., Alvarez-Lafuente, R., Urcelay, E. & Fernandez-Gutierrez, B. (2013). Alternative splicing and proteolytic rupture contribute to the generation of soluble IL-6 receptors (sIL-6R) in rheumatoid arthritis. *Cytokine* 61(3): 720-723.

Lee, H., Park, S., Kim, M., Ham, A., Anderson, L., Brown, K., D'Agati, V. & Cox, G. (2012). Interleukin-11 protects against renal ischemia and reperfusion injury. *Am J Physiol Renal Physiol* 303(8): 1216-1224.

Lee, K. A., Hai, T. Y., SivaRaman, L., Thimmappaya, B., Hurst, H. C., Jones, N. C. & Green, M. R. (1987a). A cellular protein, activating transcription factor, activates transcription of multiple E1A-inducible adenovirus early promoters. *Proc Nat Acad Sci U S A* 84(23): 8355-8359.

Lee, W., Mitchell, P. & Tjian, R. (1987b). Purified transcription factor AP-1 interacts with TPA-inducible enhancer elements. *Cell* 49(6): 741-752.

Libermann, T. A. & Baltimore, D. (1990). Activation of interleukin-6 gene expression through the NF-kappa B transcription factor. *Mol Cell Biol* 10(5): 2327-2334.

Lingwood, D. & Simons, K. (2010). Lipid rafts as a membrane-organizing principle. *Science* 327(5961): 46-50.

Lokau, J., Nitz, R., Agthe, M., Monhasery, N., Aparicio-Siegmund, S., Schumacher, N., Wolf, J., Moller-Hackbarth, K., Waetzig, G. H., Grotzinger, J., Muller-Newen, G., Rose-John, S., Scheller, J. & Garbers, C. (2016). Proteolytic Cleavage Governs Interleukin-11 Trans-signaling. *Cell Rep* 10(16)*:* 30031-30036.

Luis-Ravelo, D., Anton, I., Zandueta, C., Valencia, K., Ormazabal, C., Martinez-Canarias, S., Guruceaga, E., Perurena, N., Vicent, S., De Las Rivas, J. & Lecanda, F. (2014). A gene signature of bone metastatic colonization sensitizes for tumor-induced osteolysis and predicts survival in lung cancer. *Oncogene* 33(43): 5090-5099.

Lust, J. A., Donovan, K. A., Kline, M. P., Greipp, P. R., Kyle, R. A. & Maihle, N. J. (1992). Isolation of an mRNA encoding a soluble form of the human interleukin-6 receptor. *Cytokine* 4(2): 96-100.

Luton, F., Hexham, M. J., Zhang, M. & Mostov, K. E. (2009). Identification of a cytoplasmic signal for apical transcytosis. *Traffic* 10(8): 1128-1142.

Macia, E., Ehrlich, M., Massol, R., Boucrot, E., Brunner, C. & Kirchhausen, T. (2006). Dynasore, a cell-permeable inhibitor of dynamin. *Dev Cell* 10(6): 839-850.

Maeshima, K., Takahashi, T., Nakahira, K., Shimizu, H., Fujii, H., Katayama, H., Yokoyama, M., Morita, K., Akagi, R. & Sassa, S. (2004). A protective role of interleukin 11 on hepatic injury in acute endotoxemia. *Shock* 21(2): 134-138.

Maier, R., Ganu, V. & Lotz, M. (1993). Interleukin-11, an inducible cytokine in human articular chondrocytes and synoviocytes, stimulates the production of the tissue inhibitor of metalloproteinases. *J Biol Chem* 268(29): 21527-21532.

Martens, A. S., Bode, J. G., Heinrich, P. C. & Graeve, L. (2000). The cytoplasmic domain of the interleukin-6 receptor gp80 mediates its basolateral sorting in polarized madin-darby canine kidney cells. *J Cell Sci* 113 (20): 3593-3602.

Martin-Belmonte, F. & Mostov, K. (2008). Regulation of cell polarity during epithelial morphogenesis. *Curr Opin Cell Biol* 20(2): 227-234.

Masuda, K., Ripley, B., Nishimura, R., Mino, T., Takeuchi, O., Shioi, G., Kiyonari, H. & Kishimoto, T. (2013). Arid5a controls IL-6 mRNA stability, which contributes to elevation of IL-6 level in vivo. *Proc Nat Acad Sci U S A* 110(23): 9409-9414.

Matadeen, R., Hon, W. C., Heath, J. K., Jones, E. Y. & Fuller, S. (2007). The dynamics of signal triggering in a gp130-receptor complex. *Structure* 15(4): 441-448.

Matsusaka, T., Fujikawa, K., Nishio, Y., Mukaida, N., Matsushima, K., Kishimoto, T. & Akira, S. (1993). Transcription factors NF-IL6 and NF-kappa B synergistically activate transcription of the inflammatory cytokines, interleukin 6 and interleukin 8. *Proc Nat Acad Sci U S A* 90(21): 10193-10197.

Matter, K., Hunziker, W. & Mellman, I. (1992). Basolateral sorting of LDL receptor in MDCK cells: the cytoplasmic domain contains two tyrosine-dependent targeting determinants. *Cell* 71(5): 741-753.

Matthews, V. B., Allen, T. L., Risis, S., Chan, M. H., Henstridge, D. C., Watson, N., Zaffino, L. A., Babb, J. R., Boon, J., Meikle, P. J., Jowett, J. B., Watt, M. J., Jansson, J. O., Bruce, C. R. & Febbraio, M. A. (2010). Interleukin-6-deficient mice develop hepatic inflammation and systemic insulin resistance. *Diabetologia* 53(11): 2431-2441.

Mayor, S. & Riezman, H. (2004). Sorting GPI-anchored proteins. *Nat Rev Mol Cell Biol* 5(2): 110-120.

Medendorp, K., Vreede, L., van Groningen, J. J., Hetterschijt, L., Brugmans, L., Jansen, P. A., van den Hurk, W. H., de Bruijn, D. R. & van Kessel, A. G. (2010). The mitotic arrest deficient protein MAD2B interacts with the clathrin light chain A during mitosis. *PloS one* 5(11): e15128.

Melendez, G. C., McLarty, J. L., Levick, S. P., Du, Y., Janicki, J. S. & Brower, G. L. (2010). Interleukin 6 mediates myocardial fibrosis, concentric hypertrophy, and diastolic dysfunction in rats. *Hypertension* 56(2): 225-231.

Mellman, I. & Nelson, W. J. (2008). Coordinated protein sorting, targeting and distribution in polarized cells. *Nat Rev Mol Cell Biol* 9(11): 833-845.

Meng, X., Tian, X., Wang, X., Gao, P. & Zhang, C. (2012). A novel binding protein of single-minded 2: the mitotic arrest-deficient protein MAD2B. *Neurogenetics* 13(3): 251-260.

Miaczynska, M. & Stenmark, H. (2008). Mechanisms and functions of endocytosis. *J Cell Biol* 180(1): 7-11.

Mir, S. A., Chatterjee, A., Mitra, A., Pathak, K., Mahata, S. K. & Sarkar, S. (2012). Inhibition of signal transducer and activator of transcription 3 (STAT3) attenuates interleukin-6 (IL-6)-induced collagen synthesis and resultant hypertrophy in rat heart. *J Biol Chem* 287(4): 2666-2677.

Molmenti, E. P., Ziambaras, T. & Perlmutter, D. H. (1993). Evidence for an acute phase response in human intestinal epithelial cells. *J Biol Chem* 268(19): 14116-14124.

Morinaga, Y., Fujita, N., Ohishi, K., Zhang, Y. & Tsuruo, T. (1998). Suppression of interleukin-11-mediated bone resorption by cyclooxygenases inhibitors. *J Cell Physiol* 175(3): 247-254.

Mostov, K. E. (1994). Transepithelial transport of immunoglobulins. *Annu Rev Immunol* 12: 63-84.

Müllberg, J., Oberthur, W., Lottspeich, F., Mehl, E., Dittrich, E., Graeve, L., Heinrich, P. C. & Rose-John, S. (1994). The soluble human IL-6 receptor. Mutational characterization of the proteolytic cleavage site. *J Immunol* 152(10): 4958-4968.

Müllberg, J., Schooltink, H., Stoyan, T., Günther, M., Graeve, L., Büse, G., Mackiewicz, A., Heinrich, P. C. & Rose-John, S. (1993). The soluble interleukin-6 receptor is generated by shedding. *Eur J Immunol* 23(2): 473-480.

Musacchio, A. & Salmon, E. D. (2007). The spindle-assembly checkpoint in space and time. *Nat Rev Mol Cell Biol* 8(5): 379-393.

Nasmyth, K. (2002). Segregating sister genomes: the molecular biology of chromosome separation. *Science* 297(5581): 559-565.

Necula, L. G., Chivu-Economescu, M., Stanciulescu, E. L., Bleotu, C., Dima, S. O., Alexiu, I., Dumitru, A., Constantinescu, G., Popescu, I. & Diaconu, C. C. (2012). IL-6 and IL-11 as markers for tumor aggressiveness and prognosis in gastric adenocarcinoma patients without mutations in Gp130 subunits. *J Gastrointestin Liver Dis* 21(1): 23-29.

Neddermann, P., Graziani, R., Ciliberto, G. & Paonessa, G. (1996). Functional expression of soluble human interleukin-11 (IL-11) receptor alpha and stoichiometry of in vitro IL-11 receptor complexes with gp130. *J Biol Chem* 271(48): 30986-30991.

Nishimoto, N., Kanakura, Y., Aozasa, K., Johkoh, T., Nakamura, M., Nakano, S., Nakano, N., Ikeda, Y., Sasaki, T., Nishioka, K., Hara, M., Taguchi, H., Kimura, Y., Kato, Y., Asaoku, H., Kumagai, S., Kodama, F., Nakahara, H., Hagihara, K., Yoshizaki, K. &

Kishimoto, T. (2005). Humanized anti-interleukin-6 receptor antibody treatment of multicentric Castleman disease. *Blood* 106(8): 2627-2632.

Nishina, T., Komazawa-Sakon, S., Yanaka, S., Piao, X., Zheng, D., Piao, J., Kojima, Y., Yamashina, S., Sano, E., Putoczki, T., Doi, T., Ueno, T., Ezaki, J., Ushio, H., Ernst, M., Tsumoto, K., Okumura, K. & Nakano, H. (2012a). Interleukin-11 links oxidative stress and compensatory proliferation. *Sci Signal* 5(207): 1110-1126

Nishina, T., Komazawa-Sakon, S., Yanaka, S., Piao, X., Zheng, D. M., Piao, J. H., Kojima, Y., Yamashina, S., Sano, E., Putoczki, T., Doi, T., Ueno, T., Ezaki, J., Ushio, H., Ernst, M., Tsumoto, K., Okumura, K. & Nakano, H. (2012b). Interleukin-11 links oxidative stress and compensatory proliferation. *Sci Signal* 5(207): 108-118.

Nitz, R., Lokau, J., Aparicio-Siegmund, S., Scheller, J. & Garbers, C. (2015). Modular organization of Interleukin-6 and Interleukin-11 alpha-receptors. *Biochimie* 119: 175-182.

Nowell, M. A., Richards, P. J., Horiuchi, S., Yamamoto, N., Rose-John, S., Topley, N., Williams, A. S. & Jones, S. A. (2003). Soluble IL-6 receptor governs IL-6 activity in experimental arthritis: blockade of arthritis severity by soluble glycoprotein 130. *J Immunol* 171(6): 3202-3209.

O'Neill, T. J., Zhu, Y. & Gustafson, T. A. (1997). Interaction of MAD2 with the carboxyl terminus of the insulin receptor but not with the IGFIR. Evidence for release from the insulin receptor after activation. *J Biol Chem* 272(15): 10035-10040.

Obana M, Maeda, M., Takeda, K., Hayama, A., Mohri, T., Yamashita, T., Nakaoka, Y., Komuro, I., Takeda, K., Matsumiya, G., Azuma, J. & Fujio, Y. (2010). Therapeutic activation of signal transducer and activator of transcription 3 by interleukin-11 ameliorates cardiac fibrosis after myocardial infarction. *Circulation* 121(5): 684-691.

Oberg, H. H., Wesch, D., Grussel, S., Rose-John, S. & Kabelitz, D. (2006). Differential expression of CD126 and CD130 mediates different STAT-3 phosphorylation in CD4+CD25- and CD25high regulatory T cells. *Int Immunol* 18(4): 555-563.

Onn, I., Heidinger-Pauli, J. M., Guacci, V., Unal, E. & Koshland, D. E. (2008). Sister chromatid cohesion: a simple concept with a complex reality. *Annu Rev Cell Dev Biol* 24: 105-129.

Orlando, K. & Guo, W. (2009). Membrane organization and dynamics in cell polarity. *Cold Spring Harb Perspect Biol* 1(5): 132-143.

Orzech, E., Cohen, S., Weiss, A. & Aroeti, B. (2000). Interactions between the exocytic and endocytic pathways in polarized Madin-Darby canine kidney cells. *J Biol Chem* 275(20): 15207-15219.

Parekh, R. B., Dwek, R. A., Rademacher, T. W., Opdenakker, G. & Van Damme, J. (1992). Glycosylation of interleukin-6 purified from normal human blood mononuclear cells. *Eur J Biochem* 203(1-2): 135-141.

Paul, S. R., Bennett, F., Calvetti, J. A., Kelleher, K., Wood, C. R., O'Hara, R. M., Jr., Leary, A. C., Sibley, B., Clark, S. C., Williams, D. A. & et al. (1990). Molecular cloning of a cDNA encoding interleukin 11, a stromal cell-derived lymphopoietic and hematopoietic cytokine. *Proc Nat Acad Sci U S A* 87(19): 7512-7516.

Peters, J. M. (2006). The anaphase promoting complex/cyclosome: a machine designed to destroy. *Nat Rev Mol Cell Biol* 7(9): 644-656.

Peters, M., Solem, F., Goldschmidt, J., Schirmacher, P. & Rose-John, S. (2001). Interleukin-6 and the soluble interleukin-6 receptor induce stem cell factor and Flt-3L expression in vivo and in vitro. *Exp Hematol* 29(2): 146-155.

Pflanz, S., Timans, J. C., Cheung, J., Rosales, R., Kanzler, H., Gilbert, J., Hibbert, L., Churakova, T., Travis, M., Vaisberg, E., Blumenschein, W. M., Mattson, J. D., Wagner, J. L., To, W., Zurawski, S., McClanahan, T. K., Gorman, D. M., Bazan, J. F., de Waal Malefyt, R., Rennick, D. & Kastelein, R. A. (2002). IL-27, a heterodimeric cytokine composed of EBI3 and p28 protein, induces proliferation of naive CD4+ T cells. *Immunity* 16(6): 779-790.

Pfleger, C. M., Salic, A., Lee, E. & Kirschner, M. W. (2001). Inhibition of Cdh1-APC by the MAD2-related protein MAD2L2: a novel mechanism for regulating Cdh1. *Genes Dev* 15(14): 1759-1764.

Poli, V., Balena, R., Fattori, E., Markatos, A., Yamamoto, M., Tanaka, H., Ciliberto, G., Rodan, G. A. & Costantini, F. (1994). Interleukin-6 deficient mice are protected from bone loss caused by estrogen depletion. *EMBO J* 13(5): 1189-1196.

Putoczki, T. & Ernst, M. (2010). More than a sidekick: the IL-6 family cytokine IL-11 links inflammation to cancer. *J Leukoc Biol* 88(6): 1109-1117.

Putoczki, T., Thiem, S., Loving, A., Busuttil, R., Wilson, N., Ziegler, P., Nguyen, P., Preaudet, A., Farid, R., Edwards, K., Boglev, Y., Luwor, R., Jarnicki, A., Horst, D., Boussioutas, A., Heath, J., Sieber, O., Pleines, I., Kile, B., Nash, A., Greten, F., McKenzie, B. & M, E. (2014). Interleukin-11 is the dominant IL-6 family cytokine during gastrointestinal tumorigenesis and can be targeted therapeutically. *Cancer Cell* 24(2): 257-271.

Putoczki, T. L. & Ernst, M. (2015). IL-11 signaling as a therapeutic target for cancer. *Immunotherapy* 7(4): 441-453.

Putoczki, T. L., Thiem, S., Loving, A., Busuttil, R. A., Wilson, N. J., Ziegler, P. K., Nguyen, P. M., Preaudet, A., Farid, R., Edwards, K. M., Boglev, Y., Luwor, R. B., Jarnicki, A., Horst, D., Boussioutas, A., Heath, J. K., Sieber, O. M., Pleines, I., Kile, B. T., Nash, A., Greten, F. R., McKenzie, B. S. & Ernst, M. (2013). Interleukin-11 is the dominant IL-6 family cytokine during gastrointestinal tumorigenesis and can be targeted therapeutically. *Cancer cell* 24(2): 257-271.

Qiu, B., Pfeiffer, C. & Keith, J. J. (1996). Protection by recombinant human interleukin-11 against experimental TNB-induced colitis in rats. *Dig Dis Sci* 41(8): 1625-1630.

Rabe, B., Chalaris, A., May, U., Waetzig, G. H., Seegert, D., Williams, A. S., Jones, S. A., Rose-John, S. & Scheller, J. (2008). Transgenic blockade of interleukin 6 transsignaling abrogates inflammation. *Blood* 111(3): 1021-1028.

Rafiq, S., Frayling, T. M., Murray, A., Hurst, A., Stevens, K., Weedon, M. N., Henley, W., Ferrucci, L., Bandinelli, S., Corsi, A. M., Guralnik, J. M. & Melzer, D. (2007). A common variant of the interleukin 6 receptor (IL-6r) gene increases IL-6r and IL-6 levels, without other inflammatory effects. *Genes Immun* 8(7): 552-559.

Raiborg, C., Bache, K. G., Gillooly, D. J., Madshus, I. H., Stang, E. & Stenmark, H. (2002). Hrs sorts ubiquitinated proteins into clathrin-coated microdomains of early endosomes. *Nat Cell Biol* 4(5): 394-398.

Ray, A., Tatter, S. B., May, L. T. & Sehgal, P. B. (1988). Activation of the human "beta 2-interferon/hepatocyte-stimulating factor/interleukin 6" promoter by cytokines, viruses, and second messenger agonists. *Proc Nat Acad Sci U S A* 85(18): 6701-6705.

Redlich, C. A., Gao, X., Rockwell, S., Kelley, M. & Elias, J. A. (1996). IL-11 enhances survival and decreases TNF production after radiation-induced thoracic injury. *J Immunol* 157(4): 1705-1710.

Ren, L., Wang, X., Dong, Z., Liu, J. & Zhang, S. (2013). Bone metastasis from breast cancer involves elevated IL-11 expression and the gp130/STAT3 pathway. *Med Oncol* 30(3): 634.

Robb, L., Hilton, D. J., Brook-Carter, P. T. & Begley, C. G. (1997). Identification of a second murine interleukin-11 receptor alpha-chain gene (IL11Ra2) with a restricted pattern of expression. *Genomics* 40(3): 387-394.

Robb, L., Li, R., Hartley, L., Nandurkar, H. H., Koentgen, F. & Begley, C. G. (1998). Infertility in female mice lacking the receptor for interleukin 11 is due to a defective uterine response to implantation. *Nat Med* 4(3): 303-308.

Robledo, O., Fourcin, M., Chevalier, S., Guillet, C., Auguste, P., Pouplard-Barthelaix, A., Pennica, D. & Gascan, H. (1997). Signaling of the cardiotrophin-1 receptor. Evidence for a third receptor component. *J Biol Chem* 272(8): 4855-4863.

Rodriguez-Boulan, E. & Nelson, W. J. (1989). Morphogenesis of the polarized epithelial cell phenotype. *Science* 245(4919): 718-725.

Romas, E., Udagawa, N., Zhou, H., Tamura, T., Saito, M., Taga, T., Hilton, D. J., Suda, T., Ng, K. W. & Martin, T. J. (1996). The role of gp130-mediated signals in osteoclast development: regulation of interleukin 11 production by osteoblasts and distribution of its receptor in bone marrow cultures. *J Exp Med* 183(6): 2581-2591.

Rose-John, S. (2012). IL-6 trans-signaling via the soluble IL-6 receptor: importance for the pro-inflammatory activities of IL-6. *Int J Biol Sci* 8(9): 1237-1247.

Rose-John, S. & Heinrich, P. C. (1994). Soluble receptors for cytokines and growth factors: generation and biological function. *Biochem J* 300 (2): 281-290.

Rose-John, S., Scheller, J., Elson, G. & Jones, S. A. (2006). Interleukin-6 biology is coordinated by membrane-bound and soluble receptors: role in inflammation and cancer. *J Leukoc Biol* 80(2): 227-236.

Rothbauer, U., Zolghadr, K., Muyldermans, S., Schepers, A., Cardoso, M. C. & Leonhardt, H. (2008). A versatile nanotrap for biochemical and functional studies with fluorescent fusion proteins. *Mol Cell Proteomics* 7(2): 282-289.

Sandvig, K., Pust, S., Skotland, T. & van Deurs, B. (2011). Clathrin-independent endocytosis: mechanisms and function. *Curr Opin Cell Biol* 23(4): 413-420.

Saotome, I., Curto, M. & McClatchey, A. I. (2004). Ezrin is essential for epithelial organization and villus morphogenesis in the developing intestine. *Dev Cell* 6(6): 855-864.

Sarwar, N., Butterworth, A. S., Freitag, D. F., Gregson, J., Willeit, P., Gorman, D. N., Gao, P., Saleheen, D., Rendon, A., Nelson, C. P., Braund, P. S., Hall, A. S., Chasman, D. I., Tybjaerg-Hansen, A., Chambers, J. C., Benjamin, E. J., Franks, P. W., Clarke, R., Wilde, A. A., Trip, M. D., Steri, M., Witteman, J. C., Qi, L., van der Schoot, C. E., de Faire, U., Erdmann, J., Stringham, H. M., Koenig, W., Rader, D. J., Melzer, D., Reich, D., Psaty, B. M., Kleber, M. E., Panagiotakos, D. B., Willeit, J., Wennberg, P., Woodward, M., Adamovic, S., Rimm, E. B., Meade, T. W., Gillum, R. F., Shaffer, J. A., Hofman, A., Onat, A., Sundstrom, J., Wassertheil-Smoller, S., Mellstrom, D., Gallacher, J., Cushman, M., Tracy, R. P., Kauhanen, J., Karlsson, M., Salonen, J. T., Wilhelmsen, L., Amouyel, P., Cantin, B., Best, L. G., Ben-Shlomo, Y., Manson, J. E., Davey-Smith, G., de Bakker, P. I., O'Donnell, C. J., Wilson, J. F., Wilson, A. G., Assimes, T. L., Jansson, J. O., Ohlsson, C., Tivesten, A., Ljunggren, O., Reilly, M. P., Hamsten, A., Ingelsson, E., Cambien, F., Hung, J., Thomas, G. N., Boehnke, M., Schunkert, H., Asselbergs, F. W., Kastelein, J. J., Gudnason, V., Salomaa, V., Harris, T. B., Kooner, J. S., Allin, K. H., Nordestgaard, B. G., Hopewell, J. C., Goodall, A. H., Ridker, P. M., Holm, H., Watkins, H., Ouwehand, W. H., Samani, N. J., Kaptoge, S., Di Angelantonio, E., Harari, O. & Danesh, J. (2012). Interleukin-6 receptor pathways in coronary heart disease: a collaborative meta-analysis of 82 studies. *Lancet* 379(9822): 1205-1213.

Scheller, J., Chalaris, A., Schmidt-Arras, D. & Rose-John, S. (2011). The pro- and anti-inflammatory properties of the cytokine interleukin-6. *Biochim Biophys Acta* 1813(5): 878-888.

Scheller, J. & Rose-John, S. (2006). Interleukin-6 and its receptor: from bench to bedside. *Med Microbiol Immunol* 195(4): 173-183.

Schiel, X., Rose-John, S., Dufhues, G., Schooltink, H., Gross, V. & Heinrich, P. C. (1990). Microheterogeneity of human interleukin 6 synthesized by transfected NIH/3T3 cells: comparison with human monocytes, fibroblasts and endothelial cells. *Eur J Immunol* 20(4): 883-887.

Schmitz, J., Weissenbach, M., Haan, S., Heinrich, P. C. & Schaper, F. (2000). SOCS3 exerts its inhibitory function on interleukin-6 signal transduction through the SHP2 recruitment site of gp130. *J Biol Chem* 275(17): 12848-12856.

Sehgal, P. B., Helfgott, D. C., Santhanam, U., Tatter, S. B., Clarick, R. H., Ghrayeb, J. & May, L. T. (1988). Regulation of the acute phase and immune responses in viral disease. Enhanced expression of the beta 2-interferon/hepatocyte-stimulating factor/interleukin 6 gene in virus-infected human fibroblasts. *J Exp Med* 167(6): 1951-1956.

Sehgal, P. B. & Sagar, A. D. (1980). Heterogeneity of poly(I) x poly(C)-induced human fibroblast interferon mRNA species. *Nature* 288(5786): 95-97.

Senaldi, G., Varnum, B. C., Sarmiento, U., Starnes, C., Lile, J., Scully, S., Guo, J., Elliott, G., McNinch, J., Shaklee, C. L., Freeman, D., Manu, F., Simonet, W. S., Boone, T. & Chang, M. S. (1999). Novel neurotrophin-1/B cell-stimulating factor-3: a cytokine of the IL-6 family. *Proc Nat Acad Sci U S A* 96(20): 11458-11463.

Sheff, D. R., Kroschewski, R. & Mellman, I. (2002). Actin dependence of polarized receptor recycling in Madin-Darby canine kidney cell endosomes. *Mol Biol Cell* 13(1): 262-275.

Shimizu, H., Mitomo, K., Watanabe, T., Okamoto, S. & Yamamoto, K. (1990). Involvement of a NF-kappa B-like transcription factor in the activation of the interleukin-6 gene by inflammatory lymphokines. *Mol Cell Biol* 10(2): 561-568.

Shoshani, L., Contreras, R. G., Roldan, M. L., Moreno, J., Lazaro, A., Balda, M. S., Matter, K. & Cereijido, M. (2005). The polarized expression of Na+,K+-ATPase in epithelia depends on the association between beta-subunits located in neighboring cells. *Mol Biol Cell* 16(3): 1071-1081.

Simons, K. & Ikonen, E. (1997). Functional rafts in cell membranes. *Nature* 387(6633): 569-572.

Simons, K. & van Meer, G. (1988). Lipid sorting in epithelial cells. *Biochemistry* 27(17): 6197-6202.

Simpson, R. J., Hammacher, A., Smith, D. K., Matthews, J. M. & Ward, L. D. (1997). Interleukin-6: structure-function relationships. *Protein Sci* 6(5): 929-955.

Skibbens, J. E., Roth, M. G. & Matlin, K. S. (1989). Differential extractability of influenza virus hemagglutinin during intracellular transport in polarized epithelial cells and nonpolar fibroblasts. *J Cell Biol* 108(3): 821-832.

Skurk, T., Alberti-Huber, C., Herder, C. & Hauner, H. (2007). Relationship between adipocyte size and adipokine expression and secretion. *J Clin Endocrinol Metab* 92(3): 1023-1033.

Sofi, M. H., Li, W., Kaplan, M. H. & Chang, C. H. (2009). Elevated IL-6 expression in CD4 T cells via PKCtheta and NF-kappaB induces Th2 cytokine production. *Mol Immunol* 46(7): 1443-1450.

Sotiriou, C., Lacroix, M., Lespagnard, L., Larsimont, D., Paesmans, M. & Body, J. J. (2001). Interleukins-6 and -11 expression in primary breast cancer and subsequent development of bone metastases. *Cancer Lett* 169(1): 87-95.

Sprecher, C. A., Grant, F. J., Baumgartner, J. W., Presnell, S. R., Schrader, S. K., Yamagiwa, T., Whitmore, T. E., O'Hara, P. J. & Foster, D. F. (1998). Cloning and characterization of a novel class I cytokine receptor. *Biochem Biophys Res Commun* 246(1): 82-90.

Stein, M., Wandinger-Ness, A. & Roitbak, T. (2002). Altered trafficking and epithelial cell polarity in disease. *Trends Cell Biol* 12(8): 374-381.

Stephens, O. W., Zhang, Q., Qu, P., Zhou, Y., Chavan, S., Tian, E., Williams, D. R., Epstein, J., Barlogie, B. & Shaughnessy, J. D., Jr. (2012). An intermediate-risk multiple myeloma subgroup is defined by sIL-6r: levels synergistically increase with incidence of SNP rs2228145 and 1q21 amplification. *Blood* 119(2): 503-512.

Sudakin, V., Chan, G. K. & Yen, T. J. (2001). Checkpoint inhibition of the APC/C in HeLa cells is mediated by a complex of BUBR1, BUB3, CDC20, and MAD2. *J Cell Biol* 154(5): 925-936.

Taga, T. & Kishimoto, T. (1997). Gp130 and the interleukin-6 family of cytokines. *Annu Rev Immunol* 15: 797-819.

Takeuchi, Y., Watanabe, S., Ishii, G., Takeda, S., Nakayama, K., Fukumoto, S., Kaneta, Y., Inoue, D., Matsumoto, T., Harigaya, K. & Fujita, T. (2002). Interleukin-11 as a stimulatory factor for bone formation prevents bone loss with advancing age in mice. *J Biol Chem* 277(50): 49011-49018.

Tanaka, Y., Tanaka, N., Saeki, Y., Tanaka, K., Murakami, M., Hirano, T., Ishii, N. & Sugamura, K. (2008). c-Cbl-dependent monoubiquitination and lysosomal degradation of gp130. *Mol Cell Biol* 28(15): 4805-4818.

Tarnowski, B. I., Spinale, F. G. & Nicholson, J. H. (1991). DAPI as a useful stain for nuclear quantitation. *Biotech Histochem* 66(6): 297-302.

Tebbutt, N. C., Giraud, A. S., Inglese, M., Jenkins, B., Waring, P., Clay, F. J., Malki, S., Alderman, B. M., Grail, D., Hollande, F., Heath, J. K. & Ernst, M. (2002). Reciprocal regulation of gastrointestinal homeostasis by SHP2 and STAT-mediated trefoil gene activation in gp130 mutant mice. *Nat Med* 8(10): 1089-1097.

Torroella-Kouri, M., Keith, J. C., Ivanova, M. & Lopez, D. M. (2003). IL-11-induced reduction of C/EBP transcription factor binding may contribute to the IL-12 downregulation in tumor-bearing mice. *Int J Oncol* 22(2): 439-448.

Trepicchio, W. L., Wang, L., Bozza, M. & Dorner, A. J. (1997). IL-11 regulates macrophage effector function through the inhibition of nuclear factor-kappaB. *J Immunol* 159(11): 5661-5670.

Tuma, P. & Hubbard, A. L. (2003). Transcytosis: crossing cellular barriers. *Physiol Rev* 83(3): 871-932.

Vagin, O., Turdikulova, S. & Sachs, G. (2005). Recombinant addition of N-glycosylation sites to the basolateral Na,K-ATPase beta1 subunit results in its clustering in caveolae and apical sorting in HGT-1 cells. *J Biol Chem* 280(52): 43159-43167.

van den Hurk, W. H., Martens, G. J., Geurts van Kessel, A. & van Groningen, J. J. (2004). Isolation and characterization of the Xenopus laevis orthologs of the human papillary renal cell carcinoma-associated genes PRCC and MAD2L2 (MAD2B). *Cytogenet Genome Res* 106(1): 68-73.

Van Leuven, F., Stas, L., Hilliker, C., Miyake, Y., Bilinski, P. & Gossler, A. (1996). Molecular cloning and characterization of the human interleukin-11 receptor alpha-chain gene, IL11RA, located on chromosome 9p13. *Genomics* 31(1): 65-70.

Wallenius, V., Wallenius, K., Ahren, B., Rudling, M., Carlsten, H., Dickson, S. L., Ohlsson, C. & Jansson, J. O. (2002). Interleukin-6-deficient mice develop mature-onset obesity. *Nat Med* 8(1): 75-79.

Weich, N. S., Wang, A., Fitzgerald, M., Neben, T. Y., Donaldson, D., Giannotti, J., Yetz-Aldape, J., Leven, R. M. & Turner, K. J. (1997). Recombinant human interleukin-11 directly promotes megakaryocytopoiesis in vitro. *Blood* 90(10): 3893-3902.

Weissenbach, J., Chernajovsky, Y., Zeevi, M., Shulman, L., Soreq, H., Nir, U., Wallach, D., Perricaudet, M., Tiollais, P. & Revel, M. (1980). Two interferon mRNAs in human fibroblasts: in vitro translation and Escherichia coli cloning studies. *Proc Nat Acad Sci U S A* 77(12): 7152-7156.

Weisz, O. A. & Rodriguez-Boulan, E. (2009). Apical trafficking in epithelial cells: signals, clusters and motors. *J Cell Sci* 122(23): 4253-4266.

Wolf, J., Rose-John, S. & Garbers, C. (2014). Interleukin-6 and its receptors: a highly regulated and dynamic system. *Cytokine* 70(1): 11-20.

Wolff, S. C., Qi, A. D., Harden, T. K. & Nicholas, R. A. (2010). Charged residues in the C-terminus of the P2Y1 receptor constitute a basolateral-sorting signal. *J Cell Sci* 123(14): 2512-2520.

Yang, L., Wang, R., Gao, Y., Xu, X., Fu, K., Wang, S., Li, Y. & Peng, R. (2014). The protective role of interleukin-11 against neutron radiation injury in mouse intestines via MEK/ERK and PI3K/Akt dependent pathways. *Dig Dis Sci* 59(7): 1406-1414.

Yeaman, C., Le Gall, A. H., Baldwin, A. N., Monlauzeur, L., Le Bivic, A. &Rodriguez-Boulan, E. (1997). The O-glycosylated stalk domain is required for apical sorting of neurotrophin receptors in polarized MDCK cells. *J Cell Biol* 139(4): 929-940.

Yin, T., Yasukawa, K., Taga, T., Kishimoto, T. &Yang, Y. C. (1994). Identification of a 130-kilodalton tyrosine-phosphorylated protein induced by interleukin-11 as JAK2 tyrosine kinase, which associates with gp130 signal transducer. *Exp Hematol* 22(5): 467-472.

Yu, H. (2007). Cdc20: a WD40 activator for a cell cycle degradation machine. *Mol Cell* 27(1): 3-16.

Zhang, L., Yang, S. H. &Sharrocks, A. D. (2007). Rev7/MAD2B links c-Jun N-terminal protein kinase pathway signaling to activation of the transcription factor Elk-1. *Mol Cell Biol* 27(8): 2861-2869.

Zheng, T., Zhu, Z., Wang, J., Homer, R. J. &Elias, J. A. (2001). IL-11: insights in asthma from overexpression transgenic modeling. *J Allergy Clin Immunol* 108(4): 489-496.

Zhong, Z., Wen, Z. &Darnell, J. E., Jr. (1994). Stat3: a STAT family member activated by tyrosine phosphorylation in response to epidermal growth factor and interleukin-6. *Science* 264(5155): 95-98.

Appendix

In this study, three construct was made. The schematic illustration was shown in below.

1

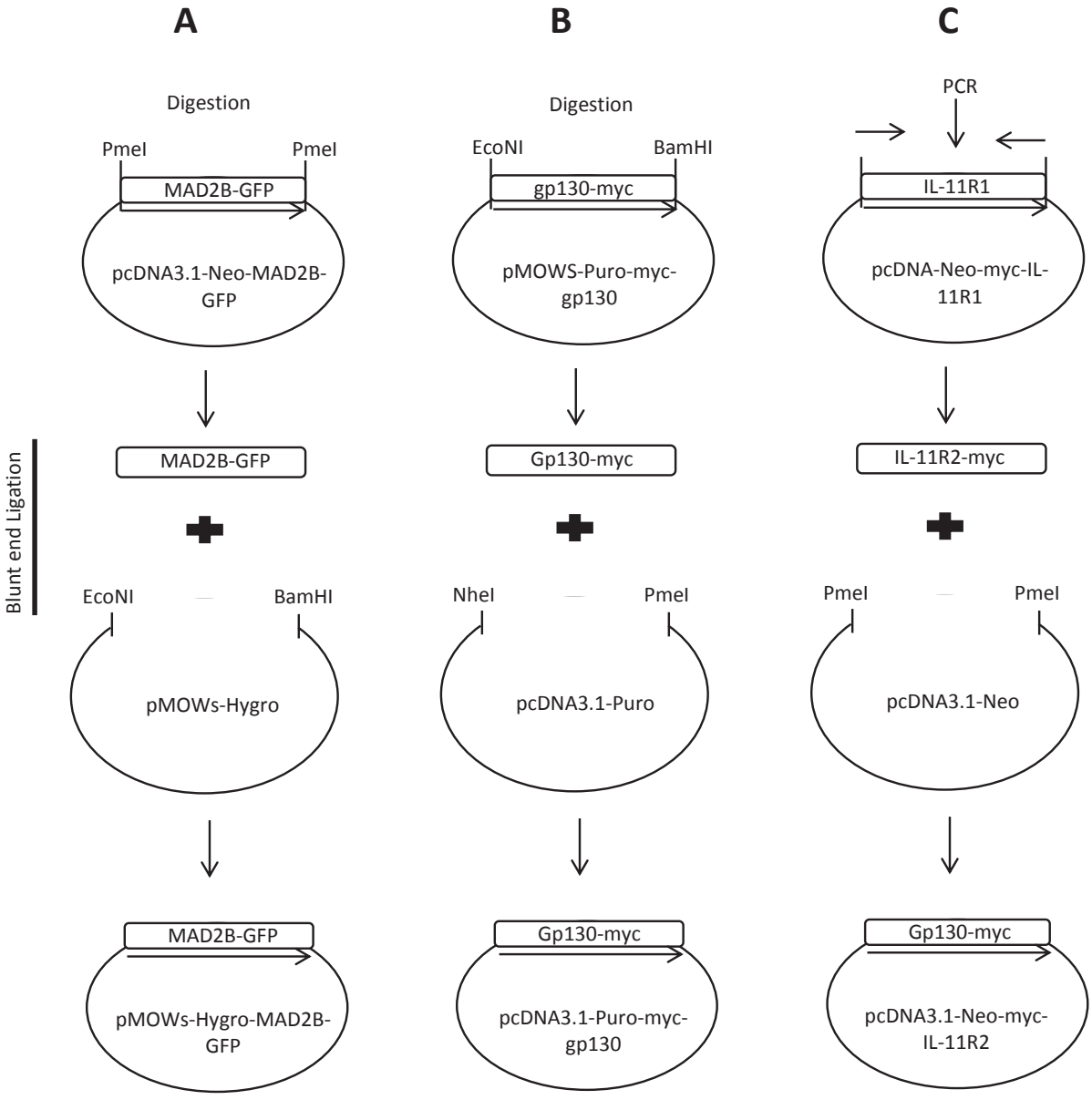

Appendix Figure: A. pcDNA3.1-Neo-MAD2B-GFP was cut by PmeI to extract MAD2B-GFP fragment. MAD2B-GFP fragment was inserted into pMOWs-puro vector which was cut by EcoNI and BamHI. The final vector was named pMOWS-Hygro-MAD2B-GFP. B. pMOWS-Puro-myc-gp130 was cut by EcoNI and BamHI

to extract the gp130-myc fragment. Gp130-myc fragment was inserted into pcDNA3.1-puro vector which was cut by NheI and PmeI. The final vector was named pcDNA3.1-puro-myc-gp130. C. IL-11R2 fragment was synthetized by PCR (primer sequences were listed in 2.1.8 part). IL-11R2 fragment was inserted into pcDNA3.1-Neo vector which was cut by PmeI. The final vector was named pcDNA3.1-Neo-myc-IL-11R2.

Abbreviations

µg	microgram
µl	microliter
µM	micromolar
ADAM	a disintegrin and metalloproteinase
Akt	protein kinase B
BCA	bicinchoninic acid assay
BSA	bovine serum albumin
cDNA	copy DNA
CLC	cardiotrophin-like-cytokine
CLF-1	cytokine-like factor 1
cm	centimetre
CNTF	ciliary neurotrophic factor α-receptor
CT-1	cardiotrophin-1
C-terminal	carboxy-terminal
DMEM	Dulbecco's modified Eagle's Medium
DMSO	dimethylsulfoxid
DNA	deoxyribonucleic acid
dNTP	deoxynucleotide
EDTA	ethylenediaminetetraacetat
EGF	epidermal growth factor
eGFP	enhanced green fluorescent protein
EGFR	epidermal growth factor receptor
EGTA	ethylen glycol tetraacetic acid
ELISA	enzyme-linked immunosorbent assay
ER	endoplasmic reticulum
ERK	extracellular regulated kinase
FCS	fetal calf serum
FERM	four-point-one, ezrin, radixin and moesin
FNIII	fibronectin Type III
g	gramm
Gab1	Brb2-associated-binding protein 1
GAPDH	glyceraldehyde 3-phosphate dehydrogenase
gp130	glycoprotein 130
GPI	glycosylphosphatidylinositol
GPL	gp130-like receptor
Grb2	growth factor receptor-bound protein 2
h	hour
IFN	interferon
Ig	immunoglobulin

Ig-like	immunoglobulin like
IL	interleukin
Jak	janus kinase
kb	kilo base
kDa	kilodalton
KIR	kinase-inhibitory region
LIF	leukemia inhibitory factor
m	murine
M	molar
MAPK	mitogen-activated protein kinase
MDCK	madin-darby canine kidney
MEF	mouse embryonic fibroblast
mg	milligram
min	minute
ml	Milliliter
mM	millimolar
ng	nanogram
NLS	nuclear localization signal
nm	nanomolar
N-terminal	amino-terminal
OSM	oncostatinM
PAGE	polyacrylamide gel electrophoresis
PBS	phosphate buffer saline
PCR	polymerase chain reaction
PEG	polyethylene glycol
PI3K	phosphoinositide 3-kinase
PIAS	protein inhibitor activated STAT
PKB	protein kinase B
POD	peroxidase
PTEN	phosphatase and tensin homologue
PVDF	Polyvinylidene fluoride
qPCR	quantitative PCR
R	receptor
Ras	rat sarcoma
RLU	relative light units
RNA	ribonucleic acid
RNase	ribonuclease
rpm	rounds per minute
RT	room temperature

s	second
SDS	sodium dodecyl sulfate
sgp130	soluble gp130
SH2	src-homology 2
SHP2	SH2 containing phosphatase
sIL-6R	soluble IL-6R
SOCS	suppressor of cytokine signaling
STAT	signal transducer and activator of transcription
TAE	tris-acetat-EDTA buffer
TBS	tris-buffered saline
TEMED	N,N,N',N'-tetramethylenediamine
Tris	tris-(hydroxymethyl-)aminomethane
Tween20	Polyoxyethylene(20)-sorbitan-monolaurate
Tyk2	non-receptor tyrosine-protein kinase
U	units
V	volt
WB	Western blot
WT	wild type

Acknowledgments

I would like to express my deepest thanks to Prof. Dr. Jürgen Scheller who accepted me in his group and also because of his continuous supports, patience, motivation, and immense knowledge. I am so thankful to him for allowing me to grow as a researcher and opening new horizons to my scientific life. I greatly appreciate him for giving me this opportunity to gain much confidence and build a strong basis for my scientific career.

I thank Prof. Dr. William F. Martin for his agreement to be co-reference of my thesis and also for his kind supports.

My sincere thanks also goes to my former colleague Dr. Christoph Garbers who was not only a simple colleague, but a great friend. I am really grateful to him for sharing his knowledge and experiences and also our wonderful collaboration and nice publications.

I would like to extend my thanks to Dr. Roland Piekorz and Prof. Dr Reza Ahmadian for their scientific discussion, advice, and motivation. I had the chance that beside my official supervisor benefited from their knowledge, experienced and insightful comments.

I am so grateful to Manuel Franke, Saeideh Nakhaeirad, Kazem Nouri, and Larissa Lamertz for our great friendship and also their help and support in correction of my thesis.

I extend my thanks to my lovely former colleague Dr. Samadhi Aparicio-Siegmund. She was not only so helpful in the lab and office work, she was so helpful and trustable person in my private life.

I would like to give a great thanks to my angle Frau Petra Oprée Jeremic. Petra, du bist ein echter Engel. I am so thankful for all your support and kindness. You never let me feel alone and sad.

I am so grateful to: Dr. Jan Sommer, Dr. Doreen Floss, Dr. Jens Moll, Alexander Lang, Ehsan Amin, Fereshte Kamrani and all other colleagues in the institute of Biochemistry and molecular biology II for our great friendship and collaboration.

Acknowledgments

My sincere thanks goes to the German Research Foundation (Deutsche Forschungsgemeinschaft; DFG) for the financial support.

The last but not the least; I would like to thank my lovely family. I cannot express my feeling with words. From deep of my heart I should say that I love and pray you. You gave me your love and taught me how to love people and my life. You taught me how to be an independent and strong person and let me free to decide for my life and fulfill my dreams. Although I am far from you, you are always in my heart and thought and feel your positive energy with myself. I love you mom, I love you dad, I love you Narges.